J Math Chem (2015) 53:260–304
DOI 10.1007/s10910-014-0426-x

ORIGINAL PAPER

Stereoisograms for three-membered heterocycles: I. Symmetry-itemized enumeration of oxiranes under an *RS*-stereoisomeric group

Shinsaku Fujita

Received: 5 August 2014 / Accepted: 4 October 2014 / Published online: 17 October 2014

Abstract For the purpose of characterizing the stereochemistry and stereoisomerism of oxirane derivatives, the *RS*-stereoisomeric group $\mathbf{C}_{2v\tilde{\sigma}\hat{I}}$ of order 8 has been defined by starting point group $\mathbf{C}_{2v}$ of order 4, which specifies the geometric features of an oxirane skeleton. The isomorphism between $\mathbf{C}_{2v\tilde{\sigma}\hat{I}}$ and the point group $\mathbf{D}_{2h}$ of order 8 is discussed algebraically and diagrammatically. The data necessary to combinatorial enumeration under $\mathbf{C}_{2v\tilde{\sigma}\hat{I}}$, e.g., the non-redundant set of subgroups, the subduction of coset representations, and the inverse of the mark table, are prepared by referring to the data of $\mathbf{D}_{2h}$. The fixed-point-matrix method and the partial-cycle-index method, which have been originally developed to accomplish combinatorial enumeration under point groups in the unit-subduced-cycle-index approach (Fujita in Symmetry and combinatorial enumeration in chemistry. Springer, Berlin, 1991), are extended and applied to the combinatorial enumeration of oxirane derivatives under the *RS*-stereoisomeric group $\mathbf{C}_{2v\tilde{\sigma}\hat{I}}$. Thereby, the numbers of inequivalent quadruplets are calculated in an itemized fashion with respect to the subgroups of $\mathbf{C}_{2v\tilde{\sigma}\hat{I}}$, where each quadruplet contained in a stereoisogram is counted once. Such quadruplets are further categorized into five types (type I–V). The enumeration of oxiranes under the point group $\mathbf{C}_{2v}$ as well as under the *RS*-permutation group $\mathbf{C}_{2\tilde{\sigma}}$ is also conducted and the results are compared with those of the *RS*-stereoisomeric group $\mathbf{C}_{2v\tilde{\sigma}\hat{I}}$.

Keywords Oxirane · Enumeration · Stereoisogram · *RS*-stereoisomeric group

S. Fujita (✉)
Shonan Institute of Chemoinformatics and Mathematical Chemistry, Kaneko 479-7 Ooimachi, Ashigara-Kami-Gun, Kanagawa-Ken 258-0019, Japan
e-mail: shinsaku_fujita@nifty.com

1 Introduction

Chiral three-membered heterocycles shown in Fig. 1 have attracted the interests of organic chemists as targets or intermediates for organic syntheses. Several reviews [1–3] have surveyed synthetic aspects of chiral oxiranes and aziridines. In particular, the Katsuki-Sharpless asymmetric epoxidation and related methods [4,5] have attracted wide interests of organic chemists, as found in many review articles [6–9]. A remarkable milestone of this field has been the Nobel Prize in Chemistry 2001 awarded to Sharpless [10]. As for chiral aziridines, the absolute configuration of 2-phenylaziridine and its derivatives has been reported by us [11], and synthetic applications of chiral aziridines have been reviewed [12]. As for chiral thiiranes, asymmetric synthesis of them from aldehydes has been reported [13].

In spite of these brilliant progresses in the synthesis of chiral three-membered rings, the total features of their stereoisomerism have not been fully investigated, e.g., the numbers of three-dimensional (3D) structures which are derived by placing four ligands on the four positions of the skeleton **1**, their symmetrical features for categorizing three-membered heterocycles as 3D structures, and theoretical and mathematical foundations for assigning stereochemical descriptors such as *R/S*-stereodescriptors of the Cahn–Ingold–Prelog (CIP) system. These items should be clarified by developing rational mathematical foundations for the purpose of discussing the total features of stereoisomerism of three-membered heterocycles.

In order to discuss geometrical features of organic compounds as 3D structures, I have pointed out the importance of coset representations and equivalence classes (orbits), where subduction of coset representations and sphericities of orbits have been emphasized as new concepts in qualitative and quantitative discussions on stereochemistry, as shown in articles [14–17] and reviews [18,19]. After unit subduced cycle indices with chirality fittingness (USCI-CFs) were proposed on the basis of these concepts, four methods of combinatorial enumeration have been developed under the collective name *the unit-subduced-cycle-index (USCI) approach* [20–24]. On the other hand, *the proligand method* has been developed as a more succinct method of combinatorial enumeration of 3D structures [25–27] and applied to combinatorial enumeration of monosubstituted alkanes [28–30] and alkanes [31–35], as summarized in a review [36] and a monograph [37]. The proligand–promolecule model has been proposed to enumerate organic compounds with rotatable ligands [38].

In addition, I have developed *the stereoisogram approach* by staring from a newly-defined concept of *stereoisograms*, which consists of a quadruplet of promolecules. Such stereoisograms are diagrammatic expressions of *RS*-stereoisomeric groups defined by integrating point-groups and *RS*-permutation groups, where the latter are generated by the restriction of usual permutation groups [39–41]. The quadruplet of

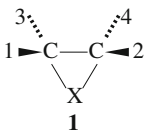

1

X = O: oxirane, epoxide
X = S: thiirane, episulfide
X = NH: aziridine

Fig. 1 Skeletons for three-membered heterocycles

promolecules in a stereoisogram is characterized by three types of relationships, i.e., enantiomeric, *RS*-diastereomeric, and holantimeric relationships [39,42]. Thereby, stereoisograms are categorized into five types, as proven in general [43].

The original version of the USCI approach [23,24] has been applied to the combinatorial enumeration of 3D structures under point groups, as shown in a recent report [44–46]. The USCI approach can be extended by incorporating the stereoisogram approach, so that it becomes capable of enumerating 3D structures under *RS*-stereoisomeric groups [47,48]. This means that the combination of the USCI approach with the stereoisogram approach is ready to conduct combinatorial enumeration of three-membered heterocycles under the corresponding *RS*-stereoisomeric group. This is the target of the present article as Part I of the present series.

2 The proligand–promolecule model for the oxirane skeleton

For the sake of simplicity, we select an oxirane skeleton **2** (Fig. 2) as a representative of three-membered heterocycles **1** (Fig. 1). The importance of the proligand–promolecule model [38] has been demonstrated by examining rigid polycyclic skeletons such as a prismane skeleton [49,50] and an adamantane skeleton [51]. The crux is the fact that the chirality or achirality of each proligand, which is decided in isolation (when detached), is identical with the chirality or achirality of the corresponding ligand with a concrete 3D structure. Note that influences due to conformational changes are avoided in terms of the proligand–promolecule model. Throughout the present article, a pair of symbols or compound numbers without and with an overbar represents a pair of enantiomeric entities (proligands, promolecules, ligands, molecules, etc.) in isolation.

The proligand–promolecule model can be applied to the oxirane skeleton **2**, which is regarded as a rigid stereoskeleton with four substitution positions (Fig. 2). These positions are numbered sequentially from 1 to 4, where the initial mode of numbering is arbitrary without losing generality.

A set of proligands is selected from a given proligand inventory:

$$\mathbf{L} = \{\mathrm{A}, \mathrm{B}, \mathrm{X}, \mathrm{Y}; \mathrm{p}, \overline{\mathrm{p}}, \mathrm{q}, \overline{\mathrm{q}}, \mathrm{r}, \overline{\mathrm{r}}, \mathrm{s}, \overline{\mathrm{s}}\}, \tag{1}$$

where the symbols, A, B, X, and Y, denote achiral proligands, while the paired symbols, p/$\overline{\mathrm{p}}$, q/$\overline{\mathrm{q}}$, r/$\overline{\mathrm{r}}$, and s/$\overline{\mathrm{s}}$, denote chiral proligands having opposite chirality senses. For example, a set of proligands, A, B, X, and Y, is applied to the skeleton **2** so as to generate a promolecule represented by **3**. Then, a molecule **4** is generated by the substitution of A = CH_3, B = CH_2CH_3, X = H, and Y = H.

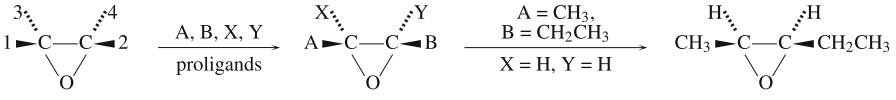

2 stereoskeleton — **3** promolecule — **4** molecule

Fig. 2 The proligand–promolecule model for an oxirane skeleton

The oxirane skeleton **2** belongs to the point group $\mathbf{C}_{2v}$ (order 4). Under the action of $\mathbf{C}_{2v}$, the orbits contained in **2** are characterized by coset representations such as $\mathbf{C}_{2v}(/\mathbf{C}_1)$ for the four substitution positions, $\mathbf{C}_{2v}(/\mathbf{C}'_s)$ for the two skeletal carbons, and $\mathbf{C}_{2v}(/\mathbf{C}_{2v})$ for the oxygen atom [15]. By adopting the numbering shown in **2**, the coset representation $\mathbf{C}_{2v}(/\mathbf{C}_1)$ is obtained as follows (cf. Table 1 of [15]):

$$\mathbf{C}_{2v} = \left\{I, C_2, \sigma_{v(1)}, \sigma_{v(2)}\right\} \tag{2}$$

$$\mathbf{C}_{2v}(/\mathbf{C}_1) = \left\{(1)(2)(3)(4), (1\ 4)(2\ 3), \overline{(1\ 2)(3\ 4)}, \overline{(1\ 3)(2\ 4)}\right\}, \tag{3}$$

where an overbar indicates the alternation of the chirality sense of each substitution position. During the generation of a promolecule, the point group $\mathbf{C}_{2v}$ is restricted to one of the subgroups (e.g., $\mathbf{C}_1$ for the promolecule **3**), where the restriction is characterized by the subduction of coset representations (e.g., $\mathbf{C}_{2v}(/\mathbf{C}_1) \downarrow \mathbf{C}_1 = 4\mathbf{C}_1(/\mathbf{C}_1)$ for the promolecule **3**) according to the USCI approach [23].

3 *RS*-stereoisomeric group for the oxirane skeleton

The operations of the point group $\mathbf{C}_{2v}$ are listed in the left part of Table 1 (two rotations in the upper-left part **A** and two reflections in the lower-left part **B**). Hence, the following coset decomposition is obtained:

$$\mathbf{C}_{2v} = \mathbf{C}_2 + \sigma\mathbf{C}_2, \tag{4}$$

where the representative σ is selected to be $\sigma_{v(1)}$ or $\sigma_{v(2)}$. These operations correspond to the symmetry elements illustrated in the top-view **6** (Fig. 3). Note that the oxygen atom with its valence bonds is hidden under the central C–C bond of the oxirane skeleton in the top-view represented by **6**.

By starting from the proper rotations of $\mathbf{C}_{2v}$, i.e., $I \sim (1)(2)(3)(4)$ and $C_2 \sim (1\ 4)(2\ 3)$, the corresponding ligand reflections (the lower-right part **D**) are generated as follows: $\widehat{I} \sim \overline{(1)(2)(3)(4)}$ and $\widehat{C}_2 \sim \overline{(1\ 4)(2\ 3)}$, where the chirality sense of each position is changed into the opposite chirality sense as denoted by an overbar. The resulting ligand-reflection group is represented as follows:

$$\mathbf{C}_{2\widehat{I}} = \mathbf{C}_2 + \widehat{I}\mathbf{C}_2 \tag{5}$$

By starting from the reflections of $\mathbf{C}_{2v}$, i.e., $\sigma_{v(1)} \sim \overline{(1\ 2)(3\ 4)}$ and $\sigma_{v(2)} \sim \overline{(1\ 3)(2\ 4)}$, the corresponding *RS*-permutations (the upper-right part **C**) are generated as follows: $\widetilde{\sigma}_{v(1)} \sim (1\ 2)(3\ 4)$ and $\widetilde{\sigma}_{v(2)} \sim (1\ 3)(2\ 4)$, where the chirality sense of each position is retained to be unchanged. The resulting *RS*-permutation group is represented as follows:

$$\mathbf{C}_{2\widetilde{\sigma}} = \mathbf{C}_2 + \widetilde{\sigma}\mathbf{C}_2 \tag{6}$$

where the representative $\widetilde{\sigma}$ is selected to be $\widetilde{\sigma}_{v(1)}$ or $\widetilde{\sigma}_{v(2)}$.

Table 1 Operations of $\mathbf{C}_{2v\widetilde{\sigma}\widehat{I}}$ and coset representation of $\mathbf{C}_{2v\widetilde{\sigma}\widehat{I}}(/\mathbf{C}_{\widehat{I}})$ versus operations of $\mathbf{D}_{2h}$ and coset representation of $\mathbf{D}_{2h}(/\mathbf{C}''_s)$

operation $g \in \mathbf{D}_{2h}$	operation $g \in \mathbf{C}_{2v\widetilde{\sigma}\widehat{I}}$	$\mathbf{D}_{2h}(/\mathbf{C}''_s)$ or $\mathbf{C}_{2v\widetilde{\sigma}\widehat{I}}(/\mathbf{C}_{\widehat{I}})$ (product of cycles)	operation $g \in \mathbf{D}_{2h}$	operation $g \in \mathbf{C}_{2v\widetilde{\sigma}\widehat{I}}$	$\mathbf{D}_{2h}(/\mathbf{C}''_s)$ or $\mathbf{C}_{2v\widetilde{\sigma}\widehat{I}}(/\mathbf{C}_{\widehat{I}})$ (product of cycles)
I	I	A (1)(2)(3)(4)	$C_{2(1)}$	$\widetilde{\sigma}_{v(1)}$	C (1 2)(3 4)
$C_{2(3)}$	C_2	(1 4)(2 3)	$C_{2(2)}$	$\widetilde{\sigma}_{v(2)}$	(1 3)(2 4)
$\sigma_{v(1)}$	$\sigma_{v(1)}$	B $\overline{(1\,2)(3\,4)}$	σ_h	$\widehat{I}$	D $\overline{(1)(2)(3)(4)}$
$\sigma_{v(2)}$	$\sigma_{v(2)}$	$\overline{(1\,3)(2\,4)}$	i	$\widehat{C}_2$	$\overline{(1\,4)(2\,3)}$

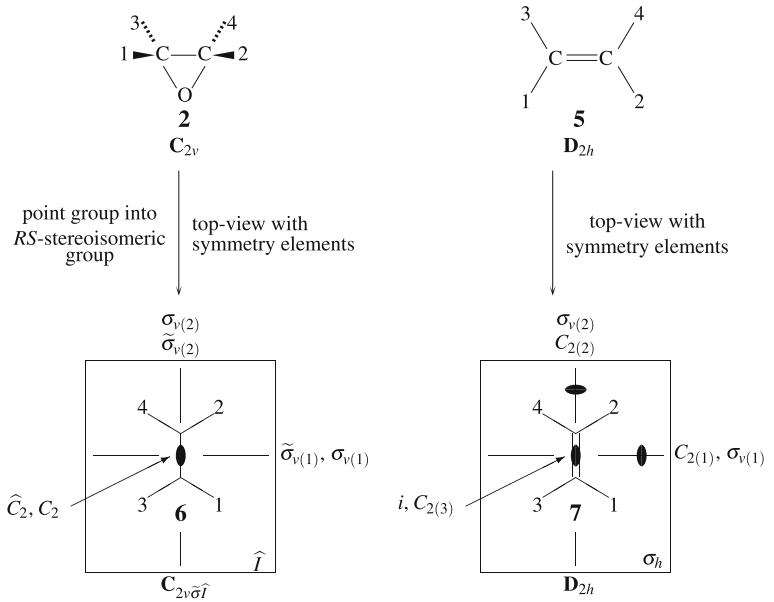

Fig. 3 An oxirane skeleton (**2**) and an ethylene skeleton (**5**). The top-view **6** shows the symmetry elements of the *RS*-stereoisomeric group $\mathbf{C}_{2v\widetilde{\sigma}\widehat{I}}$ for the oxirane skeleton (**2**), while the top-view **7** shows the symmetry elements of the isomorphic point group $\mathbf{D}_{2h}$ for the ethylene skeleton (**5**)

The coset decompositions represented by Eqs. 4, 5, and 6 are integrated to generate an *RS*-stereoisomeric group for characterizing the oxirane skeleton (**2**) as follows:

$$\mathbf{C}_{2v\widetilde{\sigma}\widehat{I}} = \mathbf{C}_2 + \sigma\mathbf{C}_2 + \widetilde{\sigma}\mathbf{C}_2 + \widehat{I}\mathbf{C}_2, \tag{7}$$

the operations of which are listed in the ($g \in \mathbf{C}_{2v\widetilde{\sigma}\widehat{I}}$)-column of Table 1. The coset representation $\mathbf{C}_{2v}(/\mathbf{C}_1)$ under the point group $\mathbf{C}_{2v}$ is extended to give the coset representation $\mathbf{C}_{2v\widetilde{\sigma}\widehat{I}}(/\mathbf{C}_{\widehat{I}})$ under the *RS*-stereoisomeric group $\mathbf{C}_{2v\widetilde{\sigma}\widehat{I}}$, as listed in Table 1.

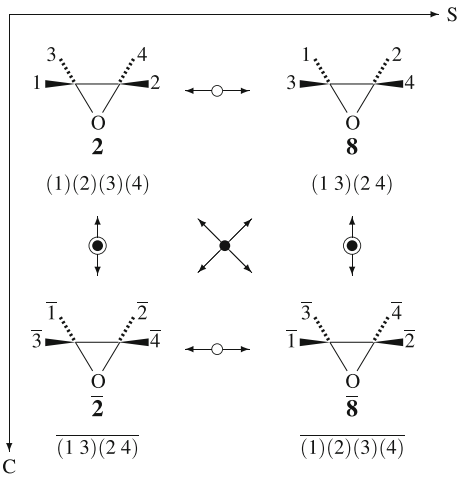

Fig. 4 Elementary stereoisogram for an oxirane skeleton

4 Stereoisograms for the oxirane skeleton

4.1 Construction of stereoisograms

Because the subgroup $\mathbf{C}_2$ is a normal subgroup of $\mathbf{C}_{2v\widetilde{\sigma}\widehat{I}}$ (Eq. 7), the corresponding factor group can be constructed as follows:

$$\mathbf{C}_{2v\widetilde{\sigma}\widehat{I}}/\mathbf{C}_2 = \left\{\mathbf{C}_2, \sigma\mathbf{C}_2, \widetilde{\sigma}\mathbf{C}_2, \widehat{I}\mathbf{C}_2\right\}, \tag{8}$$

which is isomorphic to the Klein four-group of order 4 or to the point group $\mathbf{C}_{2v}$.

Let the oxirane skeleton **2** correspond to the identity operation I ($\sim$ (1)(2)(3)(4)), which is a representative of the coset $\mathbf{C}_2$ ($= I\mathbf{C}_2$) contained in the factor group $\mathbf{C}_{2v\widetilde{\sigma}\widehat{I}}/\mathbf{C}_2$ (Eq. 8). Then, the other representatives of the cosets contained in Eq. 8 correspond to the numbered skeletons shown in Fig. 4, i.e., $\overline{\mathbf{2}}$ to $\sigma_{v(1)}$ ($\sim \overline{(1\ 3)(2\ 4)}$), **8** to $\widetilde{\sigma}_{v(1)}$ ($\sim$ (1 3)(2 4)), and $\overline{\mathbf{8}}$ to $\widehat{I}$ ($\sim \overline{(1)(2)(3)(4)}$). These four numbered skeletons are collected to give *an elementary stereoisogram* shown in Fig. 4. As found easily, each skeleton (**2**, $\overline{\mathbf{2}}$, **8**, or $\overline{\mathbf{8}}$) in Fig. 4 generates a set of homomers under the action of $\mathbf{C}_2$, so that it can be regarded as a diagrammatic representative of each coset appearing in the factor group $\mathbf{C}_{2v\widetilde{\sigma}\widehat{I}}/\mathbf{C}_2$ (Eq. 8).

When a set of proligands, A (at position 1), B (at position 2), X (at position 3), and Y (at position 4), is applied to the elementary stereoisogram (Fig. 4), there appears a stereoisogram shown in Fig. 5. The stereoisogram (Fig. 5) is characterized by the presence of diagonal equality symbols, so that it is categorized to type I (chiral, *RS*-stereogenic, and ascleral).

In general, a stereoisogram contains three kinds of relationships, i.e., (self-) enantiomeric relationships (along the vertical direction), (self-)*RS*-diastereomeric relationships (along the horizontal direction), and (self-)holantimeric relationships (along the diagonal direction). These relationships correspond to chirality/achirality, *RS*-stereogenicity/*RS*-astereogenicity, and sclerality/asclerality, respectively. A relation-

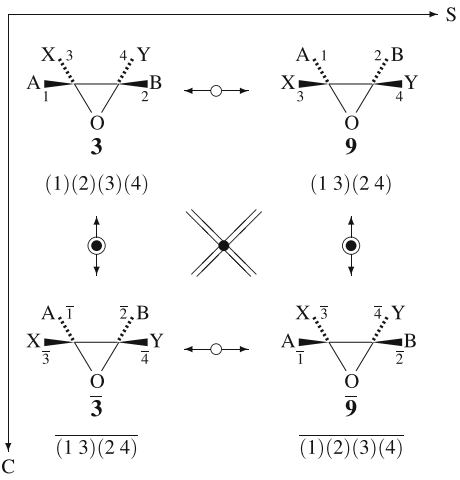

Fig. 5 Stereoisogram of type I derived from the oxirane skeleton **2**, where the proligand A is placed at position 1, B at position 2, X at position 3, and Y at position 4. Note that the proligands A, B, X, and Y are achiral in isolation. The reference promolecule **3** belongs to the *RS*-stereoisomeric group $\mathbf{C}_{\widehat{1}}$

ship with the prefix 'self-' is denoted by an equality symbol, so that the diagonal equality symbols in Fig. 5 represent self-holantimeric relationships (due to ascleral-ity).

By placing proligands selected from the proligand inventory (Eq. 1), the elementary stereoisogram (Fig. 4) is converted into a stereoisogram which contains a quadruplet of promolecules produced according to the proligand–promolecule model. There appear stereoisograms of five types, which are schematically shown in Fig. 6. The symbols **A** and $\overline{\mathbf{A}}$ (or **B** and $\overline{\mathbf{B}}$) represent a pair of enantiomers based on a given skeleton (e.g., an oxirane skeleton). For example, Fig. 5 is an example of the type-I stereoisogram shown in Fig. 6, where the **A** at the upper-left position is selected to be equal to the promolecule **3**.

4.2 Stereoisograms of five types

Just as the Klein four-group has five subgroups, the factor group $\mathbf{C}_{2v\widetilde{\sigma}\widehat{1}}/\mathbf{C}_2$ (Eq. 8) has five subgroups in accord with the general discussions on *RS*-stereoisomeric groups [43]:

$$\text{Type I:} \quad \mathbf{C}_{2\widehat{1}}/\mathbf{C}_2 = \{\mathbf{C}_2, \widehat{1}\mathbf{C}_2\} \quad \text{(cf. Eq. 5)} \tag{9}$$

$$\text{Type II:} \quad \mathbf{C}_{2\widetilde{\sigma}}/\mathbf{C}_2 = \{\mathbf{C}_2, \widetilde{\sigma}\mathbf{C}_2\} \quad \text{(cf. Eq. 6)} \tag{10}$$

$$\text{Type III:} \quad \mathbf{C}_2/\mathbf{C}_2 = \{\mathbf{C}_2\} \tag{11}$$

$$\text{Type IV:} \quad \mathbf{C}_{2v\widetilde{\sigma}\widehat{1}}/\mathbf{C}_2 = \{\mathbf{C}_2, \sigma\mathbf{C}_2, \widetilde{\sigma}\mathbf{C}_2, \widehat{1}\mathbf{C}_2\} \quad \text{(cf. Eqs. 7 and 8)} \tag{12}$$

$$\text{Type V:} \quad \mathbf{C}_{2v}/\mathbf{C}_2 = \{\mathbf{C}_2, \sigma\mathbf{C}_2\} \quad \text{(cf. Eq. 4)} \tag{13}$$

The five subgroups listed in Eqs. 9–13 correspond to the stereoisograms of five types collected in Fig. 6. Because Eq. 9 corresponds to $\mathbf{C}_{2\widehat{1}}$ (Eq. 5), it is characterized by the presence of a diagonal equality symbol, as found in the type-I stereoisogram shown in Fig. 6. Because Eq. 10 corresponds to $\mathbf{C}_{2\widetilde{\sigma}}$ (Eq. 6), it is characterized by

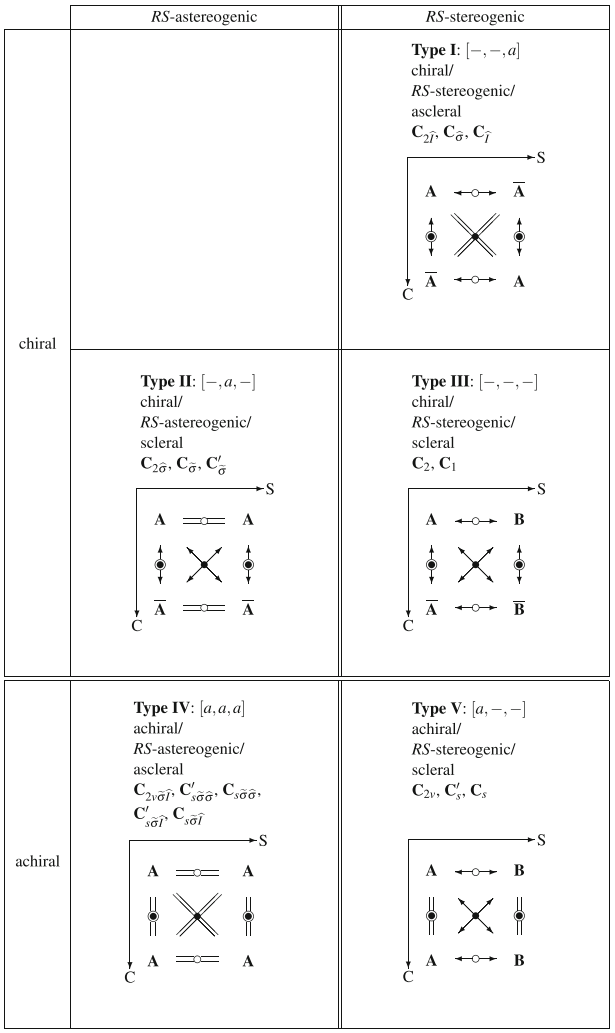

Fig. 6 Stereoisograms for representing *RS*-stereoisomers of five types. This figure is a modification of Fig. 6 of [42] and of Fig. 2 of [52], where the subgroups of $\mathbf{C}_{2v\tilde{\sigma}\hat{I}}$ for characterizing respective types are shown along with three attributes. The *symbols* **A** and $\overline{\mathbf{A}}$ (or **B** and $\overline{\mathbf{B}}$) represent a pair of enantiomers based on a given skeleton (e.g., an oxirane skeleton), where the **A** at the *upper-left* position of each stereoisogram is selected from the promolecules enumerated in the present article

the presence of a horizontal equality symbol, as found in the type-II stereoisogram shown in Fig. 6. Because Eq. 13 corresponds to $\mathbf{C}_{2v}$ (Eq. 4), it is characterized by the presence of a vertical equality symbol, as found in the type-V stereoisogram shown in Fig. 6. As an extreme case, Eq. 11 corresponding to $\mathbf{C}_2$ is characterized by the absence of equality symbols in any directions, as found in the type-III stereoisogram shown in Fig. 6. As another extreme case, Eq. 12 corresponding to $\mathbf{C}_{2v\tilde{\sigma}\hat{I}}$ (Eq. 7) indicates the presence of equality symbols in all of the directions, as found in the type-IV stereoisogram shown in Fig. 6.

5 Subgroups of the *RS*-stereoisomeric group for the oxirane skeleton

5.1 Isomorphism between the *RS*-stereoisomeric group $\mathbf{C}_{2v\tilde{\sigma}\hat{I}}$ and the point group $\mathbf{D}_{2h}$

By comparing the operations of the *RS*-stereoisomeric group $\mathbf{C}_{2v\tilde{\sigma}\hat{I}}$ with those of the point group $\mathbf{D}_{2h}$ (Table 1), they are determined to be isomorphic. The correspondence between the operations of them is clarified by comparing the top-view **6** (for the oxirane skeleton **2** of $\mathbf{C}_{2v\tilde{\sigma}\hat{I}}$) and the counterpart top-view **7** (for the ethylene skeleton **5** of $\mathbf{D}_{2h}$). It should be noted that the coset decomposition represented by Eq. 7 corresponds to the coset representation of the point group $\mathbf{D}_{2h}$:

$$\mathbf{D}_{2h} = \mathbf{C}_2 + \sigma_{v(1)}\mathbf{C}_2 + C_{2(1)}\mathbf{C}_2 + \sigma_h\mathbf{C}_2. \tag{14}$$

The isomorphism between $\mathbf{C}_{2v\tilde{\sigma}\hat{I}}$ and $\mathbf{D}_{2h}$ means that the data of the point group $\mathbf{D}_{2h}$ (e.g., the non-redundant set of subgroups, a mark table, an inverse mark able, subduction of coset representation, unit subduced cycle indices with and without chirality fittingness) [53,54] can be used in the discussions on the *RS*-stereoisomeric group $\mathbf{C}_{2v\tilde{\sigma}\hat{I}}$ after necessary modifications.

The point group $\mathbf{D}_{2h}$ has a non-redundant set of subgroups (SSG) containing 16 subgroups up to conjugacy, where the subgroups are aligned in the ascending order of their orders [53,54]:

$$\mathrm{SSG}_{\mathbf{D}_{2h}} = \left\{ \overset{1}{\mathbf{C}}_1, \overset{2}{\mathbf{C}}_2, \overset{3}{\mathbf{C}}_2', \overset{4}{\mathbf{C}}_2'', \overset{5}{\mathbf{C}}_s, \overset{6}{\mathbf{C}}_s', \overset{7}{\mathbf{C}}_s'', \overset{8}{\mathbf{C}}_i, \overset{9}{\mathbf{C}}_{2v}, \overset{10}{\mathbf{C}}_{2v}', \overset{11}{\mathbf{C}}_{2v}'', \overset{12}{\mathbf{C}}_{2h}, \overset{13}{\mathbf{C}}_{2h}', \overset{14}{\mathbf{C}}_{2h}'', \overset{15}{\mathbf{D}}_2, \overset{16}{\mathbf{D}}_{2h} \right\}. \tag{15}$$

These subgroups are numbered sequentially for the sake of cross reference. The operations contained in each of these subgroups (Eq. 15) are listed in the right part of Table 2.

Because of isomorphism, the *RS*-stereoisomeric group $\mathbf{C}_{2v\tilde{\sigma}\hat{I}}$ is characterized by a non-redundant set of subgroups (SSG) as follows:

$$\mathrm{SSG}_{\mathbf{C}_{2v\tilde{\sigma}\hat{I}}} = \left\{ \overset{1}{\mathbf{C}}_1, \overset{2}{\mathbf{C}}_2, \overset{3}{\mathbf{C}}_{\tilde{\sigma}}, \overset{4}{\mathbf{C}}_{\tilde{\sigma}}', \overset{5}{\mathbf{C}}_s, \overset{6}{\mathbf{C}}_s', \overset{7}{\mathbf{C}}_{\hat{I}}, \overset{8}{\mathbf{C}}_{\hat{\sigma}}, \overset{9}{\mathbf{C}}_{2v}, \overset{10}{\mathbf{C}}_{s\tilde{\sigma}\hat{I}}, \overset{11}{\mathbf{C}}_{s\tilde{\sigma}\hat{I}}', \overset{12}{\mathbf{C}}_{2\hat{I}}, \overset{13}{\mathbf{C}}_{s\tilde{\sigma}\hat{\sigma}}, \overset{14}{\mathbf{C}}_{s\tilde{\sigma}\hat{\sigma}}', \overset{15}{\mathbf{C}}_{2\tilde{\sigma}}, \overset{16}{\mathbf{C}}_{2v\tilde{\sigma}\hat{I}} \right\}, \tag{16}$$

where the subgroups are numbered sequentially for the sake of cross reference to the SSG of the isomorphic point group $\mathbf{D}_{2h}$. The operations contained in each of these subgroups (Eq. 16) are listed in the left part of Table 2.

As found in the left part of Table 2, the notation of each subgroup consist of a boldfaced letter and the first subscript due to its maximum point group (e.g., $\mathbf{C}_{2v}$ for

Table 2 Subgroups of the *RS*-stereoisomeric group $\mathbf{C}_{2v\widetilde{\sigma}\widehat{I}}$ and those of the isomorphic point group $\mathbf{D}_{2h}$

	RS-stereoisomeric group $\mathbf{C}_{2v\widetilde{\sigma}\widehat{I}}$		Isomorphic point group $\mathbf{D}_{2h}$	
	Type	Subgroup $\acute{\mathbf{G}}$ ($\subset \mathbf{C}_{2v\widetilde{\sigma}\widehat{I}}$)		Subgroup $\mathbf{G}$ ($\subset \mathbf{D}_{2h}$)
1	III	$\mathbf{C}_1 = \{I\}$	1	$\mathbf{C}_1 = \{I\}$
2	III	$\mathbf{C}_2 = \{I, C_2\}$	2	$\mathbf{C}_2 = \{I, C_{2(3)}\}$
3	II	$\mathbf{C}_{\widetilde{\sigma}} = \{I, \widetilde{\sigma}_{v(1)}\}$	3	$\mathbf{C}'_2 = \{I, C_{2(1)}\}$
4	II	$\mathbf{C}'_{\widetilde{\sigma}} = \{I, \widetilde{\sigma}_{v(2)}\}$	4	$\mathbf{C}''_2 = \{I, C_{2(2)}\}$
5	V	$\mathbf{C}_s = \{I, \sigma_{v(1)}\}$	5	$\mathbf{C}_s = \{I, \sigma_{v(1)}\}$
6	V	$\mathbf{C}'_s = \{I, \sigma_{v(2)}\}$	6	$\mathbf{C}'_s = \{I, \sigma_{v(2)}\}$
7	I	$\mathbf{C}_{\widehat{I}} = \{I, \widehat{I}\}$	7	$\mathbf{C}''_s = \{I, \sigma_h\}$
8	I	$\mathbf{C}_{\widehat{\sigma}} = \{I, \widehat{C}_2\}$	8	$\mathbf{C}_i = \{I, i\}$
9	V	$\mathbf{C}_{2v} = \{I, C_2, \sigma_{v(1)}, \sigma_{v(2)}\}$	9	$\mathbf{C}_{2v} = \{I, C_{2(3)}, \sigma_{v(1)}, \sigma_{v(2)}\}$
10	IV	$\mathbf{C}_{s\widetilde{\sigma}\widehat{I}} = \{I, \widetilde{\sigma}_{v(1)}, \sigma_{v(1)}, \widehat{I}\}$	10	$\mathbf{C}'_{2v} = \{I, C_{2(1)}, \sigma_{v(1)}, \sigma_h\}$
11	IV	$\mathbf{C}'_{s\widetilde{\sigma}\widehat{I}} = \{I, \widetilde{\sigma}_{v(2)}, \sigma_{v(2)}, \widehat{I}\}$	11	$\mathbf{C}''_{2v} = \{I, C_{2(2)}, \sigma_{v(2)}, \sigma_h\}$
12	I	$\mathbf{C}_{2\widehat{I}} = \{I, C_2, \widehat{I}, \widehat{C}_2\}$	12	$\mathbf{C}_{2h} = \{I, C_{2(3)}, \sigma_h, i\}$
13	IV	$\mathbf{C}_{s\widetilde{\sigma}\widehat{\sigma}} = \{I, \widetilde{\sigma}_{v(1)}, \widehat{C}_2, \sigma_{v(2)}\}$	13	$\mathbf{C}'_{2h} = \{I, C_{2(1)}, i, \sigma_{v(2)}\}$
14	IV	$\mathbf{C}'_{s\widetilde{\sigma}\widehat{\sigma}} = \{I, \widetilde{\sigma}_{v(2)}, \widehat{C}_2, \sigma_{v(1)}\}$	14	$\mathbf{C}''_{2h} = \{I, C_{2(2)}, i, \sigma_{v(1)}\}$
15	II	$\mathbf{C}_{2\widetilde{\sigma}} = \{I, C_2, \widetilde{\sigma}_{v(1)}, \widetilde{\sigma}_{v(2)}\}$	15	$\mathbf{D}_2 = \{I, C_{2(3)}, C_{2(1)}, C_{2(2)}\}$
16	IV	$\mathbf{C}_{2v\widetilde{\sigma}\widehat{I}} = \{I, C_2, \sigma_{v(1)}, \sigma_{v(2)}, \widetilde{\sigma}_{v(1)}, \widetilde{\sigma}_{v(2)}, \widehat{I}, \widehat{C}_2\}$	16	$\mathbf{D}_{2h} = \{I, C_{2(3)}, \sigma_{v(1)}, \sigma_{v(2)}, C_{2(1)}, C_{2(2)}, \sigma_h, i\}$

$\mathbf{C}_{2v\widetilde{\sigma}\widehat{I}}$), which are attached by the additional subscript $\widetilde{\sigma}$ due to the membership of *RS*-permutations (e.g., $\widetilde{\sigma}$ for $\mathbf{C}_{2v\widetilde{\sigma}\widehat{I}}$) and/or the further additional subscript $\widehat{I}$ (or $\widehat{\sigma}$) due to the membership of ligand reflections (e.g., $\widehat{I}$ for $\mathbf{C}_{2v\widetilde{\sigma}\widehat{I}}$).

5.2 Type I to V assigned to the subgroups of the *RS*-stereoisomeric group $\mathbf{C}_{2v\widetilde{\sigma}\widehat{I}}$

The data listed in Eqs. 9–13 indicate the maximum subgroup of each type, i.e., $\mathbf{C}_{2\widehat{I}}$ for type-I stereoisograms, $\mathbf{C}_{2\widetilde{\sigma}}$ for type-II stereoisograms, $\mathbf{C}_2$ for type-III stereoisograms, $\mathbf{C}_{2v\widetilde{\sigma}\widehat{I}}$ for type-IV stereoisograms, and $\mathbf{C}_{2v}$ for type-V stereoisograms. Thereby, the subgroups listed in Eq. 16 are categorized into five types, as summarized in the type-column of Table 2. For example, the subgroup $\mathbf{C}_{\widetilde{\sigma}}$ in the third row of Table 2 is concluded to be type II, because the subgroup $\mathbf{C}_{\widetilde{\sigma}}$ is a subgroup of the maximum subgroup $\mathbf{C}_{2\widetilde{\sigma}}$ of type II appearing in the 15th row. The subgroups of the *RS*-stereoisomeric group $\mathbf{C}_{2v\widetilde{\sigma}\widehat{I}}$ are categorized into type I to V (Table 2) so as to give $\mathrm{SG}^{[\mathrm{I}]}$–$\mathrm{SG}^{[\mathrm{V}]}$:

$$\mathrm{SG}^{[\mathrm{I}]} = \left\{ \overset{7}{\mathbf{C}}_{\widehat{I}}, \overset{8}{\mathbf{C}}_{\widehat{\sigma}}, \overset{12}{\mathbf{C}}_{2\widehat{I}} \right\} \tag{17}$$

$$\mathrm{SG}^{[\mathrm{II}]} = \left\{ \overset{3}{\mathbf{C}}_{\widetilde{\sigma}}, \overset{4}{\mathbf{C}}'_{\widetilde{\sigma}}, \overset{15}{\mathbf{C}}_{2\widetilde{\sigma}} \right\} \tag{18}$$

$$\mathrm{SG}^{[\mathrm{III}]} = \left\{ \overset{1}{\mathbf{C}}_1, \overset{2}{\mathbf{C}}_2 \right\} \tag{19}$$

$$\mathrm{SG}^{[\mathrm{IV}]} = \left\{ \overset{10}{\mathbf{C}}_{s\widetilde{\sigma}\widehat{I}}, \overset{11}{\mathbf{C}}'_{s\widetilde{\sigma}\widehat{I}}, \overset{13}{\mathbf{C}}_{s\widetilde{\sigma}\widehat{\sigma}}, \overset{14}{\mathbf{C}}'_{s\widetilde{\sigma}\widehat{\sigma}}, \overset{16}{\mathbf{C}}_{2v\widetilde{\sigma}\widehat{I}} \right\} \tag{20}$$

$$\mathrm{SG}^{[\mathrm{V}]} = \left\{ \overset{5}{\mathbf{C}}_s, \overset{6}{\mathbf{C}}'_s, \overset{9}{\mathbf{C}}_{2v} \right\} \tag{21}$$

These sets of subgroups are attached to the stereoisograms of the respective types shown in Fig. 6.

5.3 Subduction of the coset representation $\mathbf{C}_{2v\widetilde{\sigma}\widehat{I}}(/\mathbf{C}_{\widehat{I}})$

Each of the four substitution positions in the oxirane skeleton **2** is fixed by the subgroup $\mathbf{C}_{\widehat{I}}$ under the action of the *RS*-stereoisomeric group $\mathbf{C}_{2v\widetilde{\sigma}\widehat{I}}$. In other words, the local symmetry of each position of the oxirane skeleton **2** is determined to be $\mathbf{C}_{\widehat{I}}$ under the global symmetry $\mathbf{C}_{2v\widetilde{\sigma}\widehat{I}}$. The coset decomposition of $\mathbf{C}_{2v\widetilde{\sigma}\widehat{I}}$ by $\mathbf{C}_{\widehat{I}}$ is represented as follows:

$$\mathbf{C}_{2v\widetilde{\sigma}\widehat{I}} = \mathbf{C}_{\widehat{I}} + \sigma_{v(1)}\mathbf{C}_{\widehat{I}} + \sigma_{v(2)}\mathbf{C}_{\widehat{I}} + C_2\mathbf{C}_{\widehat{I}}, \tag{22}$$

which generates the coset representation $\mathbf{C}_{2v\widetilde{\sigma}\widehat{I}}(/\mathbf{C}_{\widehat{I}})$ for characterizing the four positions of the oxirane skeleton **2**, as collected in Table 1.

Because the subgroup $\mathbf{C}_{\widehat{I}}$ corresponds to the subgroup $\mathbf{C}''_s$ of the point group $\mathbf{D}_{2h}$ (the 7th row of Table 2), the coset decomposition (Eq. 22) corresponds to the following coset decomposition of $\mathbf{D}_{2h}$:

Table 3 Subduction of the coset representation $\mathbf{C}_{2v\widetilde{\sigma}\widehat{I}}(/\mathbf{C}_{\widehat{I}})$

j	$\acute{\mathbf{G}}_j$	Type	$\mathbf{C}_{2v\widetilde{\sigma}\widehat{I}}(/\mathbf{C}_{\widehat{I}}) \downarrow \acute{\mathbf{G}}_j$	USCI-CF
1	$\mathbf{C}_1$	III	$4\mathbf{C}_1(/\mathbf{C}_1)$	b_1^4
2	$\mathbf{C}_2$	III	$2\mathbf{C}_2(/\mathbf{C}_1)$	b_2^2
3	$\mathbf{C}_{\widetilde{\sigma}}$	II	$2\mathbf{C}_{\widetilde{\sigma}}(/\mathbf{C}_1)$	b_2^2
4	$\mathbf{C}'_{\widetilde{\sigma}}$	II	$2\mathbf{C}'_{\widetilde{\sigma}}(/\mathbf{C}_1)$	b_2^2
5	$\mathbf{C}_s$	V	$2\mathbf{C}_s(/\mathbf{C}_1)$	c_2^2
6	$\mathbf{C}'_s$	V	$2\mathbf{C}'_s(/\mathbf{C}_1)$	c_2^2
7	$\mathbf{C}_{\widehat{I}}$	I	$4\mathbf{C}_{\widehat{I}}(/\mathbf{C}_{\widehat{I}})$	a_1^4
8	$\mathbf{C}_{\widehat{\sigma}}$	I	$2\mathbf{C}_{\widehat{\sigma}}(/\mathbf{C}_1)$	c_2^2
9	$\mathbf{C}_{2v}$	V	$2\mathbf{C}_{2v}(/\mathbf{C}_1)$	c_4
10	$\mathbf{C}_{s\widetilde{\sigma}\widehat{I}}$	IV	$2\mathbf{C}_{s\widetilde{\sigma}\widehat{I}}(/\mathbf{C}_{\widehat{I}})$	a_2^2
11	$\mathbf{C}'_{s\widetilde{\sigma}\widehat{I}}$	IV	$2\mathbf{C}'_{s\widetilde{\sigma}\widehat{I}}(/\mathbf{C}_{\widehat{I}})$	a_2^2
12	$\mathbf{C}_{2\widehat{I}}$	I	$2\mathbf{C}_{2\widehat{I}}(/\mathbf{C}_{\widehat{I}})$	a_2^2
13	$\mathbf{C}_{s\widetilde{\sigma}\widehat{\sigma}}$	IV	$\mathbf{C}_{s\widetilde{\sigma}\widehat{\sigma}}(/\mathbf{C}_1)$	c_4
14	$\mathbf{C}'_{s\widetilde{\sigma}\widehat{\sigma}}$	IV	$\mathbf{C}'_{s\widetilde{\sigma}\widehat{\sigma}}(/\mathbf{C}_1)$	c_4
15	$\mathbf{C}_{2\widetilde{\sigma}}$	II	$\mathbf{C}_{2\widetilde{\sigma}}(/\mathbf{C}_1)$	b_4
16	$\mathbf{C}_{2v\widetilde{\sigma}\widehat{I}}$	IV	$\mathbf{C}_{2v\widetilde{\sigma}\widehat{I}}(/\mathbf{C}_{\widehat{I}})$	a_4

$$\mathbf{D}_{2h} = \mathbf{C}''_s + \sigma_{v(1)}\mathbf{C}''_s + \sigma_{v(2)}\mathbf{C}''_s + C_{2(3)}\mathbf{C}''_s. \tag{23}$$

It follows that the coset representation $\mathbf{D}_{2h}(/\mathbf{C}''_s)$ derived from Eq. 23 consists of an identical set of products of cycles with the coset representation $\mathbf{C}_{2v\widetilde{\sigma}\widehat{I}}(/\mathbf{C}_{\widehat{I}})$ derived from Eq. 22, as shown in Table 1.

The subduction of coset representations is a central concept of the USCI approach [23]. Because of the isomorphism between $\mathbf{D}_{2h}$ and $\mathbf{C}_{2v\widetilde{\sigma}\widehat{I}}$, the data of the subduction of $\mathbf{D}_{2h}(/\mathbf{C}''_s)$ (Table 1 of [54]) can be used to generate the counterpart data of $\mathbf{C}_{2v\widetilde{\sigma}\widehat{I}}(/\mathbf{C}_{\widehat{I}})$, as collected in Table 3. Note that the subduction $\mathbf{D}_{2h}(/\mathbf{C}''_s) \downarrow \mathbf{G}_j$ for $\mathbf{G}_j \in \mathrm{SSG}_{\mathbf{D}_{2h}}$ (Eq. 15) corresponds to the subduction $\mathbf{C}_{2v\widetilde{\sigma}\widehat{I}}(/\mathbf{C}_{\widehat{I}}) \downarrow \acute{\mathbf{G}}_j$ for $\acute{\mathbf{G}}_j \in \mathrm{SSG}_{\mathbf{C}_{2v\widetilde{\sigma}\widehat{I}}}$ (Eq. 16), where each subgroup $\acute{\mathbf{G}}_j$ corresponds to the subgroup $\mathbf{G}_j$ as shown in Table 2.

Subgroups of an *RS*-stereoisomeric group are categorized into ex-chiral or ex-achiral groups, where the prefix 'ex' is an abbreviation of the word 'extended' [47,48]. Thereby, a subgroup of type II or III is categorized to be ex-chiral (due to the absence of reflections and ligand reflections), while a subgroup of type I, IV, or V is categorized to be ex-achiral (due to the presence of reflections and ligand reflections). Then, the extended sphericity of a coset representation $\acute{\mathbf{G}}(/\acute{\mathbf{G}}_j)$ is defined as follows:

homospheric for an achiral $\acute{\mathbf{G}}$ and an achiral $\acute{\mathbf{G}}_j$,
enantiospheric for an achiral $\acute{\mathbf{G}}$ and a chiral $\acute{\mathbf{G}}_j$, and
hemispheric for a chiral $\acute{\mathbf{G}}$ and a chiral $\acute{\mathbf{G}}_j$,

which are characterized respectively by sphericity indices, a_d, c_d, and b_d ($d = |\acute{\mathbf{G}}|/|\acute{\mathbf{G}}_j|$), when the USCI approach [23] is applied in an extended fashion.

From the subduction data collected in the ($\mathbf{C}_{2v\tilde{\sigma}\hat{I}}(/\mathbf{C}_{\hat{I}}) \downarrow \acute{\mathbf{G}}_j$)-column of Table 3, the corresponding USCI-CF (unit subduced cycle index with chirality faithfulness) is calculated in a parallel way to the calculation of the USCI-CFs for the point group $\mathbf{D}_{2h}$ (cf. Table 1 of [54]). Each USCI-CF is a product of sphericity indices, which are assigned to the respective coset representations contained in the subduction data [23]. For example, the subduction $2\mathbf{C}_2(/\mathbf{C}_1)$ in the second row gives a USCI-CF b_2^2, because a sphericity index b_2 is assigned to each coset representation $\mathbf{C}_2(/\mathbf{C}_1)$, which is determined to be hemispheric and to have degree 2 ($|\mathbf{C}_2|/|\mathbf{C}_1| = 2/1 = 2$). The resulting USCI-CFs for the subduction $\mathbf{C}_{2v\tilde{\sigma}\hat{I}}(/\mathbf{C}_{\hat{I}}) \downarrow \acute{\mathbf{G}}_j$ are collected in the (UCSI-CF)-column of Table 3.

6 Combinatorial enumeration under the *RS*-stereoisomeric group $\mathbf{C}_{2v\tilde{\sigma}\hat{I}}$

6.1 The fixed-point matrix method of the USCI approach

Although the fixed-point matrix (FPM) method of the USCI approach has been originally developed for the purpose of itemized enumeration under the point groups [23], it can be applied to the present enumeration under the *RS*-stereoisomeric group $\mathbf{C}_{2v\tilde{\sigma}\hat{I}}$, where the original procedure [23] is useful by adopting extended sphericities described above. For an application of the FPM method to the *RS*-stereoisomeric group $\mathbf{T}_{d\tilde{\sigma}\hat{I}}$, see [47].

6.1.1 Fixed-point vectors for symmetry-itemized enumeration

According to Def. 19.3 of [23], each of the USCI-CFs collected in Table 3 can be used as a subduced cycle index with chirality fittingness (SCI-CF), because the four positions of the oxirane skeleton **2** construct a single orbit under the *RS*-stereoisomeric group $\mathbf{C}_{2v\tilde{\sigma}\hat{I}}$.

Suppose that substituents for the four positions of the oxirane skeleton **2** are selected from the proligand inventory represented by Eq. 1. Then, we use the following ligand-inventory functions (Lemma 19.2 of [23]):

$$a_d = \mathrm{A}^d + \mathrm{B}^d + \mathrm{X}^d + \mathrm{Y}^d \tag{24}$$

$$c_d = \mathrm{A}^d + \mathrm{B}^d + \mathrm{X}^d + \mathrm{Y}^d + 2\mathrm{p}^{d/2}\overline{\mathrm{p}}^{d/2} + 2\mathrm{q}^{d/2}\overline{\mathrm{q}}^{d/2} + 2\mathrm{r}^{d/2}\overline{\mathrm{r}}^{d/2} + 2\mathrm{s}^{d/2}\overline{\mathrm{s}}^{d/2} \tag{25}$$

$$b_d = \mathrm{A}^d + \mathrm{B}^d + \mathrm{X}^d + \mathrm{Y}^d + \mathrm{p}^d + \mathrm{q}^d + \mathrm{r}^d + \mathrm{s}^d + \overline{\mathrm{p}}^d + \overline{\mathrm{q}}^d + \overline{\mathrm{r}}^d + \overline{\mathrm{s}}^d. \tag{26}$$

These ligand-inventory functions are introduced into each SCI-CF (the same as the USCI-CF for the corresponding subgroup collected in Table 3) to give a generating function, which is a polynomial concerning A, B, X, Y, p, $\overline{\mathrm{p}}$, q, $\overline{\mathrm{q}}$, r, $\overline{\mathrm{r}}$, s, and $\overline{\mathrm{s}}$. The coefficient of the term $\mathrm{A}^a\mathrm{B}^b\mathrm{X}^x\mathrm{Y}^y\mathrm{p}^p\overline{\mathrm{p}}^{\overline{p}}\mathrm{q}^q\overline{\mathrm{q}}^{\overline{q}}\mathrm{r}^r\overline{\mathrm{r}}^{\overline{r}}\mathrm{s}^s\overline{\mathrm{q}}^{\overline{s}}$ in each generating function indicates the number of fixed promolecules to be counted. This term can be represented by the following partition:

$$[\theta] = [a, b, x, y;\ p, \overline{p}, q, \overline{q}, r, \overline{r}, s, \overline{s}], \tag{27}$$

where we put $a \geq b \geq x \geq y$, $p \geq \overline{p}$, $q \geq \overline{q}$, $r \geq \overline{r}$, $s \geq \overline{s}$, and $p \geq q \geq r \geq s$, because A, B, etc. appear symmetrically in general.

For the purpose of systematic enumeration of epoxides, the same partitions as adopted in the enumeration of tetrahedral promolecules [47] can be used as follows:

$$[\theta]_1 = [4, 0, 0, 0; 0, 0, 0, 0, 0, 0, 0, 0] \quad (\text{for } A^4 \text{ etc.}) \tag{28}$$
$$[\theta]_2 = [3, 1, 0, 0; 0, 0, 0, 0, 0, 0, 0, 0] \quad (\text{for } A^3B \text{ etc.}) \tag{29}$$
$$[\theta]_3 = [3, 0, 0, 0; 1, 0, 0, 0, 0, 0, 0, 0] \quad (\text{for } A^3p \text{ etc.}) \tag{30}$$
$$[\theta]_4 = [2, 2, 0, 0; 0, 0, 0, 0, 0, 0, 0, 0] \quad (\text{for } A^2B^2 \text{ etc.}) \tag{31}$$
$$[\theta]_5 = [2, 0, 0, 0; 2, 0, 0, 0, 0, 0, 0, 0] \quad (\text{for } A^2p^2 \text{ etc.}) \tag{32}$$
$$[\theta]_6 = [2, 1, 1, 0; 0, 0, 0, 0, 0, 0, 0, 0] \quad (\text{for } A^2BX \text{ etc.}) \tag{33}$$
$$[\theta]_7 = [2, 1, 0, 0; 1, 0, 0, 0, 0, 0, 0, 0] \quad (\text{for } A^2Bp \text{ etc.}) \tag{34}$$
$$[\theta]_8 = [2, 0, 0, 0; 1, 1, 0, 0, 0, 0, 0, 0] \quad (\text{for } A^2p\overline{p} \text{ etc.}) \tag{35}$$
$$[\theta]_9 = [2, 0, 0, 0; 1, 0, 1, 0, 0, 0, 0, 0] \quad (\text{for } A^2pq \text{ etc.}) \tag{36}$$
$$[\theta]_{10} = [1, 1, 1, 1; 0, 0, 0, 0, 0, 0, 0, 0] \quad (\text{for ABXY}) \tag{37}$$
$$[\theta]_{11} = [1, 1, 1, 0; 1, 0, 0, 0, 0, 0, 0, 0] \quad (\text{for ABXp etc.}) \tag{38}$$
$$[\theta]_{12} = [1, 1, 0, 0; 2, 0, 0, 0, 0, 0, 0, 0] \quad (\text{for } ABp^2 \text{ etc.}) \tag{39}$$
$$[\theta]_{13} = [1, 1, 0, 0; 1, 1, 0, 0, 0, 0, 0, 0] \quad (\text{for } ABp\overline{p} \text{ etc.}) \tag{40}$$
$$[\theta]_{14} = [1, 1, 0, 0; 1, 0, 1, 0, 0, 0, 0, 0] \quad (\text{for ABpq etc.}) \tag{41}$$
$$[\theta]_{15} = [1, 0, 0, 0; 3, 0, 0, 0, 0, 0, 0, 0] \quad (\text{for } Ap^3 \text{ etc.}) \tag{42}$$
$$[\theta]_{16} = [1, 0, 0, 0; 2, 1, 0, 0, 0, 0, 0, 0] \quad (\text{for } Ap^2\overline{p} \text{ etc.}) \tag{43}$$
$$[\theta]_{17} = [1, 0, 0, 0; 2, 0, 1, 0, 0, 0, 0, 0] \quad (\text{for } Ap^2q \text{ etc.}) \tag{44}$$
$$[\theta]_{18} = [1, 0, 0, 0; 1, 1, 1, 0, 0, 0, 0, 0] \quad (\text{for } Ap\overline{p}q \text{ etc.}) \tag{45}$$
$$[\theta]_{19} = [1, 0, 0, 0; 1, 0, 1, 0, 1, 0, 0, 0] \quad (\text{for Apqr etc.}) \tag{46}$$

In addition, partitions with no achiral proligands are listed as follows:

$$[\theta]_{20} = [0, 0, 0, 0; 4, 0, 0, 0, 0, 0, 0, 0] \quad (\text{for } p^4 \text{ etc.}) \tag{47}$$
$$[\theta]_{21} = [0, 0, 0, 0; 3, 1, 0, 0, 0, 0, 0, 0] \quad (\text{for } p^3\overline{p} \text{ etc.}) \tag{48}$$
$$[\theta]_{22} = [0, 0, 0, 0; 3, 0, 1, 0, 0, 0, 0, 0] \quad (\text{for } p^3q \text{ etc.}) \tag{49}$$
$$[\theta]_{23} = [0, 0, 0, 0; 2, 2, 0, 0, 0, 0, 0, 0] \quad (\text{for } p^2\overline{p}^2 \text{ etc.}) \tag{50}$$
$$[\theta]_{24} = [0, 0, 0, 0; 2, 1, 1, 0, 0, 0, 0, 0] \quad (\text{for } p^2\overline{p}q \text{ etc.}) \tag{51}$$
$$[\theta]_{25} = [0, 0, 0, 0; 2, 0, 2, 0, 0, 0, 0, 0] \quad (\text{for } p^2q^2 \text{ etc.}) \tag{52}$$
$$[\theta]_{26} = [0, 0, 0, 0; 2, 0, 1, 1, 0, 0, 0, 0] \quad (\text{for } p^2q\overline{q} \text{ etc.}) \tag{53}$$
$$[\theta]_{27} = [0, 0, 0, 0; 2, 0, 1, 0, 1, 0, 0, 0] \quad (\text{for } p^2qr \text{ etc.}) \tag{54}$$
$$[\theta]_{28} = [0, 0, 0, 0; 1, 1, 1, 1, 0, 0, 0, 0] \quad (\text{for } p\overline{p}q\overline{q} \text{ etc.}) \tag{55}$$
$$[\theta]_{29} = [0, 0, 0, 0; 1, 1, 1, 0, 1, 0, 0, 0] \quad (\text{for } p\overline{p}qr \text{ etc.}) \tag{56}$$

$$[\theta]_{30} = [0, 0, 0, 0; 1, 0, 1, 0, 1, 0, 1, 0] \quad \text{(for pqrs etc.)} \tag{57}$$

For example, the ligand-inventory functions (Eqs. 24–26) are introduced into the SCI-CF (USCI-CF) c_2^2 for $\mathbf{C}_{2v\tilde{\sigma}\hat{I}}(/\mathbf{C}_{\hat{I}}) \downarrow \mathbf{C}_s$ (the 5th row of Table 3). The resulting equation is expanded to give the following generating function:

$$\begin{aligned} g_{\mathbf{C}_s} &= (\mathrm{A}^2 + \mathrm{B}^2 + \mathrm{X}^2 + \mathrm{Y}^2 + 2\mathrm{p}\overline{\mathrm{p}} + 2\mathrm{q}\overline{\mathrm{q}} + 2\mathrm{r}\overline{\mathrm{r}} + 2\mathrm{s}\overline{\mathrm{s}})^2 \\ &= \{\mathrm{A}^4 + \mathrm{B}^4 + \mathrm{X}^4 + \mathrm{Y}^4\}_{[\theta]_1} + \{2\mathrm{A}^2\mathrm{B}^2 + 2\mathrm{A}^2\mathrm{X}^2 + \cdots\}_{[\theta]_4} \\ &\quad + \{4\mathrm{A}^2\mathrm{p}\overline{\mathrm{p}} + 4\mathrm{A}^2\mathrm{q}\overline{\mathrm{q}} + \cdots\}_{[\theta]_8} + \{4\mathrm{p}^2\overline{\mathrm{p}}^2 + 4\mathrm{p}^2\overline{\mathrm{q}}^2 + \cdots\}_{[\theta]_{23}} \\ &\quad + \{8\mathrm{p}\overline{\mathrm{p}}\mathrm{q}\overline{\mathrm{q}} + 8\mathrm{p}\overline{\mathrm{p}}\mathrm{r}\overline{\mathrm{r}} + \cdots\}_{[\theta]_{28}} \end{aligned} \tag{58}$$

where a partition selected form $[\theta]_i$ (i = 1–30) is attached to each pair of braces. Let the symbol $\rho_{[\theta]_i\acute{\mathbf{G}}_j}$ be the number of fixed points (fixed promolecule), which appears as the coefficient of the term corresponding to $[\theta]_i$ (i = 1–30) and $\acute{\mathbf{G}}_j$ ($\subset \mathbf{D}_{2d\tilde{\sigma}\hat{I}}$). The terms in the right-hand side of Eq. 58 give the following values:

$$\rho_{[\theta]_1\mathbf{C}_s} = 1,\ \rho_{[\theta]_4\mathbf{C}_s} = 2,\ \rho_{[\theta]_8\mathbf{C}_s} = 4,\ \rho_{[\theta]_{23}\mathbf{C}_s} = 4,\ \rho_{[\theta]_{28}\mathbf{C}_s} = 8, \tag{59}$$

where the remaining values are equal to zero, i.e., $\rho_{[\theta]_i\mathbf{C}_s} = 0$. By examining all of the subgroups collected Table 3, the USCI-CFs are treated similarly so as to give $\rho_{[\theta]_i\acute{\mathbf{G}}_j}$ for $\acute{\mathbf{G}}_j$ ($\in \mathrm{SSG}_{\mathbf{D}_{2d\tilde{\sigma}\hat{I}}}$) and for $[\theta]_i$ (i = 1–30). The resulting values of $\rho_{[\theta]_i\acute{\mathbf{G}}_j}$ are collected to give a fixed-point matrix (FPM) as a 30 × 16 matrix, where the 19 × 16 part (FPM_1) concerning achiral and chiral proligands is represented as follows:

$$\mathrm{FPM}_1 = \begin{array}{c} [\theta]_1 \\ [\theta]_2 \\ [\theta]_3 \\ [\theta]_4 \\ [\theta]_5 \\ [\theta]_6 \\ [\theta]_7 \\ [\theta]_8 \\ [\theta]_9 \\ [\theta]_{10} \\ [\theta]_{11} \\ [\theta]_{12} \\ [\theta]_{13} \\ [\theta]_{14} \\ [\theta]_{15} \\ [\theta]_{16} \\ [\theta]_{17} \\ [\theta]_{18} \\ [\theta]_{19} \end{array} \begin{pmatrix} 1 & 1 & 1 & 1 & 1 & 1 & 1 & 1 & 1 & 1 & 1 & 1 & 1 & 1 & 1 & 1 \\ 4 & 0 & 0 & 0 & 0 & 0 & 4 & 0 & 0 & 0 & 0 & 0 & 0 & 0 & 0 & 0 \\ 4 & 0 & 0 & 0 & 0 & 0 & 0 & 0 & 0 & 0 & 0 & 0 & 0 & 0 & 0 & 0 \\ 6 & 2 & 2 & 2 & 2 & 2 & 6 & 2 & 0 & 2 & 2 & 2 & 0 & 0 & 0 & 0 \\ 6 & 2 & 2 & 2 & 0 & 0 & 0 & 0 & 0 & 0 & 0 & 0 & 0 & 0 & 0 & 0 \\ 12 & 0 & 0 & 0 & 0 & 0 & 12 & 0 & 0 & 0 & 0 & 0 & 0 & 0 & 0 & 0 \\ 12 & 0 & 0 & 0 & 0 & 0 & 0 & 0 & 0 & 0 & 0 & 0 & 0 & 0 & 0 & 0 \\ 12 & 0 & 0 & 0 & 4 & 4 & 0 & 4 & 0 & 0 & 0 & 0 & 0 & 0 & 0 & 0 \\ 12 & 0 & 0 & 0 & 0 & 0 & 0 & 0 & 0 & 0 & 0 & 0 & 0 & 0 & 0 & 0 \\ 24 & 0 & 0 & 0 & 0 & 0 & 24 & 0 & 0 & 0 & 0 & 0 & 0 & 0 & 0 & 0 \\ 24 & 0 & 0 & 0 & 0 & 0 & 0 & 0 & 0 & 0 & 0 & 0 & 0 & 0 & 0 & 0 \\ 12 & 0 & 0 & 0 & 0 & 0 & 0 & 0 & 0 & 0 & 0 & 0 & 0 & 0 & 0 & 0 \\ 24 & 0 & 0 & 0 & 0 & 0 & 0 & 0 & 0 & 0 & 0 & 0 & 0 & 0 & 0 & 0 \\ 24 & 0 & 0 & 0 & 0 & 0 & 0 & 0 & 0 & 0 & 0 & 0 & 0 & 0 & 0 & 0 \\ 4 & 0 & 0 & 0 & 0 & 0 & 0 & 0 & 0 & 0 & 0 & 0 & 0 & 0 & 0 & 0 \\ 12 & 0 & 0 & 0 & 0 & 0 & 0 & 0 & 0 & 0 & 0 & 0 & 0 & 0 & 0 & 0 \\ 12 & 0 & 0 & 0 & 0 & 0 & 0 & 0 & 0 & 0 & 0 & 0 & 0 & 0 & 0 & 0 \\ 24 & 0 & 0 & 0 & 0 & 0 & 0 & 0 & 0 & 0 & 0 & 0 & 0 & 0 & 0 & 0 \\ 24 & 0 & 0 & 0 & 0 & 0 & 0 & 0 & 0 & 0 & 0 & 0 & 0 & 0 & 0 & 0 \end{pmatrix} \tag{60}$$

and the 11 × 16 part (FPM_2) concerning chiral proligands only is represented as follows:

$$\mathrm{FPM}_2 = \begin{array}{c} [\theta]_{20} \\ [\theta]_{21} \\ [\theta]_{22} \\ [\theta]_{23} \\ [\theta]_{24} \\ [\theta]_{25} \\ [\theta]_{26} \\ [\theta]_{27} \\ [\theta]_{28} \\ [\theta]_{29} \\ [\theta]_{30} \end{array} \begin{pmatrix} 1 & 1 & 1 & 1 & 0 & 0 & 0 & 0 & 0 & 0 & 0 & 0 & 0 & 0 & 1 & 0 \\ 4 & 0 & 0 & 0 & 0 & 0 & 0 & 0 & 0 & 0 & 0 & 0 & 0 & 0 & 0 & 0 \\ 4 & 0 & 0 & 0 & 0 & 0 & 0 & 0 & 0 & 0 & 0 & 0 & 0 & 0 & 0 & 0 \\ 6 & 2 & 2 & 2 & 4 & 4 & 0 & 4 & 2 & 0 & 0 & 0 & 2 & 2 & 0 & 0 \\ 12 & 0 & 0 & 0 & 0 & 0 & 0 & 0 & 0 & 0 & 0 & 0 & 0 & 0 & 0 & 0 \\ 6 & 2 & 2 & 2 & 0 & 0 & 0 & 0 & 0 & 0 & 0 & 0 & 0 & 0 & 0 & 0 \\ 12 & 0 & 0 & 0 & 0 & 0 & 0 & 0 & 0 & 0 & 0 & 0 & 0 & 0 & 0 & 0 \\ 12 & 0 & 0 & 0 & 0 & 0 & 0 & 0 & 0 & 0 & 0 & 0 & 0 & 0 & 0 & 0 \\ 24 & 0 & 0 & 0 & 8 & 8 & 0 & 8 & 0 & 0 & 0 & 0 & 0 & 0 & 0 & 0 \\ 24 & 0 & 0 & 0 & 0 & 0 & 0 & 0 & 0 & 0 & 0 & 0 & 0 & 0 & 0 & 0 \\ 24 & 0 & 0 & 0 & 0 & 0 & 0 & 0 & 0 & 0 & 0 & 0 & 0 & 0 & 0 & 0 \end{pmatrix}. \quad (61)$$

The respective columns in FPM_1 and FPM_2 are aligned in accord with the $SSG_{\mathbf{C}_{2v\tilde{\sigma}\hat{I}}}$ (Eq. 16). The number of fixed points (fixed promolecule), i.e., $\rho_{[\theta]_i \acute{\mathbf{G}}_j}$, appears as the $([\theta]_i, j)$-element of FPM_1 or FPM_2 at the intersection between the $[\theta]_i$-row and the $\acute{\mathbf{G}}_j$-column. Note that the values shown in Eq. 59 appear in the 5th ($\mathbf{C}_s$) columns of FPM_1 (in the $[\theta]_1$-, $[\theta]_4$-, and $[\theta]_8$-row) and FPM_2 (in the $[\theta]_{23}$- and $[\theta]_{28}$-row). As for the $SSG_{\mathbf{C}_{2v\tilde{\sigma}\hat{I}}}$ indicating the columns of FPM_1 and FPM_2, see Eq. 16. As for the partitions indicating the rows of FPM_1 and FPM_2, see Eqs. 28–57.

The calculations of FPM_1 and FPM_2 are conducted by the Maple system after writing a Maple program in a similar way to the enumeration under point groups, which was based on the original FPM method of the USCI approach [44].

The inverse mark table $M^{-1}_{\mathbf{C}_{2v\tilde{\sigma}\hat{I}}}$ is calculated by starting from the mark table $M_{\mathbf{C}_{2v\tilde{\sigma}\hat{I}}}$, which is identical with the mark table $M_{\mathbf{D}_{2h}}$ reported previously in [53,54]. Thus, we obtain:

$$M^{-1}_{\mathbf{C}_{2v\tilde{\sigma}\hat{I}}} = M^{-1}_{\mathbf{D}_{2h}} = (\overline{m}_{ji}) = \begin{pmatrix} 1/8 & 0 & 0 & 0 & 0 & 0 & 0 & 0 & 0 & 0 & 0 & 0 & 0 & 0 & 0 & 0 \\ -1/8 & 1/4 & 0 & 0 & 0 & 0 & 0 & 0 & 0 & 0 & 0 & 0 & 0 & 0 & 0 & 0 \\ -1/8 & 0 & 1/4 & 0 & 0 & 0 & 0 & 0 & 0 & 0 & 0 & 0 & 0 & 0 & 0 & 0 \\ -1/8 & 0 & 0 & 1/4 & 0 & 0 & 0 & 0 & 0 & 0 & 0 & 0 & 0 & 0 & 0 & 0 \\ -1/8 & 0 & 0 & 0 & 1/4 & 0 & 0 & 0 & 0 & 0 & 0 & 0 & 0 & 0 & 0 & 0 \\ -1/8 & 0 & 0 & 0 & 0 & 1/4 & 0 & 0 & 0 & 0 & 0 & 0 & 0 & 0 & 0 & 0 \\ -1/8 & 0 & 0 & 0 & 0 & 0 & 1/4 & 0 & 0 & 0 & 0 & 0 & 0 & 0 & 0 & 0 \\ -1/8 & 0 & 0 & 0 & 0 & 0 & 0 & 1/4 & 0 & 0 & 0 & 0 & 0 & 0 & 0 & 0 \\ 1/4 & -1/4 & 0 & 0 & -1/4 & -1/4 & 0 & 0 & 1/2 & 0 & 0 & 0 & 0 & 0 & 0 & 0 \\ 1/4 & 0 & -1/4 & 0 & -1/4 & 0 & -1/4 & 0 & 0 & 1/2 & 0 & 0 & 0 & 0 & 0 & 0 \\ 1/4 & 0 & 0 & -1/4 & 0 & -1/4 & -1/4 & 0 & 0 & 0 & 1/2 & 0 & 0 & 0 & 0 & 0 \\ 1/4 & -1/4 & 0 & 0 & 0 & 0 & -1/4 & -1/4 & 0 & 0 & 0 & 1/2 & 0 & 0 & 0 & 0 \\ 1/4 & 0 & -1/4 & 0 & 0 & -1/4 & 0 & -1/4 & 0 & 0 & 0 & 0 & 1/2 & 0 & 0 & 0 \\ 1/4 & 0 & 0 & -1/4 & -1/4 & 0 & 0 & -1/4 & 0 & 0 & 0 & 0 & 0 & 1/2 & 0 & 0 \\ 1/4 & -1/4 & -1/4 & -1/4 & 0 & 0 & 0 & 0 & 0 & 0 & 0 & 0 & 0 & 0 & 1/2 & 0 \\ -1 & 1/2 & 1/2 & 1/2 & 1/2 & 1/2 & 1/2 & 1/2 & -1/2 & -1/2 & -1/2 & -1/2 & -1/2 & -1/2 & -1/2 & 1 \end{pmatrix} \quad (62)$$

According to Theorem 19.4 (coupled with Theorem 15.4) in [23], the FPMs are multiplied by the inverse $M^{-1}_{\mathbf{C}_{2v\tilde{\sigma}\hat{I}}}$ to give the following isomer-counting matrices (ICMs):

$$\mathrm{ICM}_1 = \mathrm{FPM}_1 \times M^{-1}_{\mathbf{C}_{2v\tilde{\sigma}\hat{I}}} = \begin{array}{c} \\ [\theta]_1 \\ [\theta]_2 \\ [\theta]_3 \\ [\theta]_4 \\ [\theta]_5 \\ [\theta]_6 \\ [\theta]_7 \\ [\theta]_8 \\ [\theta]_9 \\ [\theta]_{10} \\ [\theta]_{11} \\ [\theta]_{12} \\ [\theta]_{13} \\ [\theta]_{14} \\ [\theta]_{15} \\ [\theta]_{16} \\ [\theta]_{17} \\ [\theta]_{18} \\ [\theta]_{19} \end{array} \begin{pmatrix} 0 & 0 & 0 & 0 & 0\,0\,0\,0\,0\,0\,0\,0\,0\,0\,0 & 1 \\ 0 & 0 & 0 & 0 & 0\,0\,1\,0\,0\,0\,0\,0\,0\,0\,0 & 0 \\ 1/2 & 0 & 0 & 0 & 0\,0\,0\,0\,0\,0\,0\,0\,0\,0\,0 & 0 \\ 0 & 0 & 0 & 0 & 0\,0\,0\,0\,0\,1\,1\,1\,0\,0\,0 & 0 \\ 0 & 1/2 & 1/2 & 1/2 & 0\,0\,0\,0\,0\,0\,0\,0\,0\,0\,0 & 0 \\ 0 & 0 & 0 & 0 & 0\,0\,3\,0\,0\,0\,0\,0\,0\,0\,0 & 0 \\ 3/2 & 0 & 0 & 0 & 0\,0\,0\,0\,0\,0\,0\,0\,0\,0\,0 & 0 \\ 0 & 0 & 0 & 0 & 1\,1\,0\,1\,0\,0\,0\,0\,0\,0\,0 & 0 \\ 3/2 & 0 & 0 & 0 & 0\,0\,0\,0\,0\,0\,0\,0\,0\,0\,0 & 0 \\ 0 & 0 & 0 & 0 & 0\,0\,6\,0\,0\,0\,0\,0\,0\,0\,0 & 0 \\ 3 & 0 & 0 & 0 & 0\,0\,0\,0\,0\,0\,0\,0\,0\,0\,0 & 0 \\ 3/2 & 0 & 0 & 0 & 0\,0\,0\,0\,0\,0\,0\,0\,0\,0\,0 & 0 \\ 3 & 0 & 0 & 0 & 0\,0\,0\,0\,0\,0\,0\,0\,0\,0\,0 & 0 \\ 3 & 0 & 0 & 0 & 0\,0\,0\,0\,0\,0\,0\,0\,0\,0\,0 & 0 \\ 1/2 & 0 & 0 & 0 & 0\,0\,0\,0\,0\,0\,0\,0\,0\,0\,0 & 0 \\ 3/2 & 0 & 0 & 0 & 0\,0\,0\,0\,0\,0\,0\,0\,0\,0\,0 & 0 \\ 3/2 & 0 & 0 & 0 & 0\,0\,0\,0\,0\,0\,0\,0\,0\,0\,0 & 0 \\ 3 & 0 & 0 & 0 & 0\,0\,0\,0\,0\,0\,0\,0\,0\,0\,0 & 0 \\ 3 & 0 & 0 & 0 & 0\,0\,0\,0\,0\,0\,0\,0\,0\,0\,0 & 0 \end{pmatrix} \tag{63}$$

$$\mathrm{ICM}_2 = \mathrm{FPM}_2 \times M^{-1}_{\mathbf{C}_{2v\tilde{\sigma}\hat{I}}} = \begin{array}{c} \\ [\theta]_{20} \\ [\theta]_{21} \\ [\theta]_{22} \\ [\theta]_{23} \\ [\theta]_{24} \\ [\theta]_{25} \\ [\theta]_{26} \\ [\theta]_{27} \\ [\theta]_{28} \\ [\theta]_{29} \\ [\theta]_{30} \end{array} \begin{pmatrix} 0 & 0 & 0 & 0 & 0\,0\,0\,0\,0\,0\,0\,0\,0\,0\,0 & 1/2 & 0 \\ 1/2 & 0 & 0 & 0 & 0\,0\,0\,0\,0\,0\,0\,0\,0\,0\,0 & 0 & 0 \\ 1/2 & 0 & 0 & 0 & 0\,0\,0\,0\,0\,0\,0\,0\,0\,0\,0 & 0 & 0 \\ 0 & 0 & 0 & 0 & 0\,0\,0\,0\,1\,0\,0\,0\,1\,1 & 0 & 0 \\ 3/2 & 0 & 0 & 0 & 0\,0\,0\,0\,0\,0\,0\,0\,0\,0\,0 & 0 & 0 \\ 0 & 1/2 & 1/2 & 1/2 & 0\,0\,0\,0\,0\,0\,0\,0\,0\,0\,0 & 0 & 0 \\ 3/2 & 0 & 0 & 0 & 0\,0\,0\,0\,0\,0\,0\,0\,0\,0\,0 & 0 & 0 \\ 3/2 & 0 & 0 & 0 & 0\,0\,0\,0\,0\,0\,0\,0\,0\,0\,0 & 0 & 0 \\ 0 & 0 & 0 & 0 & 2\,2\,0\,2\,0\,0\,0\,0\,0\,0 & 0 & 0 \\ 3 & 0 & 0 & 0 & 0\,0\,0\,0\,0\,0\,0\,0\,0\,0\,0 & 0 & 0 \\ 3 & 0 & 0 & 0 & 0\,0\,0\,0\,0\,0\,0\,0\,0\,0\,0 & 0 & 0 \end{pmatrix} \tag{64}$$

The $([\theta]_i, j)$-element of ICM_1 (Eq. 63) or ICM_2 (Eq. 64) represents the number of quadruplets with the partition $[\theta]_i$ ($i = 1$–30) and the *RS*-stereoisomeric subgroup $\acute{\mathbf{G}}_j$ ($\in \mathrm{SSG}_{\mathbf{C}_{2v\tilde{\sigma}\hat{I}}}$, Eq. 16):

1. For example, the value 1/2 at the intersection between the $[\theta]_3$-row and the first column ($\mathbf{C}_1$-column) stems from the term $\frac{1}{2}(\mathrm{A}^3\mathrm{p} + \mathrm{A}^3\overline{\mathrm{p}})$ (or other $[\theta]_3$-terms), which indicates the presence of one quadruplet of promolecules with the composition $\mathrm{A}^3\mathrm{p}$ (or $\mathrm{A}^3\overline{\mathrm{p}}$).
2. The value 3/2 at the intersection between the $[\theta]_7$-row and the first column ($\mathbf{C}_1$-column) stems from the term $\frac{3}{2}(\mathrm{A}^2\mathrm{Bp} + \mathrm{A}^2\mathrm{B}\overline{\mathrm{p}})$ (or other $[\theta]_7$-terms), which is

interpreted to be $3 \times \frac{1}{2}(\mathrm{A}^2\mathrm{Bp} + \mathrm{AB}\overline{\mathrm{p}})$. This means the presence of three quadruplets of promolecules with the composition $\mathrm{A}^2\mathrm{Bp}$ (or $\mathrm{A}^2\mathrm{B}\overline{\mathrm{p}}$).

3. The value 3 at the intersection between the $[\theta]_{30}$-row and the first column ($\mathbf{C}_1$-column) stems from the term $3(\mathrm{pqrs} + \overline{\mathrm{pqrs}})$, which is interpreted to be $6 \times \frac{1}{2}(\mathrm{pqrs} + \overline{\mathrm{pqrs}})$. This means the presence of six quadruplets of promolecules with the composition pqrs (or $\overline{\mathrm{pqrs}}$).
4. On the other hand, The value 1 at the intersection between the $[\theta]_2$-row and the 7-th column ($\mathbf{C}_{\widehat{I}}$-column) stems from the term $\mathrm{A}^3\mathrm{B}$ (or other $[\theta]_2$-terms), which indicates the presence of one quadruplet of promolecules with the composition $\mathrm{A}^3\mathrm{B}$. Note that the $\mathbf{C}_{\widehat{I}}$-promolecule in this quadruplet belongs to a type-I stereoisogram (chiral, *RS*-stereogenic, and ascleral).

6.2 The partial-cycle-index method of the USCI approach

The partial-cycle-index (PCI) method of the USCI approach, which has been originally developed for the purpose of itemized enumeration under the point groups [23], can be applied to the present enumeration under the *RS*-stereoisomeric group $\mathbf{C}_{2v\widetilde{\sigma}\widehat{I}}$. For an application of the PCI method to the *RS*-stereoisomeric group $\mathbf{T}_{d\widetilde{\sigma}\widehat{I}}$, see [48].

6.2.1 Partial cycle indices with chirality fittingness (PCI-CFs)

According to the USCI approach [23], the USCI-CFs listed in Table 3 are regarded as subduced-cycle-indices (SCI-CFs) and collected to form a row vector:

$$\begin{aligned}&\text{SCI-CF}_{\mathbf{C}_{2v\widetilde{\sigma}\widehat{I}}(/\mathbf{C}_{\widehat{I}})}\\ &= \left(b_1^4, b_2^2, b_2^2, b_2^2, c_2^2, c_2^2, a_1^4, c_2^2, c_4, a_2^2, a_2^2, a_2^2, c_4, c_4, b_4, a_4\right)\end{aligned} \tag{65}$$

PCI-CFs for enumerating quadruplets are calculated by using the $\text{SCI-CF}_{\mathbf{C}_{2v\widetilde{\sigma}\widehat{I}}(/\mathbf{C}_{\widehat{I}})}$ (Eq. 65) according to Def. 19.6 of [23]. The row vector (Eq. 65) is multiplied by the inverse mark table $M^{-1}_{\mathbf{C}_{2v\widetilde{\sigma}\widehat{I}}}$ (Eq. 62) as follows:

$$\text{SCI-CF}_{\mathbf{C}_{2v\widetilde{\sigma}\widehat{I}}(/\mathbf{C}_{\widehat{I}})} \times M^{-1}_{\mathbf{C}_{2v\widetilde{\sigma}\widehat{I}}} = \left(\text{PCI-CF}(\mathbf{C}_1), \ldots, \text{PCI-CF}(\acute{\mathbf{G}}_j), \ldots, \text{PCI-CF}(\mathbf{C}_{2v\widetilde{\sigma}\widehat{I}})\right), \tag{66}$$

where $\acute{\mathbf{G}}_j$ runs to cover the $\text{SSG}_{\mathbf{C}_{2v\widetilde{\sigma}\widehat{I}}}$ (Eq. 16). The j-th component $\text{PCI-CF}(\acute{\mathbf{G}}_j)$ of Eq. 66 can be regarded as a polynomial, which is the PCI-CF for the subgroup $\acute{\mathbf{G}}_j$ ($\in \text{SSG}_{\mathbf{C}_{2v\widetilde{\sigma}\widehat{I}}}$):

$$\text{PCI-CF}(\mathbf{C}_1) \underset{\text{III}}{\overset{1}{=}} \frac{1}{8}b_1^4 - \frac{1}{8}a_1^4 - \frac{3}{8}b_2^2 + \frac{3}{4}a_2^2 - \frac{3}{8}c_2^2 + \frac{3}{4}c_4 + \frac{1}{4}b_4 - a_4 \tag{67}$$

$$\text{PCI-CF}(\mathbf{C}_2) \underset{\text{III}}{\overset{2}{=}} \frac{1}{4}b_2^2 - \frac{1}{4}a_2^2 - \frac{1}{4}c_4 - \frac{1}{4}b_4 + \frac{1}{2}a_4 \tag{68}$$

$$\text{PCI-CF}(\mathbf{C}_{\widetilde{\sigma}}) \underset{\text{II}}{\overset{3}{=}} \frac{1}{4}b_2^2 - \frac{1}{4}a_2^2 - \frac{1}{4}c_4 - \frac{1}{4}b_4 + \frac{1}{2}a_4 \tag{69}$$

$$\mathrm{PCI\text{-}CF}(\mathbf{C}'_{\widetilde{\sigma}}) \underset{\mathrm{II}}{\overset{4}{=}} \frac{1}{4}b_2^2 - \frac{1}{4}a_2^2 - \frac{1}{4}c_4 - \frac{1}{4}b_4 + \frac{1}{2}a_4 \tag{70}$$

$$\mathrm{PCI\text{-}CF}(\mathbf{C}_s) \underset{\mathrm{V}}{\overset{5}{=}} -\frac{1}{4}a_2^2 + \frac{1}{4}c_2^2 - \frac{1}{2}c_4 + \frac{1}{2}a_4 \tag{71}$$

$$\mathrm{PCI\text{-}CF}(\mathbf{C}'_s) \underset{\mathrm{V}}{\overset{6}{=}} -\frac{1}{4}a_2^2 + \frac{1}{4}c_2^2 - \frac{1}{2}c_4 + \frac{1}{2}a_4 \tag{72}$$

$$\mathrm{PCI\text{-}CF}(\mathbf{C}_{\widehat{I}}) \underset{\mathrm{I}}{\overset{7}{=}} \frac{1}{4}a_1^4 - \frac{3}{4}a_2^2 + \frac{1}{2}a_4 \tag{73}$$

$$\mathrm{PCI\text{-}CF}(\mathbf{C}_{\widehat{\sigma}}) \underset{\mathrm{I}}{\overset{8}{=}} -\frac{1}{4}a_2^2 + \frac{1}{4}c_2^2 - \frac{1}{2}c_4 + \frac{1}{2}a_4 \tag{74}$$

$$\mathrm{PCI\text{-}CF}(\mathbf{C}_{2v}) \underset{\mathrm{V}}{\overset{9}{=}} \frac{1}{2}c_4 - \frac{1}{2}a_4 \tag{75}$$

$$\mathrm{PCI\text{-}CF}(\mathbf{C}_{s\widetilde{\sigma}\widehat{I}}) \underset{\mathrm{IV}}{\overset{10}{=}} \frac{1}{2}a_2^2 - \frac{1}{2}a_4 \tag{76}$$

$$\mathrm{PCI\text{-}CF}(\mathbf{C}'_{s\widetilde{\sigma}\widehat{I}}) \underset{\mathrm{IV}}{\overset{11}{=}} \frac{1}{2}a_2^2 - \frac{1}{2}a_4 \tag{77}$$

$$\mathrm{PCI\text{-}CF}(\mathbf{C}_{2\widehat{I}}) \underset{\mathrm{I}}{\overset{12}{=}} \frac{1}{2}a_2^2 - \frac{1}{2}a_4 \tag{78}$$

$$\mathrm{PCI\text{-}CF}(\mathbf{C}_{s\widetilde{\sigma}\widehat{\sigma}}) \underset{\mathrm{IV}}{\overset{13}{=}} \frac{1}{2}c_4 - \frac{1}{2}a_4 \tag{79}$$

$$\mathrm{PCI\text{-}CF}(\mathbf{C}'_{s\widetilde{\sigma}\widehat{\sigma}}) \underset{\mathrm{IV}}{\overset{14}{=}} \frac{1}{2}c_4 - \frac{1}{2}a_4 \tag{80}$$

$$\mathrm{PCI\text{-}CF}(\mathbf{C}_{2\widetilde{\sigma}}) \underset{\mathrm{II}}{\overset{15}{=}} \frac{1}{2}b_4 - \frac{1}{2}a_4 \tag{81}$$

$$\mathrm{PCI\text{-}CF}(\mathbf{C}_{2v\widetilde{\sigma}\widehat{I}}) \underset{\mathrm{IV}}{\overset{16}{=}} a_4 \tag{82}$$

Note that a Roman numeral below each equality symbol represents the stereoisogram type at issue (types I–V), as categorized in Table 3.

6.2.2 Generating functions for symmetry-itemized enumeration

According to the USCI approach (Theorem 19.6 of [23]), the ligand-inventory functions (Eqs. 24–26) are introduced into the PCI-CFs (Eqs. 67–82). Thereby, the generating functions $f_{\hat{\mathbf{G}}_j}$ for the subgroup $\hat{\mathbf{G}}_j \in \mathrm{SSG}_{\mathbf{C}_{2v\widetilde{\sigma}\widehat{I}}}$ (Eq. 16) are obtained as follows:

$$\begin{aligned} f_{\mathbf{C}_1} \underset{\mathrm{III}}{\overset{1}{=}} & \left\{\frac{1}{2}(\mathrm{A}^3\mathrm{p} + \mathrm{A}^3\overline{\mathrm{p}}) + \cdots\right\}_{[\theta]_3} + \left\{\frac{3}{2}(\mathrm{A}^2\mathrm{Bp} + \mathrm{A}^2\mathrm{B}\overline{\mathrm{p}}) + \cdots\right\}_{[\theta]_7} \\ & + \left\{\frac{3}{2}(\mathrm{A}^2\mathrm{pq} + \mathrm{A}^2\overline{\mathrm{pq}}) + \cdots\right\}_{[\theta]_9} + \{3(\mathrm{ABXp} + \mathrm{ABX}\overline{\mathrm{p}}) + \cdots\}_{[\theta]_{11}} \\ & + \{3\mathrm{ABp}\overline{\mathrm{p}} + \cdots\}_{[\theta]_{13}} + \left\{\frac{3}{2}(\mathrm{ABp}^2 + \mathrm{AB}\overline{\mathrm{p}}^2) + \cdots\right\}_{[\theta]_{12}} \end{aligned}$$

$$
\begin{aligned}
&+\{3(\mathrm{ABpq}+\mathrm{AB}\overline{\mathrm{pq}})+\cdots\}_{[\theta]_{14}}+\left\{\frac{3}{2}(\mathrm{Ap}^2\overline{\mathrm{p}}+\mathrm{Ap}\overline{\mathrm{p}}^2)+\cdots\right\}_{[\theta]_{16}}\\
&+\left\{\frac{3}{2}(\mathrm{Ap}^2\mathrm{q}+\mathrm{A}\overline{\mathrm{p}}^2\overline{\mathrm{q}})+\cdots\right\}_{[\theta]_{17}}+\left\{\frac{1}{2}(\mathrm{Ap}^3+\mathrm{A}\overline{\mathrm{p}}^3)+\cdots\right\}_{[\theta]_{15}}\\
&+\{3(\mathrm{Ap}\overline{\mathrm{p}}\mathrm{q}+\mathrm{Ap}\overline{\mathrm{pq}})+\cdots\}_{[\theta]_{18}}+\{3(\mathrm{Apqr}+\mathrm{A}\overline{\mathrm{pqr}})+\cdots\}_{[\theta]_{19}}\\
&+\left\{\frac{1}{2}(\mathrm{p}^3\overline{\mathrm{p}}+\mathrm{p}\overline{\mathrm{p}}^3)+\cdots\right\}_{[\theta]_{21}}+\left\{\frac{1}{2}(\mathrm{p}^3\mathrm{q}+\overline{\mathrm{p}}^3\overline{\mathrm{q}})+\cdots\right\}_{[\theta]_{22}}\\
&+\left\{\frac{3}{2}(\mathrm{p}^2\overline{\mathrm{p}}\mathrm{q}+\mathrm{p}\overline{\mathrm{p}}^2\overline{\mathrm{q}})+\cdots\right\}_{[\theta]_{24}}+\left\{\frac{3}{2}(\mathrm{p}^2\mathrm{q}\overline{\mathrm{q}}+\overline{\mathrm{p}}^2\mathrm{q}\overline{\mathrm{q}})+\cdots\right\}_{[\theta]_{26}}\\
&+\left\{\frac{3}{2}(\mathrm{p}^2\mathrm{qr}+\overline{\mathrm{p}}^2\overline{\mathrm{qr}})+\cdots\right\}_{[\theta]_{27}}+\{3(\mathrm{p}\overline{\mathrm{p}}\mathrm{qr}+\mathrm{p}\overline{\mathrm{pqr}})+\cdots\}_{[\theta]_{29}}\\
&+\{3(\mathrm{pqrs}+\overline{\mathrm{pqrs}})+\cdots\}_{[\theta]_{30}}
\end{aligned}
\tag{83}
$$

$$f_{\mathbf{C}_2}\overset{2}{\underset{\mathrm{III}}{=}}\left\{\frac{1}{2}(\mathrm{A}^2\mathrm{p}^2+\mathrm{A}^2\overline{\mathrm{p}}^2)+\cdots\right\}_{[\theta]_5}+\left\{\frac{1}{2}(\mathrm{p}^2\mathrm{q}^2+\overline{\mathrm{p}}^2\overline{\mathrm{q}}^2)+\cdots\right\}_{[\theta]_{25}} \tag{84}$$

$$f_{\mathbf{C}_{\tilde{\sigma}}}\overset{3}{\underset{\mathrm{II}}{=}}\left\{\frac{1}{2}(\mathrm{A}^2\mathrm{p}^2+\mathrm{A}^2\overline{\mathrm{p}}^2)+\cdots\right\}_{[\theta]_5}+\left\{\frac{1}{2}(\mathrm{p}^2\mathrm{q}^2+\overline{\mathrm{p}}^2\overline{\mathrm{q}}^2)+\cdots\right\}_{[\theta]_{25}} \tag{85}$$

$$f_{\mathbf{C}_{\tilde{\sigma}'}}\overset{4}{\underset{\mathrm{II}}{=}}\left\{\frac{1}{2}(\mathrm{A}^2\mathrm{p}^2+\mathrm{A}^2\overline{\mathrm{p}}^2)+\cdots\right\}_{[\theta]_5}+\left\{\frac{1}{2}(\mathrm{p}^2\mathrm{q}^2+\overline{\mathrm{p}}^2\overline{\mathrm{q}}^2)+\cdots\right\}_{[\theta]_{25}} \tag{86}$$

$$f_{\mathbf{C}_s}\overset{5}{\underset{\mathrm{V}}{=}}\left\{(\mathrm{A}^2\mathrm{p}\overline{\mathrm{p}})+\cdots\right\}_{[\theta]_8}+\{2(\mathrm{p}\overline{\mathrm{p}}\mathrm{q}\overline{\mathrm{q}})+\cdots\}_{[\theta]_{28}} \tag{87}$$

$$f_{\mathbf{C}'_s}\overset{6}{\underset{\mathrm{V}}{=}}\left\{(\mathrm{A}^2\mathrm{p}\overline{\mathrm{p}})+\cdots\right\}_{[\theta]_8}+\{2(\mathrm{p}\overline{\mathrm{p}}\mathrm{q}\overline{\mathrm{q}})+\cdots\}_{[\theta]_{28}} \tag{88}$$

$$f_{\mathbf{C}_{\hat{I}}}\overset{7}{\underset{\mathrm{I}}{=}}\left\{(\mathrm{A}^3\mathrm{B})+\cdots\right\}_{[\theta]_2}+\left\{3(\mathrm{A}^2\mathrm{BX})+\cdots\right\}_{[\theta]_6}+\{6(\mathrm{ABXY})+\cdots\}_{[\theta]_{10}} \tag{89}$$

$$f_{\mathbf{C}_{\hat{\sigma}}}\overset{8}{\underset{\mathrm{I}}{=}}\left\{(\mathrm{A}^2\mathrm{p}\overline{\mathrm{p}})+\cdots\right\}_{[\theta]_8}+\{2(\mathrm{p}\overline{\mathrm{p}}\mathrm{q}\overline{\mathrm{q}})+\cdots\}_{[\theta]_{28}} \tag{90}$$

$$f_{\mathbf{C}_{2v}}\overset{9}{\underset{\mathrm{V}}{=}}\left\{(\mathrm{p}^2\overline{\mathrm{p}}^2)+\cdots\right\}_{[\theta]_{23}} \tag{91}$$

$$f_{\mathbf{C}_{s\tilde{\sigma}\hat{I}}}\overset{10}{\underset{\mathrm{IV}}{=}}\left\{(\mathrm{A}^2\mathrm{B}^2)+\cdots\right\}_{[\theta]_4} \tag{92}$$

$$f_{\mathbf{C}'_{s\tilde{\sigma}\hat{I}}}\overset{11}{\underset{\mathrm{IV}}{=}}\left\{(\mathrm{A}^2\mathrm{B}^2)+\cdots\right\}_{[\theta]_4} \tag{93}$$

$$f_{\mathbf{C}_{2\hat{I}}}\overset{12}{\underset{\mathrm{I}}{=}}\left\{(\mathrm{A}^2\mathrm{B}^2)+\cdots\right\}_{[\theta]_4} \tag{94}$$

$$f_{\mathbf{C}_{s\tilde{\sigma}\hat{\sigma}}}\overset{13}{\underset{\mathrm{IV}}{=}}\left\{(\mathrm{p}^2\overline{\mathrm{p}}^2)+\cdots\right\}_{[\theta]_{23}} \tag{95}$$

$$f_{\mathbf{C}'_{s\tilde{\sigma}\hat{\sigma}}}\overset{14}{\underset{\mathrm{IV}}{=}}\left\{(\mathrm{p}^2\overline{\mathrm{p}}^2)+\cdots\right\}_{[\theta]_{23}} \tag{96}$$

$$f_{\mathbf{C}_{2\tilde{\sigma}}}\overset{15}{\underset{\mathrm{II}}{=}}\left\{\frac{1}{2}(\mathrm{p}^4+\overline{\mathrm{p}}^4)+\cdots\right\}_{[\theta]_{20}} \tag{97}$$

$$f_{\mathbf{C}_{2v\widetilde{\sigma}\widehat{I}}} \overset{16}{\underset{\mathrm{IV}}{=}} \left\{(\mathrm{A}^4) + \cdots\right\}_{[\theta]_1} \tag{98}$$

Note that a Roman numeral below each equality symbol represents the stereoisogram type at issue (types I–V), as categorized in Table 3. Each pair of braces contains terms having the same partition, which is shown in the subscript attached to the ending brace. For example, the $\frac{1}{2}(\mathrm{ABXp} + \mathrm{ABX}\overline{\mathrm{p}})$ (Eq. 83) indicates the presence of one quadruplet of promolecules with ABXp or $\mathrm{ABX}\overline{\mathrm{p}}$ ($[\theta]_{11}$) under the *RS*-stereoisomeric-group symmetry.

The calculations of the generating functions (Eqs. 83–98) are conducted by the Maple system after writing a Maple program in a similar way to the enumeration under point groups, which was based on the original PCI method of the USCI approach [45].

The generating function $f_{\acute{\mathbf{G}}_j}$ for the subgroup $\acute{\mathbf{G}}_j$ (j = 1–16, Eqs. 83–98) corresponds to the $\acute{\mathbf{G}}_j$-columns (j = 1–16) of the isomer-counting matrices, ICM_1 (Eq. 63) and ICM_2 (Eq. 64). For example, the generating function $f_{\mathbf{C}_2}$ ($\acute{\mathbf{G}}_2 = \mathbf{C}_2$ in Eq. 84) corresponds to the second columns of ICM_1 (Eq. 63) and ICM_2 (Eq. 64), so that the terms appearing in $f_{\mathbf{C}_2}$ correspond to the $([\theta]_5, 2)$-element of ICM_1 and to the $([\theta]_{25}, 2)$-element of ICM_2.

6.3 Type-itemized enumeration

6.3.1 Type-enumeration matrices

According to the categories shown in Eqs. 17–21, quadruplets are enumerated in an itemized fashion, after the type-enumeration matrix (TEM) is defined. Let $\overline{m}_{ji}$ be the ji-element of the inverse mark table $M^{-1}_{\mathbf{C}_{2v\widetilde{\sigma}\widehat{I}}}$ (Eq. 62). The $\acute{\mathbf{G}}_j$-row is tentatively fixed and the row is summed up according to the categorization of type I–V as follows:

$$\widehat{N}_j^{(\mathrm{Tp})} = \sum_{\acute{\mathbf{G}}_i \in \mathrm{SG}^{[\mathrm{Tp}]}} \overline{m}_{ji} \tag{99}$$

where $\mathrm{SG}^{[\mathrm{Tp}]}$ (Tp = I, II, III, IV, or V) is selected from Eqs. 17–21. All the elements in the j-row are summed up to give:

$$\widehat{N}_j = \sum_{\acute{\mathbf{G}}_i \in \mathrm{SSG}_{\mathbf{C}_{2v\widetilde{\sigma}\widehat{I}}}} \overline{m}_{ji} = \widehat{N}_j^{(\mathrm{I})} + \widehat{N}_j^{(\mathrm{II})} + \widehat{N}_j^{(\mathrm{III})} + \widehat{N}_j^{(\mathrm{IV})} + \widehat{N}_j^{(\mathrm{V})}. \tag{100}$$

Let us consider a 16×6 type-enumeration matrix (TEM) where the j-th row (TEM_j) as a row vector is represented as follows:

$$\mathrm{TEM}_j = \left(\widehat{N}_j, \widehat{N}_j^{(\mathrm{I})}, \widehat{N}_j^{(\mathrm{II})}, \widehat{N}_j^{(\mathrm{III})}, \widehat{N}_j^{(\mathrm{IV})}, \widehat{N}_j^{(\mathrm{V})}\right). \tag{101}$$

Then $\acute{\mathbf{G}}_j$ runs to cover the SSG (Eq. 16) so as to give 16 row vectors TEM_j ($j = 1$–16), which are collected to give the following type-enumeration matrix (TEM):

$$\mathrm{TEM}_{\mathbf{C}_{2v\tilde{\sigma}\hat{I}}} = \begin{pmatrix} 1/8 & 0 & 0 & 1/8 & 0 & 0 \\ 1/8 & 0 & 0 & 1/8 & 0 & 0 \\ 1/8 & 0 & 1/4 & -1/8 & 0 & 0 \\ 1/8 & 0 & 1/4 & -1/8 & 0 & 0 \\ 1/8 & 0 & 0 & -1/8 & 0 & 1/4 \\ 1/8 & 0 & 0 & -1/8 & 0 & 1/4 \\ 1/8 & 1/4 & 0 & -1/8 & 0 & 0 \\ 1/8 & 1/4 & 0 & -1/8 & 0 & 0 \\ 0 & 0 & 0 & 0 & 0 & 0 \\ 0 & -1/4 & -1/4 & 1/4 & 1/2 & -1/4 \\ 0 & -1/4 & -1/4 & 1/4 & 1/2 & -1/4 \\ 0 & 0 & 0 & 0 & 0 & 0 \\ 0 & -1/4 & -1/4 & 1/4 & 1/2 & -1/4 \\ 0 & -1/4 & -1/4 & 1/4 & 1/2 & -1/4 \\ 0 & 0 & 0 & 0 & 0 & 0 \\ 0 & 1/2 & 1/2 & -1/2 & -1 & 1/2 \end{pmatrix} \tag{102}$$

Because the FPM_1 (Eq. 60) and the FPM_2 (Eq. 61) consist of 16 columns, they are multiplied by the TEM (Eq. 102) as a 16×6 matrix. Thereby, isomer-type-counting matrices (ITCM_1 and ITCM_2) are obtained as follows:

$$\mathrm{ITCM}_1 = \mathrm{FPM}_1 \times \mathrm{TEM}_{\mathbf{C}_{2v\tilde{\sigma}\hat{I}}} = \begin{matrix} [\theta]_1 \\ [\theta]_2 \\ [\theta]_3 \\ [\theta]_4 \\ [\theta]_5 \\ [\theta]_6 \\ [\theta]_7 \\ [\theta]_8 \\ [\theta]_9 \\ [\theta]_{10} \\ [\theta]_{11} \\ [\theta]_{12} \\ [\theta]_{13} \\ [\theta]_{14} \\ [\theta]_{15} \\ [\theta]_{16} \\ [\theta]_{17} \\ [\theta]_{18} \\ [\theta]_{19} \end{matrix} \begin{pmatrix} 1 & 0 & 0 & 0 & 1 & 0 \\ 1 & 1 & 0 & 0 & 0 & 0 \\ 1/2 & 0 & 0 & 1/2 & 0 & 0 \\ 3 & 1 & 0 & 0 & 2 & 0 \\ 3/2 & 0 & 1 & 1/2 & 0 & 0 \\ 3 & 3 & 0 & 0 & 0 & 0 \\ 3/2 & 0 & 0 & 3/2 & 0 & 0 \\ 3 & 1 & 0 & 0 & 0 & 2 \\ 3/2 & 0 & 0 & 3/2 & 0 & 0 \\ 6 & 6 & 0 & 0 & 0 & 0 \\ 3 & 0 & 0 & 3 & 0 & 0 \\ 3/2 & 0 & 0 & 3/2 & 0 & 0 \\ 3 & 0 & 0 & 3 & 0 & 0 \\ 3 & 0 & 0 & 3 & 0 & 0 \\ 1/2 & 0 & 0 & 1/2 & 0 & 0 \\ 3/2 & 0 & 0 & 3/2 & 0 & 0 \\ 3/2 & 0 & 0 & 3/2 & 0 & 0 \\ 3 & 0 & 0 & 3 & 0 & 0 \\ 3 & 0 & 0 & 3 & 0 & 0 \end{pmatrix} \tag{103}$$

$$\mathrm{ITCM}_2 = \mathrm{FPM}_2 \times \mathrm{TEM}_{\mathbf{C}_{2v\widetilde{\sigma}\widehat{I}}} = \begin{matrix}[\theta]_{20}\\ [\theta]_{21}\\ [\theta]_{22}\\ [\theta]_{23}\\ [\theta]_{24}\\ [\theta]_{25}\\ [\theta]_{26}\\ [\theta]_{27}\\ [\theta]_{28}\\ [\theta]_{29}\\ [\theta]_{30}\end{matrix} \begin{pmatrix} 1/2 & 0 & 1/2 & 0 & 0 & 0\\ 1/2 & 0 & 0 & 1/2 & 0 & 0\\ 1/2 & 0 & 0 & 1/2 & 0 & 0\\ 3 & 0 & 0 & 0 & 2 & 1\\ 3/2 & 0 & 0 & 3/2 & 0 & 0\\ 3/2 & 0 & 1 & 1/2 & 0 & 0\\ 3/2 & 0 & 0 & 3/2 & 0 & 0\\ 3/2 & 0 & 0 & 3/2 & 0 & 0\\ 6 & 2 & 0 & 0 & 0 & 4\\ 3 & 0 & 0 & 3 & 0 & 0\\ 3 & 0 & 0 & 3 & 0 & 0 \end{pmatrix} \tag{104}$$

Note that the six columns of each ITCM contain the numbers of total quadruplets (the first column) and those of quadruplets of the respective types (the second to 6th columns). Obviously, ITCM_1 (Eq. 103) and ITCM_2 (Eq. 104) can be alternatively obtained by starting from ICM_1 (Eq. 63) and ICM_2 (Eq. 64), where the columns corresponding to each type are summed up.

In place of the inverse mark table $M^{-1}_{\mathbf{C}_{2v\widetilde{\sigma}\widehat{I}}}$ used in Eq. 66, let us use the type-enumeration matrix (TEM) shown in Eq. 102. Then, we obtain cycle indices for enumerating quadruples categorized with respect to five types:

$$\begin{aligned}&\mathrm{SCI\text{-}CF}_{\mathbf{C}_{2v\widetilde{\sigma}\widehat{I}}(/\mathbf{C}_{\widehat{I}})} \times \mathrm{TEM}_{\mathbf{C}_{2v\widetilde{\sigma}\widehat{I}}}\\ &\quad = \left(\mathrm{CI\text{-}CF}^{[\mathrm{G}]}, \mathrm{CI\text{-}CF}^{[\mathrm{I}]}, \mathrm{CI\text{-}CF}^{[\mathrm{II}]}, \mathrm{CI\text{-}CF}^{[\mathrm{III}]}, \mathrm{CI\text{-}CF}^{[\mathrm{IV}]}, \mathrm{CI\text{-}CF}^{[\mathrm{V}]}\right),\end{aligned} \tag{105}$$

where $\mathrm{CI\text{-}CF}^{[\mathrm{G}]}$ is the cycle index with chirality fittingness for gross enumeration, while the remaining cycle indices are concerned with respective types.

These cycle indices $\mathrm{CI\text{-}CF}^{[\mathrm{I}]}$–$\mathrm{CI\text{-}CF}^{[\mathrm{V}]}$ can be alternatively calculated by summing up the PCI-CFs listed in Eqs. 67–82 in accord with $\mathrm{SG}^{[\mathrm{I}]}$–$\mathrm{SG}^{[\mathrm{V}]}$ (Eqs. 17–21):

$$\mathrm{CI\text{-}CF}^{[\mathrm{I}]} = \mathrm{PCI\text{-}CF}\left(\overset{7}{\mathbf{C}}_{\widehat{I}}\right) + \mathrm{PCI\text{-}CF}\left(\overset{8}{\mathbf{C}}_{\widehat{\sigma}}\right) + \mathrm{PCI\text{-}CF}\left(\overset{12}{\mathbf{C}}_{2\widehat{I}}\right) \tag{106}$$

$$\mathrm{CI\text{-}CF}^{[\mathrm{II}]} = \mathrm{PCI\text{-}CF}\left(\overset{3}{\mathbf{C}}_{\widetilde{\sigma}}\right) + \mathrm{PCI\text{-}CF}\left(\overset{4}{\mathbf{C}'}_{\widetilde{\sigma}}\right) + \mathrm{PCI\text{-}CF}\left(\overset{15}{\mathbf{C}}_{2\widetilde{\sigma}}\right) \tag{107}$$

$$\mathrm{CI\text{-}CF}^{[\mathrm{III}]} = \mathrm{PCI\text{-}CF}\left(\overset{1}{\mathbf{C}}_{1}\right) + \mathrm{PCI\text{-}CF}\left(\overset{2}{\mathbf{C}}_{2}\right) \tag{108}$$

$$\begin{aligned}\mathrm{CI\text{-}CF}^{[\mathrm{IV}]} = {} & \mathrm{PCI\text{-}CF}\left(\overset{10}{\mathbf{C}}_{s\widetilde{\sigma}\widehat{I}}\right) + \mathrm{PCI\text{-}CF}\left(\overset{11}{\mathbf{C}'}_{s\widetilde{\sigma}\widehat{I}}\right) + \mathrm{PCI\text{-}CF}\left(\overset{13}{\mathbf{C}}_{s\widetilde{\sigma}\widehat{\sigma}}\right)\\ & + \mathrm{PCI\text{-}CF}\left(\overset{14}{\mathbf{C}'}_{s\widetilde{\sigma}\widehat{\sigma}}\right) + \mathrm{PCI\text{-}CF}\left(\overset{16}{\mathbf{C}}_{2v\widetilde{\sigma}\widehat{I}}\right)\end{aligned} \tag{109}$$

$$\mathrm{CI\text{-}CF}^{[\mathrm{V}]} = \mathrm{PCI\text{-}CF}\left(\overset{5}{\mathbf{C}}_{s}\right) + \mathrm{PCI\text{-}CF}\left(\overset{6}{\mathbf{C}'}_{s}\right) + \mathrm{PCI\text{-}CF}\left(\overset{9}{\mathbf{C}}_{2v}\right) \tag{110}$$

The calculations based on Eq. 105 and on Eqs. 106–110 give an identical set of cycle indices with chirality fittingness as follows:

$$\text{CI-CF}^{[\text{I}]} = \frac{1}{4}a_1^4 - \frac{1}{2}a_2^2 + \frac{1}{4}c_2^2 + \frac{1}{2}a_4 - \frac{1}{2}c_4 \tag{111}$$

$$\text{CI-CF}^{[\text{II}]} = \frac{1}{2}b_2^2 - \frac{1}{2}a_2^2 - \frac{1}{2}c_4 + \frac{1}{2}a_4 \tag{112}$$

$$\text{CI-CF}^{[\text{III}]} = \frac{1}{8}b_1^4 - \frac{1}{8}a_1^4 - \frac{1}{8}b_2^2 + \frac{1}{2}a_2^2 - \frac{3}{8}c_2^2 + \frac{1}{2}c_4 - \frac{1}{2}a_4 \tag{113}$$

$$\text{CI-CF}^{[\text{IV}]} = a_2^2 - a_4 + c_4 \tag{114}$$

$$\text{CI-CF}^{[\text{V}]} = \frac{1}{2}c_2^2 - \frac{1}{2}a_2^2 - \frac{1}{2}c_4 + \frac{1}{2}a_4 \tag{115}$$

By applying the USCI approach (Theorem 19.6 of [23]) in a modified fashion, the ligand-inventory functions (Eqs. 24–26) are introduced into the CI-CFs (Eqs. 111–115). Thereby, the generating functions for type I to type V are obtained as follows:

$$\begin{aligned} f^{[\text{I}]} &= f_{\mathbf{C}_{\hat{1}}} + f_{\mathbf{C}_{\hat{\sigma}}} + f_{\mathbf{C}_{2\hat{1}}} \\ &= \left\{(\text{A}^3\text{B}) + \cdots\right\}_{[\theta]_2} + \left\{3(\text{A}^2\text{BX}) + \cdots\right\}_{[\theta]_6} + \{6(\text{ABXY}) + \cdots\}_{[\theta]_{10}} \\ &\quad + \left\{(\text{A}^2\text{p}\overline{\text{p}}) + \cdots\right\}_{[\theta]_8} + \{2(\text{p}\overline{\text{p}}\text{q}\overline{\text{q}}) + \cdots\}_{[\theta]_{28}} + \left\{(\text{A}^2\text{B}^2) + \cdots\right\}_{[\theta]_4} \end{aligned} \tag{116}$$

$$\begin{aligned} f^{[\text{II}]} &= f_{\mathbf{C}_{\tilde{\sigma}}} + f_{\mathbf{C}_{\tilde{\sigma}'}} + f_{\mathbf{C}_{2\tilde{\sigma}}} \\ &= \left\{(\text{A}^2\text{p}^2 + \text{A}^2\overline{\text{p}}^2) + \cdots\right\}_{[\theta]_5} + \left\{(\text{p}^2\text{q}^2 + \overline{\text{p}}^2\overline{\text{q}}^2) + \cdots\right\}_{[\theta]_{25}} \\ &\quad + \left\{\frac{1}{2}(\text{p}^4 + \overline{\text{p}}^4) + \cdots\right\}_{[\theta]_{20}} \end{aligned} \tag{117}$$

$$\begin{aligned} f^{[\text{III}]} &= f_{\mathbf{C}_1} + f_{\mathbf{C}_2} \\ &= \left\{\frac{1}{2}(\text{A}^3\text{p} + \text{A}^3\overline{\text{p}}) + \cdots\right\}_{[\theta]_3} + \left\{\frac{3}{2}(\text{A}^2\text{Bp} + \text{A}^2\text{B}\overline{\text{p}}) + \cdots\right\}_{[\theta]_7} \\ &\quad + \left\{\frac{3}{2}(\text{A}^2\text{pq} + \text{A}^2\overline{\text{pq}}) + \cdots\right\}_{[\theta]_9} + \{3(\text{ABXp} + \text{ABX}\overline{\text{p}}) + \cdots\}_{[\theta]_{11}} \\ &\quad + \{3\text{ABp}\overline{\text{p}} + \cdots\}_{[\theta]_{13}} + \left\{\frac{3}{2}(\text{ABp}^2 + \text{AB}\overline{\text{p}}^2) + \cdots\right\}_{[\theta]_{12}} \\ &\quad + \{3(\text{ABpq} + \text{AB}\overline{\text{pq}}) + \cdots\}_{[\theta]_{14}} + \left\{\frac{3}{2}(\text{Ap}^2\overline{\text{p}} + \text{Ap}\overline{\text{p}}^2) + \cdots\right\}_{[\theta]_{16}} \\ &\quad + \left\{\frac{3}{2}(\text{Ap}^2\text{q} + \text{A}\overline{\text{p}}^2\overline{\text{q}}) + \cdots\right\}_{[\theta]_{17}} + \left\{\frac{1}{2}(\text{Ap}^3 + \text{A}\overline{\text{p}}^3) + \cdots\right\}_{[\theta]_{15}} \\ &\quad + \{3(\text{Ap}\overline{\text{p}}\text{q} + \text{Ap}\overline{\text{pq}}) + \cdots\}_{[\theta]_{18}} + \{3(\text{Apqr} + \text{A}\overline{\text{pqr}}) + \cdots\}_{[\theta]_{19}} \\ &\quad + \left\{\frac{1}{2}(\text{p}^3\overline{\text{p}} + \text{p}\overline{\text{p}}^3) + \cdots\right\}_{[\theta]_{21}} + \left\{\frac{1}{2}(\text{p}^3\text{q} + \overline{\text{p}}^3\overline{\text{q}}) + \cdots\right\}_{[\theta]_{22}} \end{aligned}$$

$$+\left\{\frac{3}{2}(\mathrm{p}^2\overline{\mathrm{p}}\mathrm{q}+\mathrm{p}\overline{\mathrm{p}}^2\overline{\mathrm{q}})+\cdots\right\}_{[\theta]_{24}}+\left\{\frac{3}{2}(\mathrm{p}^2\mathrm{q}\overline{\mathrm{q}}+\overline{\mathrm{p}}^2\mathrm{q}\overline{\mathrm{q}})+\cdots\right\}_{[\theta]_{26}}$$
$$+\left\{\frac{3}{2}(\mathrm{p}^2\mathrm{q}\mathrm{r}+\overline{\mathrm{p}}^2\overline{\mathrm{q}\mathrm{r}})+\cdots\right\}_{[\theta]_{27}}+\{3(\mathrm{p}\overline{\mathrm{p}}\mathrm{q}\mathrm{r}+\mathrm{p}\overline{\mathrm{p}\mathrm{q}\mathrm{r}})+\cdots\}_{[\theta]_{29}}$$
$$+\{3(\mathrm{p}\mathrm{q}\mathrm{r}\mathrm{s}+\overline{\mathrm{p}\mathrm{q}\mathrm{r}\mathrm{s}})+\cdots\}_{[\theta]_{30}}$$
$$+\left\{\frac{1}{2}(\mathrm{A}^2\mathrm{p}^2+\mathrm{A}^2\overline{\mathrm{p}}^2)+\cdots\right\}_{[\theta]_5}+\left\{\frac{1}{2}(\mathrm{p}^2\mathrm{q}^2+\overline{\mathrm{p}}^2\overline{\mathrm{q}}^2)+\cdots\right\}_{[\theta]_{25}} \quad (118)$$

$$f^{[\mathrm{IV}]}=f_{\mathbf{C}_{s\tilde{\sigma}\hat{I}}}+f_{\mathbf{C}'_{s\tilde{\sigma}\hat{I}}}+f_{\mathbf{C}_{s\tilde{\sigma}\hat{\sigma}}}+f_{\mathbf{C}'_{s\tilde{\sigma}\hat{\sigma}}}+f_{\mathbf{C}_{2v\tilde{\sigma}\hat{I}}}$$
$$=\left\{2(\mathrm{A}^2\mathrm{B}^2)+\cdots\right\}_{[\theta]_4}+\left\{2(\mathrm{p}^2\overline{\mathrm{p}}^2)+\cdots\right\}_{[\theta]_{23}}+\left\{(\mathrm{A}^4)+\cdots\right\}_{[\theta]_1} \quad (119)$$

$$f^{[\mathrm{V}]}=f_{\mathbf{C}_s}+f_{\mathbf{C}'_s}+f_{\mathbf{C}_{2v}}$$
$$=\left\{2(\mathrm{A}^2\mathrm{p}\overline{\mathrm{p}})+\cdots\right\}_{[\theta]_8}+\{4(\mathrm{p}\overline{\mathrm{p}}\mathrm{q}\overline{\mathrm{q}})+\cdots\}_{[\theta]_{28}}+\left\{(\mathrm{p}^2\overline{\mathrm{p}}^2)+\cdots\right\}_{[\theta]_{23}} \quad (120)$$

These generating functions contain equivalent values to those of ITCM_1 (Eq. 103) and ITCM_2 (Eq. 104). Note that each of the second (type I) to 6th (type V) columns of these ITCMs contains the coefficients of terms appearing in the generating function of the type at issue.

Alternatively, another set of generating functions identical with Eqs. 116–120 can be calculated by starting from the generating functions of the respective subgroups (Eqs. 83–98), which are summed up in accord with $\mathrm{SG}^{[\mathrm{I}]}$–$\mathrm{SG}^{[\mathrm{V}]}$ (Eqs. 17–21).

7 Catalogs of promolecules derived from the oxirane skeleton

7.1 Type-I promolecules

The representative promolecules of type-I stereoisograms, the numbers of which are collected in the second columns of ITCM_1 (Eq. 103) and ITCM_2 (Eq. 104) or equivalently in the generating function for type I ($f^{[\mathrm{I}]}$, Eq. 116), are depicted in Fig. 7. They are itemized with respect to *RS*-stereoisomeric groups, i.e., $\mathbf{C}_{\hat{I}}$ (Eq. 89), $\mathbf{C}_{\hat{\sigma}}$ (Eq. 90), and $\mathbf{C}_{2\hat{I}}$ (Eq. 94), the values of which are also listed in the 7th, 8th, and 12th columns of ICM_1 (Eq. 63) and ICM_2 (Eq. 64).

For example, one promolecule **10** with the partition $[\theta]_2$ belongs to the *RS*-stereoisomeric group $\mathbf{C}_{\hat{I}}$, where the number of *RS*-stereoisomers is shown at the intersection between the $[\theta]_2$-row and the 7th ($\mathbf{C}_{\hat{I}}$) column in ICM_1 (Eq. 63) or equivalently appears as the coefficient of the term $\mathrm{A}^3\mathrm{B}$ ($[\theta]_2$) contained in the generating function $f_{\mathbf{C}_{\hat{I}}}$ (Eq. 89). The number 3 of the term $3\mathrm{A}^2\mathrm{BX}$ ($[\theta]_6$) appearing in $f_{\mathbf{C}_{\hat{I}}}$ (Eq. 89) correspond to the promolecules **11**, **12**, and **13**. For this value, see also the intersection between the $[\theta]_6$-row and the 7th ($\mathbf{C}_{\hat{I}}$) column in ICM_1 (Eq. 63). On the other hand, the number 6 of the term 6ABXY ($[\theta]_{10}$) appearing in $f_{\mathbf{C}_{\hat{I}}}$ (Eq. 89) correspond to the promolecules **14**–**19**. For this value, see also the intersection between the $[\theta]_{10}$-row and the 7th ($\mathbf{C}_{\hat{I}}$) column in ICM_1 (Eq. 63).

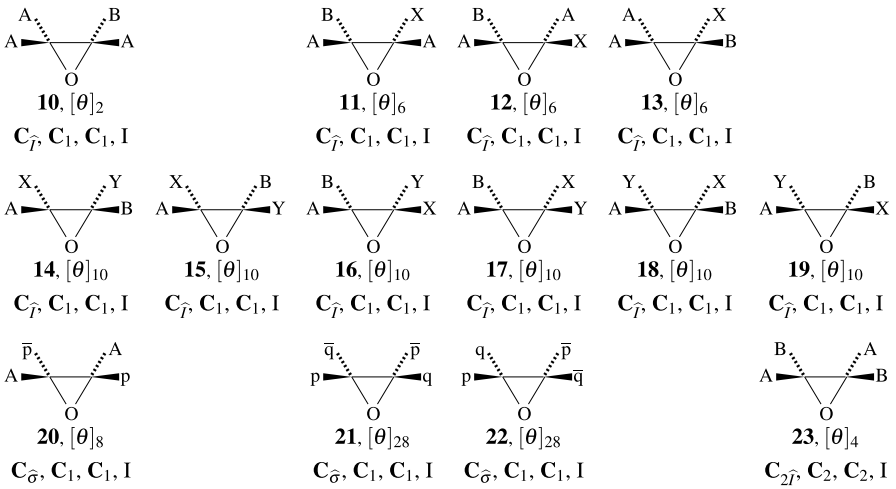

Fig. 7 Representative promolecules for type-I stereoisograms of oxiranes. Each representative is attached by a partition and characterized by a *RS*-stereoisomeric group, a point group, *RS*-permutation group, and a stereoisogram type

Each of the representatives Fig. 7 is accompanied with a quadruplet of promolecules, which are contained in a type-I stereoisogram shown in Fig. 6. Such a type-I stereoisogram is characterized by chirality, *RS*-stereogenicity, and asclerality, so that an enantiomeric relationship is coincident with an *RS*-diastereomeric relationship as indicated by diagonal equality symbols.

For example, **14** (= **3**) belonging to the *RS*-stereoisomeric group $\mathbf{C}_{\hat{1}}$ generates a type-I stereoisogram shown in Fig. 5. Another example of a type-I stereoisogram is shown in Fig. 8. The enantiomeric relationship between **23** and $\overline{\mathbf{23}}$ is coincident with an *RS*-diastereomeric relationship between **23** and **24** (= $\overline{\mathbf{23}}$). The promolecule **23** is ascleral so that it is self-holantimeric with $\overline{\mathbf{24}}$ (=**23**), as indicated by diagonal equality symbols.

The promolecule **23** with the partition $[\theta]_4$ belongs to the *RS*-stereoisomeric group $\mathbf{C}_{2\hat{1}}$, to the point group $\mathbf{C}_2$, and to the *RS*-permutation group $\mathbf{C}_2$. The corresponding stereoisogram exhibits type-I properties, as shown in Fig. 8. The enantiomeric relationship between **23** and $\overline{\mathbf{23}}$ is coincident with the *RS*-diastereomeric relationship between **23** and **24** (= $\overline{\mathbf{23}}$).

7.2 Type-II promolecules

The numbers of quadruplets having type-II stereoisograms are shown in the third columns of ITCM_1 (Eq. 103) and ITCM_2 (Eq. 104) or equivalently in the generating function for type II ($f^{[\mathrm{II}]}$, Eq. 117). The representative promolecules of the quadruplets of type II are depicted in Fig. 9. They are itemized with respect to *RS*-stereoisomeric groups, i.e., $\mathbf{C}_{\tilde{\sigma}}$ (Eq. 85), $\mathbf{C}'_{\tilde{\sigma}}$ (Eq. 86), $\mathbf{C}_{2\tilde{\sigma}}$ (Eq. 97), the values of which are also listed in the third, 4th, and 15th columns of ICM_1 (Eq. 63) and ICM_2 (Eq. 64).

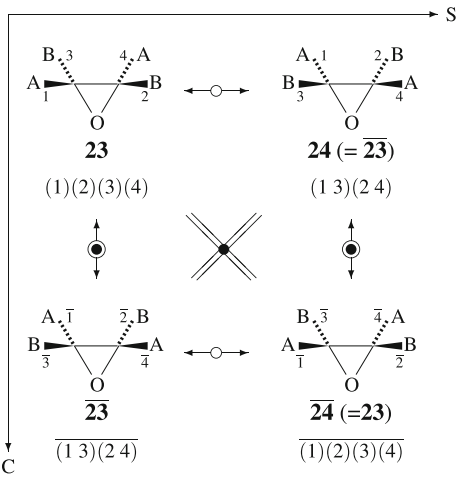

Fig. 8 Stereoisogram of type I derived from the oxirane skeleton **2**, where achiral proligand A's are placed at positions 1 and 4, while achiral proligands B's at positions 2 and 3. The reference promolecule **23** belongs to the *RS*-stereoisomeric group $\mathbf{C}_{2\hat{I}}$

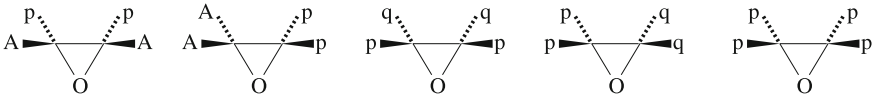

$\mathbf{C}_{\widetilde{\sigma}}, \mathbf{C}_1, \mathbf{C}_{\widetilde{\sigma}}$, II $\quad \mathbf{C}'_{\widetilde{\sigma}}, \mathbf{C}_1, \mathbf{C}'_{\widetilde{\sigma}}$, II $\quad \mathbf{C}_{\widetilde{\sigma}}, \mathbf{C}_1, \mathbf{C}_{\widetilde{\sigma}}$, II $\quad \mathbf{C}'_{\widetilde{\sigma}}, \mathbf{C}_1, \mathbf{C}'_{\widetilde{\sigma}}$, II $\quad \mathbf{C}_{2\widetilde{\sigma}}, \mathbf{C}_2, \mathbf{C}_{2\widetilde{\sigma}}$, II

Fig. 9 Representative promolecules for type-II stereoisograms of oxiranes. Each representative is attached by a partition and characterized by a *RS*-stereoisomeric group, a point group, *RS*-permutation group, and a stereoisogram type

Note that a stereoisogram of type II consists of one pair of enantiomers, which is counted once under the action of *RS*-stereoisomeric groups. For example, one promolecule **25** with the partition $[\theta]_5$ belongs to the *RS*-stereoisomeric group $\mathbf{C}_{\widetilde{\sigma}}$. The number is shown at the intersection between the $[\theta]_5$-row and the 3rd ($\mathbf{C}_{\widetilde{\sigma}}$) column in ICM_1 (Eq. 63), where the value $\frac{1}{2}$ indicates the presence of one quadruplet because of the term $\frac{1}{2}(\mathrm{A}^2\mathrm{p}^2 + \mathrm{A}^2\overline{\mathrm{p}}^2)$. The value $\frac{1}{2}$ appears equivalently as the coefficient of the term $\frac{1}{2}(\mathrm{A}^2\mathrm{p}^2 + \mathrm{A}^2\overline{\mathrm{p}}^2)$ ($[\theta]_5$) contained in the generating function $f_{\mathbf{C}_{\widetilde{\sigma}}}$ (Eq. 85).

All of the promolecules listed in Fig. 9 are characterized by type-II stereoisograms under the *RS*-stereoisomeric group $\mathbf{C}_{2v\widetilde{\sigma}\hat{I}}$. For example, the promolecule **25** generates a type-II stereoisogram shown in Fig. 10. The type-II stereoisogram (Fig. 10) is characterized by chirality, *RS*-astereogenicity, and sclerality, so that the horizontal equality symbols show the self-*RS*-diastereomeric relationship between **25** and **30** (= **25**) or between $\overline{\mathbf{25}}$ and $\overline{\mathbf{30}}$ (= $\overline{\mathbf{25}}$). Note that **25** and **30** (or $\overline{\mathbf{25}}$ and $\overline{\mathbf{30}}$) are homomeric under the action of $\mathbf{C}_2$, so that they coincide with each other under rotations.

The relationship between **25** and **26** or between **27** and **28** is determined not to be stereoisomeric. This relationship is usually referred to as being constitutional isomeric under the modern stereochemistry. The relationship **25**/**26** (or **27**/**28**) is determined more definitely to be isoskeletal-isomeric because the present proligand–promolecule model emphasizes the oxirane skeleton as a common stereoskeleton.

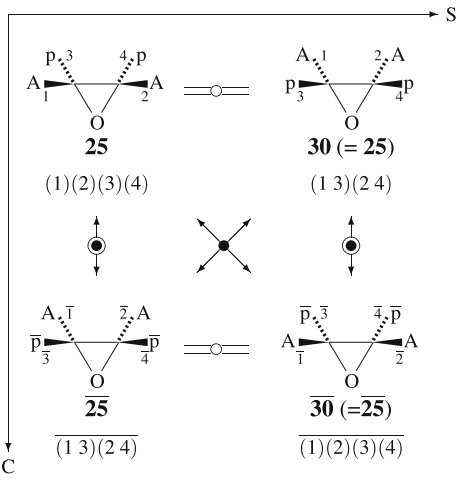

Fig. 10 Stereoisogram of type II derived from the oxirane skeleton **2**, where achiral proligand A's are placed at positions 1 and 2, while chiral proligands p's at positions 3 and 4. The reference promolecule **25** belongs to the *RS*-stereoisomeric group $\mathbf{C}_{\widetilde{\sigma}}$

7.3 Type-III promolecules

The numbers of quadruplets having type-III stereoisograms are shown in the 4th columns of ITCM_1 (Eq. 103) and ITCM_2 (Eq. 104) or equivalently in the generating function for type III ($f^{[\mathrm{III}]}$, Eq. 118). The representative promolecules of the quadruplets of type III are depicted in Fig. 11 (for the partitions $[\theta]_1$–$[\theta]_{19}$) and Fig. 12 (for the partitions $[\theta]_{20}$–$[\theta]_{30}$). They are itemized with respect to *RS*-stereoisomeric groups, i.e., $\mathbf{C}_1$ (Eq. 83) and $\mathbf{C}_2$ (Eq. 84), the values of which are also listed in the first and second columns of ICM_1 (Eq. 63) and ICM_2 (Eq. 64).

Although a stereoisogram of type III consists of two pair of enantiomers, the quadruplet of the type-III stereoisogram is counted once under the action of *RS*-stereoisomeric groups. For example, one promolecule **31** with the partition $[\theta]_3$ belongs to the *RS*-stereoisomeric group $\mathbf{C}_1$. The number appears at the intersection between the $[\theta]_3$-row and the first ($\mathbf{C}_1$) column in ICM_1 (Eq. 63), where the value $\frac{1}{2}$ indicates the presence of one quadruplet according to the term $\frac{1}{2}(\mathrm{A}^3\mathrm{p}+\mathrm{A}^3\overline{\mathrm{p}})$. The value $\frac{1}{2}$ appears equivalently as the coefficient of the term $\frac{1}{2}(\mathrm{A}^3\mathrm{p}+\mathrm{A}^3\overline{\mathrm{p}})$ ($[\theta]_3$) contained in the generating function $f_{\mathbf{C}_1}$ (Eq. 83).

All of the promolecules listed in Figs. 11 and 12 are characterized by type-III stereoisograms under the *RS*-stereoisomeric group $\mathbf{C}_{2v\widetilde{\sigma}\widehat{I}}$. For example, the promolecule **31** generates a type-III stereoisogram shown in Fig. 13. The type-III stereoisogram (Fig. 13) is characterized by chirality, *RS*-stereogenicity, and sclerality, so that there appear no equality symbols in the vertical, horizontal, and diagonal directions.

7.4 Type-IV promolecules

The numbers of quadruplets having type-IV stereoisograms are shown in the 5th columns of ITCM_1 (Eq. 103) and ITCM_2 (Eq. 104) or equivalently in the generating function for type IV ($f^{[\mathrm{IV}]}$, Eq. 119). The representative promolecules of the quadruplets of type IV are depicted in Fig. 14. They are itemized with respect to

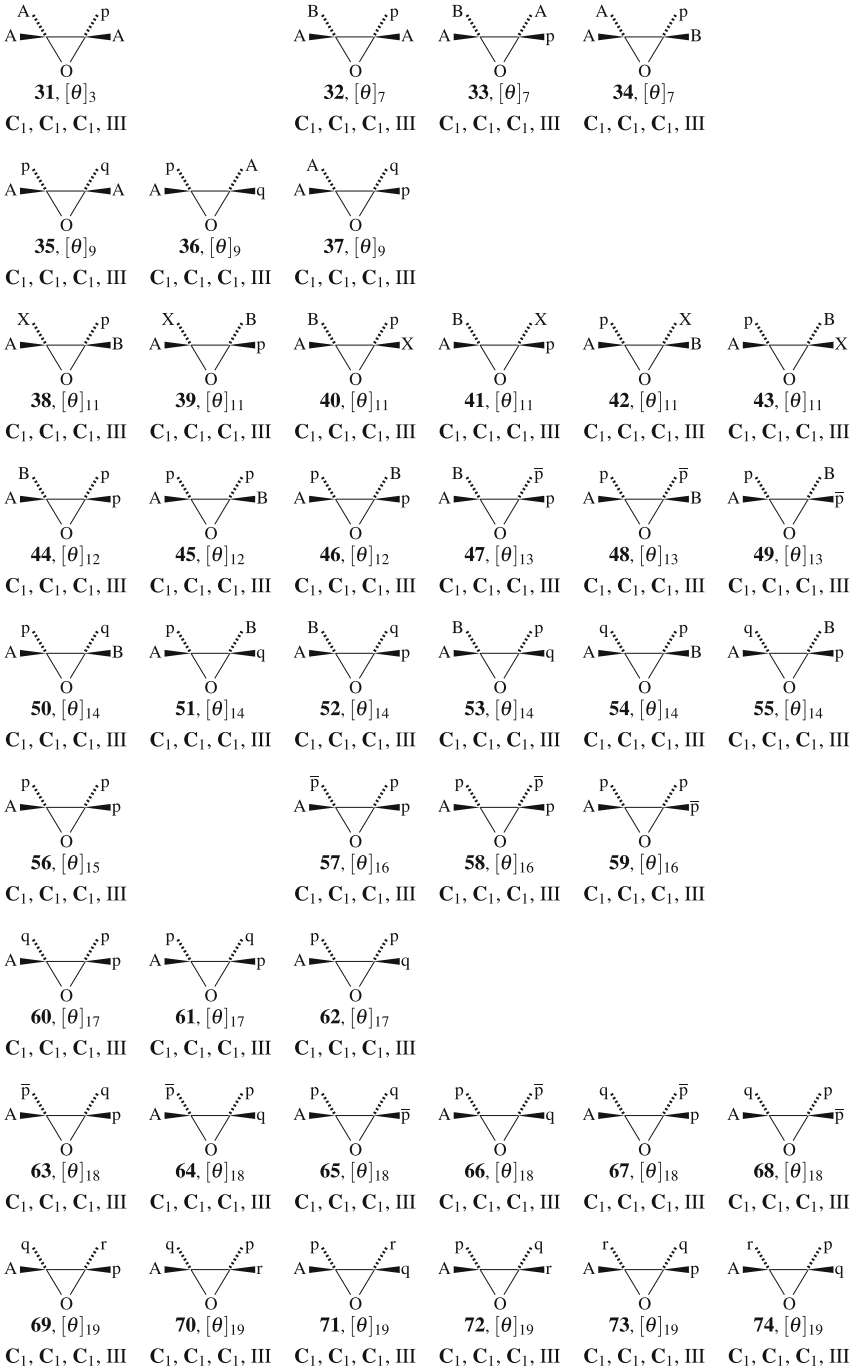

Fig. 11 Representative promolecules for type-III stereoisograms of oxiranes (List 1). Each representative is attached by a partition and characterized by a *RS*-stereoisomeric group, a point group, *RS*-permutation group, and a stereoisogram type

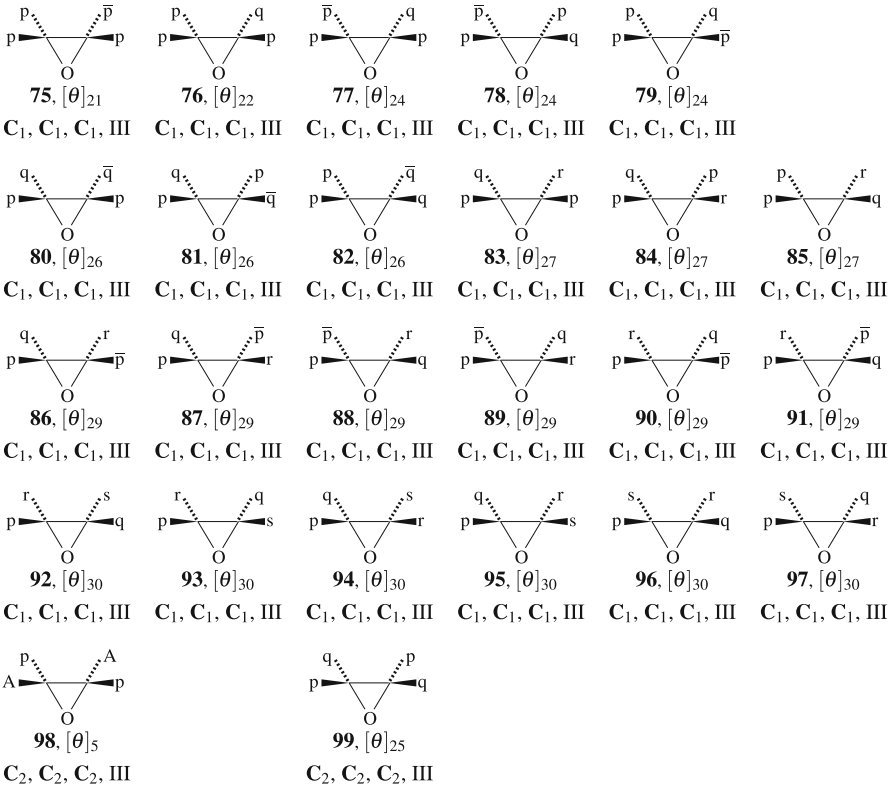

Fig. 12 Representative promolecules for type-III stereoisograms of oxiranes (List 2). Each representative is attached by a partition and characterized by a *RS*-stereoisomeric group, a point group, *RS*-permutation group, and a stereoisogram type

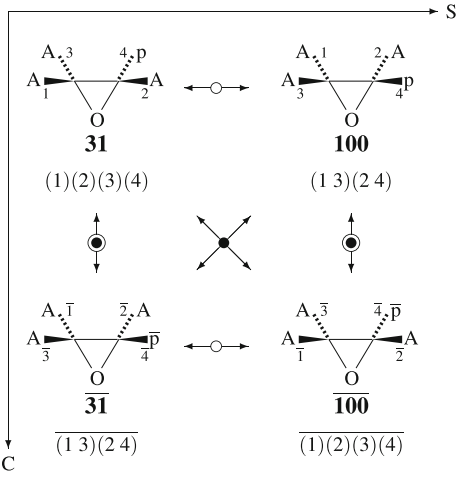

Fig. 13 Stereoisogram of type III derived from the oxirane skeleton **2**, where achiral proligand A's are placed at positions 1, 2, and 3, while a chiral proligand p at position 4. The reference promolecule **31** belongs to the *RS*-stereoisomeric group $\mathbf{C}_1$

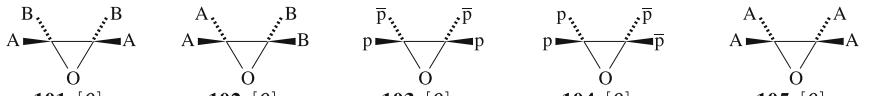

Fig. 14 Representative promolecules for type-IV stereoisograms of oxiranes. Each representative is attached by a partition and characterized by a *RS*-stereoisomeric group, a point group, *RS*-permutation group, and a stereoisogram type

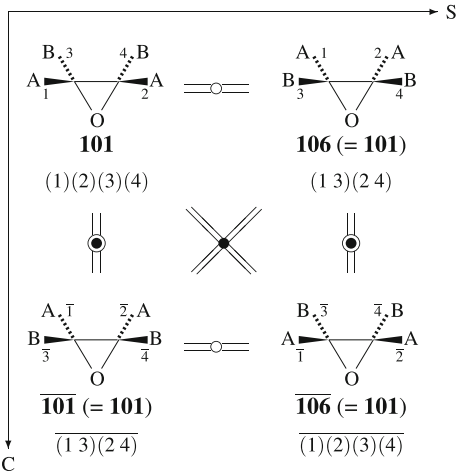

Fig. 15 Stereoisogram of type IV derived from the oxirane skeleton **2**, where achiral proligand A's are placed at positions 1 and 2, while achiral proligands B at position 3 and 4. The reference promolecule **101** belongs to the *RS*-stereoisomeric group $\mathbf{C}_{2v\tilde{\sigma}\hat{I}}$

RS-stereoisomeric groups, i.e., $\mathbf{C}_{s\tilde{\sigma}\hat{I}}$ (Eq. 92), $\mathbf{C}'_{s\tilde{\sigma}\hat{I}}$ (Eq. 93), $\mathbf{C}_{s\tilde{\sigma}\hat{\sigma}}$ (Eq. 95), $\mathbf{C}'_{s\tilde{\sigma}\hat{\sigma}}$ (Eq. 96), and $\mathbf{C}_{2v\tilde{\sigma}\hat{I}}$ (Eq. 98), the values of which are also listed in the 10th, 11th, 13th, 14th and 16th columns of ICM_1 (Eq. 63) and ICM_2 (Eq. 64).

Because a stereoisogram of type IV consists of one achiral promolecule, the quadruplet of the type-IV stereoisogram is counted once under the action of *RS*-stereoisomeric groups. For example, one promolecule **101** with the partition $[\theta]_4$ belongs to the *RS*-stereoisomeric group $\mathbf{C}_{s\tilde{\sigma}\hat{I}}$. The number appears at the intersection between the $[\theta]_4$-row and the 10th ($\mathbf{C}_{s\tilde{\sigma}\hat{I}}$) column in ICM_1 (Eq. 63), where the value 1 indicates the presence of one quadruplet according to the term $\mathrm{A}^2\mathrm{B}^2$. The value 1 appears equivalently as the coefficient of the term $\mathrm{A}^2\mathrm{B}^2$ ($[\theta]_4$) contained in the generating function $f_{\mathbf{C}_{s\tilde{\sigma}\hat{I}}}$ (Eq. 92).

All of the promolecules listed in Fig. 14 are characterized by type-IV stereoisograms under the *RS*-stereoisomeric group $\mathbf{C}_{2v\tilde{\sigma}\hat{I}}$. For example, the promolecule **101** generates a type-IV stereoisogram shown in Fig. 15. The type-IV stereoisogram (Fig. 15) is characterized by achirality, *RS*-astereogenicity, and asclerality so that the four promolecules in the type-IV stereoisogram are identical with one another to give a single promolecule.

7.5 Type-V promolecules

The numbers of quadruplets having type-V stereoisograms are shown in the 6th columns of ITCM_1 (Eq. 103) and ITCM_2 (Eq. 104) or equivalently in the generating

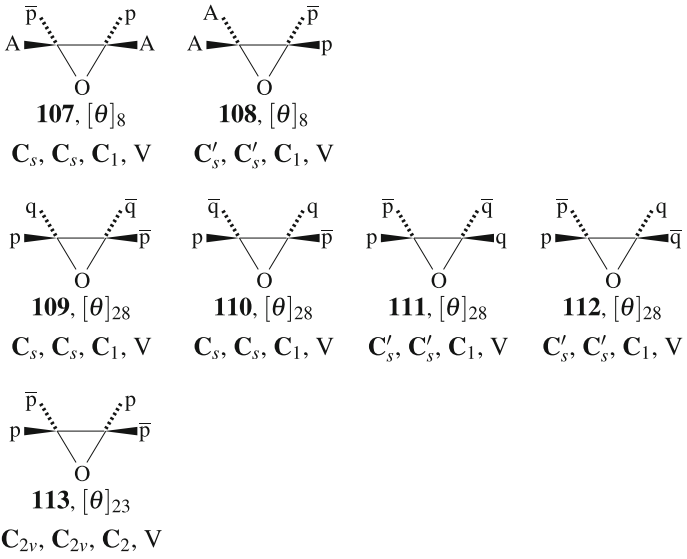

Fig. 16 Representative promolecules for type-V stereoisograms of oxiranes. Each representative is attached by a partition and characterized by a *RS*-stereoisomeric group, a point group, *RS*-permutation group, and a stereoisogram type

function for type V ($f^{[V]}$, Eq. 120). The representative promolecules of the quadruplets of type V are depicted in Fig. 16. They are itemized with respect to *RS*-stereoisomeric groups, i.e., $\mathbf{C}_s$ (Eq. 87), $\mathbf{C}'_s$ (Eq. 88), and $\mathbf{C}_{2v}$ (Eq. 91), the values of which are also listed in the 5th, 6th, and 9th columns of ICM_1 (Eq. 63) and ICM_2 (Eq. 64).

Although a stereoisogram of type V consists of two achiral promolecules, the quadruplet of the type-V stereoisogram is counted once under the action of *RS*-stereoisomeric groups. For example, one promolecule **107** with the partition $[\theta]_8$ belongs to the *RS*-stereoisomeric group $\mathbf{C}_s$. The number appears at the intersection between the $[\theta]_8$-row and the 5th ($\mathbf{C}_s$) column in ICM_1 (Eq. 63), where the value 1 indicates the presence of one quadruplet according to the term $\mathrm{A}^2\mathrm{p}\overline{\mathrm{p}}$. The value 1 appears equivalently as the coefficient of the term $\mathrm{A}^2\mathrm{p}\overline{\mathrm{p}}$ ($[\theta]_8$) contained in the generating function $f_{\mathbf{C}_s}$ (Eq. 87).

All of the promolecules listed in Fig. 16 are characterized by type-V stereoisograms under the *RS*-stereoisomeric group $\mathbf{C}_{2v\widetilde{\sigma}\widehat{I}}$. For example, the promolecule **107** generates a type-V stereoisogram shown in Fig. 17. The type-V stereoisogram (Fig. 17) is characterized by achirality, *RS*-stereogenicity, and sclerality.

The type-V stereoisograms of the promolecules shown in Fig. 16 can be regarded as being pseudoasymmetric in an extended fashion, because the oxirane skeleton with $\mathrm{A}^2\mathrm{p}\overline{\mathrm{p}}$ etc. at the four positions (**107**) exhibits achirality but *RS*-stereogenicity. Thereby, there emerges a pair of *RS*-diastereomers **107**/**114**. On the other hand, a tetrahedral skeleton with $\mathrm{ABp}\overline{\mathrm{p}}$ etc. at the four positions exhibits achirality but *RS*-stereogenicity, so that there emerges a pair of *RS*-diastereomers due to pseudoasymmetry. Note that the oxirane skeleton is selected as a stereoskeleton, just as the tetrahedral skeleton is selected as a stereoskeleton in accord with the proligand–promolecule model.

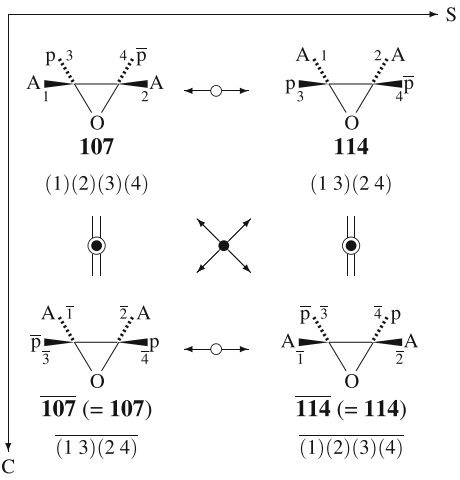

Fig. 17 Stereoisogram of type V derived from the oxirane skeleton **2**, where achiral proligand A's are placed at positions 1 and 2, while chiral proligands p's at position 3 and 4. The reference promolecule **107** belongs to the *RS*-stereoisomeric group $\mathbf{C}_s$

The extended pseudoasymmetry of **107** cannot be detected so long as we obey the modern stereochemistry, because the modern stereochemistry does not adopt the oxirane skeleton as a 'stereogenic unit'. On the other hand, the pseudoasymmetry of **108** can be detected even in the modern stereochemistry, because a carbon atom attached by a pair of p/$\overline{\text{p}}$ can be regarded as a 'pseudoasymmetric center', i.e., one of 'stereogenic units', in the light of the conventional terminology. To develop comprehensive discussions on stereochemistry, however, even the case of **108** should be regarded as an extended pseudoasymmetric case, where the oxirane skeleton **2** is taken into consideration in a parallel way to the case of **107**.

8 Combinatorial enumeration under subgroups

8.1 Enumeration of oxiranes under the point group $\mathbf{C}_{2v}$

8.1.1 The FPM method

Suppose that the oxirane skeleton **2** is considered to belong to the point group $\mathbf{C}_{2v}$ in place of the *RS*-stereoisomeric group $\mathbf{C}_{2v\tilde{\sigma}\hat{I}}$. The four positions of **2** construct an orbit governed by the coset representation $\mathbf{C}_{2v}(/\mathbf{C}_1)$ under the point group $\mathbf{C}_{2v}$ in place of the coset representation $\mathbf{C}_{2v\tilde{\sigma}\hat{I}}(/\mathbf{C}_{\hat{I}})$ under the *RS*-stereoisomeric group $\mathbf{C}_{2v\tilde{\sigma}\hat{I}}$.

The point group $\mathbf{C}_{2v}$ has the following non-redundant set of subgroups (SSG):

$$\text{SSG}_{\mathbf{C}_{2v}} = \left\{ \overset{1}{\mathbf{C}_1}, \overset{2}{\mathbf{C}_2}, \overset{5}{\mathbf{C}_s}, \overset{6}{\mathbf{C}'_s}, \overset{9}{\mathbf{C}_{2v}} \right\}, \tag{121}$$

where the subgroups are aligned in the ascending order of their orders and attached by the sequential numbers of the subgroups listed in Eq. 16. (cf. $\text{SG}^{[\text{III}]}$ in Eq. 19 and $\text{SG}^{[\text{V}]}$ in Eq. 21). The mark table $M_{\mathbf{C}_{2v}}$ (Table A.5 of [23]) and the inverse mark table $M^{-1}_{\mathbf{C}_{2v}}$ (Table B.5 of [23]) are cited for the sake of convenience as follows:

$$M_{\mathbf{C}_{2v}} = M_{\mathbf{C}_{2\tilde{\sigma}}} = \begin{pmatrix} 4 & 0 & 0 & 0 & 0 \\ 2 & 2 & 0 & 0 & 0 \\ 2 & 0 & 2 & 0 & 0 \\ 2 & 0 & 0 & 2 & 0 \\ 1 & 1 & 1 & 1 & 1 \end{pmatrix} \tag{122}$$

$$M^{-1}_{\mathbf{C}_{2v}} = M^{-1}_{\mathbf{C}_{2\tilde{\sigma}}} = \begin{pmatrix} \frac{1}{4} & 0 & 0 & 0 & 0 \\ -\frac{1}{4} & \frac{1}{2} & 0 & 0 & 0 \\ -\frac{1}{4} & 0 & \frac{1}{2} & 0 & 0 \\ -\frac{1}{4} & 0 & 0 & \frac{1}{2} & 0 \\ \frac{1}{2} & -\frac{1}{2} & -\frac{1}{2} & -\frac{1}{2} & 1 \end{pmatrix}. \tag{123}$$

The USCI-CFs corresponding to $\mathbf{C}_{2v}(/\mathbf{C}_1)$ are obtained according to the USCI approach (Table E.5 of Ref. [23]). These USCI-CFs are regarded as SCI-CFs of the symmetry-restricted skeletons derived from **2**, so that the subduced-cycle-indices (SCI-CFs) are obtained to form the following row vector:

$$\text{SCI-CF}_{\mathbf{C}_{2v}(/\mathbf{C}_1)} = \left(b_1^4, b_2^2, c_2^2, c_2^2, c_4\right). \tag{124}$$

Compare this vector with $\text{SCI-CF}_{\mathbf{C}_{2v\tilde{\sigma}\tilde{I}}(/\mathbf{C}_{\tilde{I}})}$ (Eq. 65).

The ligand-inventory functions (Eqs. 24–26) are introduced into each SCI-CF collected in $\text{SCI-CF}_{\mathbf{C}_{2v}(/\mathbf{C}_1)}$ (Eq. 124). Thereby, the corresponding fixed-point matrices, FPM'_1 and FPM'_2 are obtained in a similar way to FPM_1 (Eq. 60) and FPM_2 (Eq. 61). These FPM'_1 and FPM'_2 are multiplied by the inverse mark table $M^{-1}_{\mathbf{C}_{2v}}$ (Eq. 123) to give the corresponding isomer-counting matrices, ICM'_1 and ICM'_2, respectively:

$$\text{ICM}'_1 = \text{FPM}'_1 \times M^{-1}_{\mathbf{C}_{2v}}$$

$$\begin{matrix} [\theta]_1 \\ [\theta]_2 \\ [\theta]_3 \\ [\theta]_4 \\ [\theta]_5 \\ [\theta]_6 \\ [\theta]_7 \\ [\theta]_8 \\ [\theta]_9 \\ [\theta]_{10} \\ [\theta]_{11} \\ [\theta]_{12} \\ [\theta]_{13} \\ [\theta]_{14} \\ [\theta]_{15} \\ [\theta]_{16} \\ [\theta]_{17} \\ [\theta]_{18} \\ [\theta]_{19} \end{matrix} \begin{pmatrix} 1 & 1 & 1 & 1 & 1 \\ 4 & 0 & 0 & 0 & 0 \\ 4 & 0 & 0 & 0 & 0 \\ 6 & 2 & 2 & 2 & 0 \\ 6 & 2 & 0 & 0 & 0 \\ 12 & 0 & 0 & 0 & 0 \\ 12 & 0 & 0 & 0 & 0 \\ 12 & 0 & 4 & 4 & 0 \\ 12 & 0 & 0 & 0 & 0 \\ 24 & 0 & 0 & 0 & 0 \\ 24 & 0 & 0 & 0 & 0 \\ 12 & 0 & 0 & 0 & 0 \\ 24 & 0 & 0 & 0 & 0 \\ 24 & 0 & 0 & 0 & 0 \\ 4 & 0 & 0 & 0 & 0 \\ 12 & 0 & 0 & 0 & 0 \\ 12 & 0 & 0 & 0 & 0 \\ 24 & 0 & 0 & 0 & 0 \\ 24 & 0 & 0 & 0 & 0 \end{pmatrix} \begin{pmatrix} \frac{1}{4} & 0 & 0 & 0 & 0 \\ -\frac{1}{4} & \frac{1}{2} & 0 & 0 & 0 \\ -\frac{1}{4} & 0 & \frac{1}{2} & 0 & 0 \\ -\frac{1}{4} & 0 & 0 & \frac{1}{2} & 0 \\ \frac{1}{2} & -\frac{1}{2} & -\frac{1}{2} & -\frac{1}{2} & 1 \end{pmatrix} = \begin{matrix} [\theta]_1 \\ [\theta]_2 \\ [\theta]_3 \\ [\theta]_4 \\ [\theta]_5 \\ [\theta]_6 \\ [\theta]_7 \\ [\theta]_8 \\ [\theta]_9 \\ [\theta]_{10} \\ [\theta]_{11} \\ [\theta]_{12} \\ [\theta]_{13} \\ [\theta]_{14} \\ [\theta]_{15} \\ [\theta]_{16} \\ [\theta]_{17} \\ [\theta]_{18} \\ [\theta]_{19} \end{matrix} \begin{pmatrix} 0 & 0 & 0 & 0 & 1 \\ 1 & 0 & 0 & 0 & 0 \\ 1 & 0 & 0 & 0 & 0 \\ 0 & 1 & 1 & 1 & 0 \\ 1 & 1 & 0 & 0 & 0 \\ 3 & 0 & 0 & 0 & 0 \\ 3 & 0 & 0 & 0 & 0 \\ 1 & 0 & 2 & 2 & 0 \\ 3 & 0 & 0 & 0 & 0 \\ 6 & 0 & 0 & 0 & 0 \\ 6 & 0 & 0 & 0 & 0 \\ 3 & 0 & 0 & 0 & 0 \\ 6 & 0 & 0 & 0 & 0 \\ 6 & 0 & 0 & 0 & 0 \\ 1 & 0 & 0 & 0 & 0 \\ 3 & 0 & 0 & 0 & 0 \\ 3 & 0 & 0 & 0 & 0 \\ 6 & 0 & 0 & 0 & 0 \\ 6 & 0 & 0 & 0 & 0 \end{pmatrix} \tag{125}$$

$$
\begin{aligned}
\mathrm{ICM}'_2 &= \mathrm{FPM}'_2 \times M^{-1}_{\mathbf{C}_{2v}} \\
&= \begin{matrix}[\theta]_{20}\\ [\theta]_{21}\\ [\theta]_{22}\\ [\theta]_{23}\\ [\theta]_{24}\\ [\theta]_{25}\\ [\theta]_{26}\\ [\theta]_{27}\\ [\theta]_{28}\\ [\theta]_{29}\\ [\theta]_{30}\end{matrix}
\begin{pmatrix} 1 & 1 & 0 & 0 & 0 \\ 4 & 0 & 0 & 0 & 0 \\ 4 & 0 & 0 & 0 & 0 \\ 6 & 2 & 4 & 4 & 2 \\ 12 & 0 & 0 & 0 & 0 \\ 6 & 2 & 0 & 0 & 0 \\ 12 & 0 & 0 & 0 & 0 \\ 12 & 0 & 0 & 0 & 0 \\ 24 & 0 & 8 & 8 & 0 \\ 24 & 0 & 0 & 0 & 0 \\ 24 & 0 & 0 & 0 & 0 \end{pmatrix}
\begin{pmatrix} \frac{1}{4} & 0 & 0 & 0 & 0 \\ -\frac{1}{4} & \frac{1}{2} & 0 & 0 & 0 \\ -\frac{1}{4} & 0 & \frac{1}{2} & 0 & 0 \\ -\frac{1}{4} & 0 & 0 & \frac{1}{2} & 0 \\ \frac{1}{2} & -\frac{1}{2} & -\frac{1}{2} & -\frac{1}{2} & 1 \end{pmatrix} \\
&= \begin{matrix}[\theta]_{20}\\ [\theta]_{21}\\ [\theta]_{22}\\ [\theta]_{23}\\ [\theta]_{24}\\ [\theta]_{25}\\ [\theta]_{26}\\ [\theta]_{27}\\ [\theta]_{28}\\ [\theta]_{29}\\ [\theta]_{30}\end{matrix}
\begin{pmatrix} 0 & 1/2 & 0 & 0 & 0 \\ 1 & 0 & 0 & 0 & 0 \\ 1 & 0 & 0 & 0 & 0 \\ 0 & 0 & 1 & 1 & 2 \\ 3 & 0 & 0 & 0 & 0 \\ 1 & 1 & 0 & 0 & 0 \\ 3 & 0 & 0 & 0 & 0 \\ 3 & 0 & 0 & 0 & 0 \\ 2 & 0 & 4 & 4 & 0 \\ 6 & 0 & 0 & 0 & 0 \\ 6 & 0 & 0 & 0 & 0 \end{pmatrix}. \qquad (126)
\end{aligned}
$$

The columns of ICM'_1 (Eq. 125) or ICM'_2 (Eq. 126) are aligned in the order of subgroups listed in $\mathrm{SSG}_{\mathbf{C}_{2v}}$ (Eq. 121). The value 1/2 at the intersection between the $[\theta]_{20}$-row and 2nd $\mathbf{C}_2$-column corresponds to the term $\frac{1}{2}(\mathrm{p}^4 + \overline{\mathrm{p}}^4)$, which indicates the presence of one pair of enantiomeric promolecules with the partition $[\theta]_{20}$ and the point group $\mathbf{C}_2$.

8.1.2 The PCI method

According to the PCI method of the USCI approach [23], the multiplication of the set of SCI-CFs (Eq. 124) by the inverse mark table (Eq. 123), i.e., $\text{SCI-CF}_{\mathbf{C}_{2v}(/\mathbf{C}_1)} \times M^{-1}_{\mathbf{C}_{2v}}$, gives the PCI-CFs as follows:

$$\text{PCI-CF}'(\mathbf{C}_1) = \frac{1}{4}b_1^4 - \frac{1}{4}b_2^2 - \frac{1}{2}c_2^2 + \frac{1}{2}c_4 \qquad (127)$$

$$\text{PCI-CF}'(\mathbf{C}_2) = \frac{1}{2}b_2^2 - \frac{1}{2}c_4 \qquad (128)$$

$$\text{PCI-CF}'(\mathbf{C}_s) = \frac{1}{2}c_2^2 - \frac{1}{2}c_4 \qquad (129)$$

$$\text{PCI-CF}'(\mathbf{C}'_s) = \frac{1}{2}c_2^2 - \frac{1}{2}c_4 \qquad (130)$$

$$\text{PCI-CF}'(\mathbf{C}_{2v}) = c_4 \qquad (131)$$

The ligand-inventory functions (Eqs. 24–26) are introduced in the PCI-CFs (Eqs. 127–131). The resulting equations are expanded to give the following generating functions:

$$
\begin{aligned}
f'_{\mathbf{C}_1} = {} & \left\{(\mathrm{A}^3\mathrm{p} + \mathrm{A}^3\overline{\mathrm{p}}) + \cdots\right\}_{[\theta]_3} + \left\{3(\mathrm{A}^2\mathrm{Bp} + \mathrm{A}^2\mathrm{B}\overline{\mathrm{p}}) + \cdots\right\}_{[\theta]_7} \\
& + \left\{3(\mathrm{A}^2\mathrm{pq} + \mathrm{A}^2\overline{\mathrm{pq}}) + \cdots\right\}_{[\theta]_9} + \{6(\mathrm{ABXp} + \mathrm{ABX}\overline{\mathrm{p}}) + \cdots\}_{[\theta]_{11}} \\
& + \{6\mathrm{ABp}\overline{\mathrm{p}} + \cdots\}_{[\theta]_{13}} + \left\{3(\mathrm{ABp}^2 + \mathrm{AB}\overline{\mathrm{p}}^2) + \cdots\right\}_{[\theta]_{12}} \\
& + \{6(\mathrm{ABpq} + \mathrm{AB}\overline{\mathrm{pq}}) + \cdots\}_{[\theta]_{14}} + \left\{3(\mathrm{Ap}^2\overline{\mathrm{p}} + \mathrm{Ap}\overline{\mathrm{p}}^2) + \cdots\right\}_{[\theta]_{16}}
\end{aligned}
$$

$$
\begin{aligned}
&+\left\{3(\mathrm{Ap}^2\mathrm{q}+\mathrm{A}\overline{\mathrm{p}}^2\overline{\mathrm{q}})+\cdots\right\}_{[\theta]_{17}}+\left\{(\mathrm{Ap}^3+\mathrm{A}\overline{\mathrm{p}}^3)+\cdots\right\}_{[\theta]_{15}}\\
&+\{6(\mathrm{Ap}\overline{\mathrm{p}}\mathrm{q}+\mathrm{Ap}\overline{\mathrm{p}}\overline{\mathrm{q}})+\cdots\}_{[\theta]_{18}}+\{6(\mathrm{Apqr}+\mathrm{A}\overline{\mathrm{pqr}})+\cdots\}_{[\theta]_{19}}\\
&+\left\{(\mathrm{p}^3\overline{\mathrm{p}}+\mathrm{p}\overline{\mathrm{p}}^3)+\cdots\right\}_{[\theta]_{21}}+\left\{(\mathrm{p}^3\mathrm{q}+\overline{\mathrm{p}}^3\overline{\mathrm{q}})+\cdots\right\}_{[\theta]_{22}}\\
&+\left\{3(\mathrm{p}^2\overline{\mathrm{p}}\mathrm{q}+\mathrm{p}\overline{\mathrm{p}}^2\overline{\mathrm{q}})+\cdots\right\}_{[\theta]_{24}}+\left\{3(\mathrm{p}^2\mathrm{q}\overline{\mathrm{q}}+\overline{\mathrm{p}}^2\mathrm{q}\overline{\mathrm{q}})+\cdots\right\}_{[\theta]_{26}}\\
&+\left\{3(\mathrm{p}^2\mathrm{qr}+\overline{\mathrm{p}}^2\overline{\mathrm{qr}})+\cdots\right\}_{[\theta]_{27}}+\{6(\mathrm{p}\overline{\mathrm{p}}\mathrm{qr}+\mathrm{p}\overline{\mathrm{pqr}})+\cdots\}_{[\theta]_{29}}+\{6(\mathrm{pqrs}+\overline{\mathrm{pqrs}})+\cdots\}_{[\theta]_{30}}\\
&+\left\{(\mathrm{A}^2\mathrm{p}^2+\mathrm{A}^2\overline{\mathrm{p}}^2)+\cdots\right\}_{[\theta]_5}+\left\{(\mathrm{p}^2\mathrm{q}^2+\overline{\mathrm{p}}^2\overline{\mathrm{q}}^2)+\cdots\right\}_{[\theta]_{25}}\\
&+\left\{(\mathrm{A}^3\mathrm{B})+\cdots\right\}_{[\theta]_2}+\left\{3(\mathrm{A}^2\mathrm{BX})+\cdots\right\}_{[\theta]_6}+\{6(\mathrm{ABXY})+\cdots\}_{[\theta]_{10}}\\
&+\left\{(\mathrm{A}^2\mathrm{p}\overline{\mathrm{p}})+\cdots\right\}_{[\theta]_8}+\{2(\mathrm{p}\overline{\mathrm{p}}\mathrm{q}\overline{\mathrm{q}})+\cdots\}_{[\theta]_{28}} \qquad (132)
\end{aligned}
$$

$$
\begin{aligned}
f'_{\mathbf{C}_2} &= \left\{(\mathrm{A}^2\mathrm{p}^2+\mathrm{A}^2\overline{\mathrm{p}}^2)+\cdots\right\}_{[\theta]_5}+\left\{(\mathrm{p}^2\mathrm{q}^2+\overline{\mathrm{p}}^2\overline{\mathrm{q}}^2)+\cdots\right\}_{[\theta]_{25}}\\
&+\left\{(\mathrm{A}^2\mathrm{B}^2)+\cdots\right\}_{[\theta]_4}+\left\{\frac{1}{2}(\mathrm{p}^4+\overline{\mathrm{p}}^4)+\cdots\right\}_{[\theta]_{20}} \qquad (133)
\end{aligned}
$$

$$
\begin{aligned}
f'_{\mathbf{C}_s} &= \left\{2(\mathrm{A}^2\mathrm{p}\overline{\mathrm{p}})+\cdots\right\}_{[\theta]_8}+\{4(\mathrm{p}\overline{\mathrm{p}}\mathrm{q}\overline{\mathrm{q}})+\cdots\}_{[\theta]_{28}}\\
&+\left\{(\mathrm{A}^2\mathrm{B}^2)+\cdots\right\}_{[\theta]_4}+\left\{(\mathrm{p}^2\overline{\mathrm{p}}^2)+\cdots\right\}_{[\theta]_{23}} \qquad (134)
\end{aligned}
$$

$$
\begin{aligned}
f'_{\mathbf{C}'_s} &= \left\{2(\mathrm{A}^2\mathrm{p}\overline{\mathrm{p}})+\cdots\right\}_{[\theta]_8}+\{4(\mathrm{p}\overline{\mathrm{p}}\mathrm{q}\overline{\mathrm{q}})+\cdots\}_{[\theta]_{28}}\\
&+\left\{(\mathrm{A}^2\mathrm{B}^2)+\cdots\right\}_{[\theta]_4}+\left\{(\mathrm{p}^2\overline{\mathrm{p}}^2)+\cdots\right\}_{[\theta]_{23}} \qquad (135)
\end{aligned}
$$

$$
f'_{\mathbf{C}_{2v}} = \left\{2(\mathrm{p}^2\overline{\mathrm{p}}^2)+\cdots\right\}_{[\theta]_{23}}+\left\{(\mathrm{A}^4)+\cdots\right\}_{[\theta]_1} \qquad (136)
$$

Each pair of braces in the generating functions (Eqs. 132–136) contains terms having the same partition, which is shown in the subscript attached to the ending brace. For example, the term $\{6(\mathrm{ABXp}+\mathrm{ABX}\overline{\mathrm{p}})+\cdots\}_{[\theta]_{11}}$ (Eq. 132) indicates the presence of twelve pairs of enantiomeric $\mathbf{C}_1$-promolecules with ABXp or ABX$\overline{\mathrm{p}}$ ($[\theta]_{11}$) under the point-group symmetry. The value 6 due to the PCI method is identical with the counterpart value due to the FPM method, which appears at the intersection between the $[\theta]_{11}$-row and the first $\mathbf{C}_1$-column of the isomer-counting matrix ICM'_1 (Eq. 125). In general, the generating function $f'_{\mathbf{G}_j}$ for the subgroup $\mathbf{G}_j$ (j = 1–5, Eqs. 132–136) corresponds to the $\mathbf{G}_j$-columns (j = 1–5) of the isomer-counting matrices, ICM'_1 (Eq. 125) and ICM'_2 (Eq. 126).

8.1.3 The RS-stereoisomeric group $\mathbf{C}_{2v\widetilde{\sigma}\widehat{I}}$ versus the point group $\mathbf{C}_{2v}$

The PCI-CFs for the point group $\mathbf{C}_{2v}$ (Eqs. 127–131) can be derived by starting the PCI-CFs for the *RS*-stereoisomeric group $\mathbf{C}_{2v\widetilde{\sigma}\widehat{I}}$ (Eqs. 67–82). Note that a set of *RS*-stereoisomeric subgroups coalesces to give the common maximum point subgroup. For example, $\overset{1}{\mathbf{C}}_1$, $\overset{3}{\mathbf{C}}_{\widetilde{\sigma}}$, $\overset{4}{\mathbf{C}}'_{\widetilde{\sigma}}$, $\overset{7}{\mathbf{C}}_{\widehat{I}}$, and $\overset{8}{\mathbf{C}}_{\widehat{\sigma}}$ coalesce to give the point group

$\mathbf{C}_1$ as the common maximum subgroup. By referring to Fig. 6, each quadruplet of type III or V under the *RS*-stereoisomeric group corresponds to two pairs of enantiomers or two achiral promolecules under the point group, while each quadruplet of type I, II, or IV under the *RS*-stereoisomeric group corresponds to one pair of enantiomers or one achiral promolecule under the point group. It follows that the following relationships between the PCI-CFs for the point group $\mathbf{C}_{2v}$ (Eqs. 127–131) and the PCI-CFs for the *RS*-stereoisomeric group $\mathbf{C}_{2v\tilde{\sigma}\hat{I}}$ (Eqs. 67–82) are obtained:

$$\begin{aligned}\text{PCI-CF}'(\mathbf{C}_1) = 2\text{PCI-CF}\left(\overset{1}{\mathbf{C}}_1\right) + \text{PCI-CF}\left(\overset{3}{\mathbf{C}}_{\tilde{\sigma}}\right) + \text{PCI-CF}\left(\overset{4}{\mathbf{C}}'_{\tilde{\sigma}}\right) \\ + \text{PCI-CF}\left(\overset{7}{\mathbf{C}}_{\hat{I}}\right) + \text{PCI-CF}\left(\overset{8}{\mathbf{C}}_{\hat{\sigma}}\right)\end{aligned} \tag{137}$$

$$\text{PCI-CF}'(\mathbf{C}_2) = 2\text{PCI-CF}\left(\overset{2}{\mathbf{C}}_2\right) + \text{PCI-CF}\left(\overset{12}{\mathbf{C}}_{2\hat{I}}\right) + \text{PCI-CF}\left(\overset{15}{\mathbf{C}}_{2\tilde{\sigma}}\right) \tag{138}$$

$$\text{PCI-CF}'(\mathbf{C}_s) = 2\text{PCI-CF}\left(\overset{5}{\mathbf{C}}_s\right) + \text{PCI-CF}\left(\overset{10}{\mathbf{C}}_{s\tilde{\sigma}\hat{I}}\right) + \text{PCI-CF}\left(\overset{14}{\mathbf{C}}'_{s\tilde{\sigma}\hat{\sigma}}\right) \tag{139}$$

$$\text{PCI-CF}'\left(\mathbf{C}'_s\right) = 2\text{PCI-CF}\left(\overset{6}{\mathbf{C}}'_s\right) + \text{PCI-CF}\left(\overset{11}{\mathbf{C}}'_{s\tilde{\sigma}\hat{I}}\right) + \text{PCI-CF}\left(\overset{13}{\mathbf{C}}_{s\tilde{\sigma}\hat{\sigma}}\right) \tag{140}$$

$$\text{PCI-CF}'(\mathbf{C}_{2v}) = 2\text{PCI-CF}\left(\overset{9}{\mathbf{C}}_{2v}\right) + \text{PCI-CF}\left(\overset{16}{\mathbf{C}}_{2v\tilde{\sigma}\hat{I}}\right) \tag{141}$$

In a parallel way, the relationships between the generating functions for the point group $\mathbf{C}_{2v}$ (Eqs. 132–136) and those for the *RS*-stereoisomeric group $\mathbf{C}_{2v\tilde{\sigma}\hat{I}}$ (Eqs. 83–98) are obtained as follows:

$$f'_{\mathbf{C}_1} = 2f_{\mathbf{C}_1} + f_{\mathbf{C}_{\tilde{\sigma}}} + f_{\mathbf{C}'_{\tilde{\sigma}}} + f_{\mathbf{C}_{\hat{I}}} + f_{\mathbf{C}_{\hat{\sigma}}} \tag{142}$$

$$f'_{\mathbf{C}_2} = 2f_{\mathbf{C}_2} + f_{\mathbf{C}_{2\hat{I}}} + f_{\mathbf{C}_{2\tilde{\sigma}}} \tag{143}$$

$$f'_{\mathbf{C}_s} = 2f_{\mathbf{C}_s} + f_{\mathbf{C}_{s\tilde{\sigma}\hat{I}}} + f_{\mathbf{C}'_{s\tilde{\sigma}\hat{\sigma}}} \tag{144}$$

$$f'_{\mathbf{C}'_s} = 2f_{\mathbf{C}'_s} + f_{\mathbf{C}'_{s\tilde{\sigma}\hat{I}}} + f_{\mathbf{C}_{s\tilde{\sigma}\hat{\sigma}}} \tag{145}$$

$$f'_{\mathbf{C}_{2v}} = 2f_{\mathbf{C}_{2v}} + f_{\mathbf{C}_{2v\tilde{\sigma}\hat{I}}} \tag{146}$$

By keeping these relationships in mind, each column of ICM'_1 (Eq. 125) or ICM'_2 (Eq. 126) can be calculated by summing up an appropriate set of columns of ICM_1 (Eq. 60) or ICM_2 (Eq. 61). For example, the first (duplicated), third, 4th, 7th, and 8th columns of ICM_1 (Eq. 60) or ICM_2 (Eq. 61) are summed up to give the first column of ICM'_1 (Eq. 125) or ICM'_2 (Eq. 126) in agreement with Eq. 142 (cf. Eq. 137).

Each of the representative promolecules shown in Figs. 7 (type I), 9 (type II), 11 (type III, list 1), 12 (type III, list 2), 14 (type IV), and 16 (type V) contains the data of relevant groups, e.g., $\mathbf{C}_{\hat{I}}$, $\mathbf{C}_1$, $\mathbf{C}_1$, I (*RS*-stereoisomeric group, point group, *RS*-permutation group, and stereoisogram type) for the promolecule **10**.

The enumeration under the point group $\mathbf{C}_{2v}$ (Eqs. 142–146) are divided into two parts, i.e., chiral subgroups (Eqs. 142 and 143) and achiral subgroups (Eqs. 144–146). See the division by a horizontal double line in Fig. 6.

The set of chiral subgroups (Eqs. 142 and 143) under the point-group symmetry is correlated to stereoisograms of type I, II, and III, which are characterized by the chirality along the vertical direction under the *RS*-stereoisomeric-group symmetry.

1. In accord with Eq. 142, the point group $\mathbf{C}_1$ corresponds to all the type-III ($\mathbf{C}_1$) promolecules listed in Figs. 11 and 12 (except **98** and **99**), all the type-II ($\mathbf{C}_{\tilde{\sigma}}$ and $\mathbf{C}'_{\tilde{\sigma}}$) promolecules listed in Fig. 9 (except **29**), and all the type-I ($\mathbf{C}_{\hat{1}}$ and $\mathbf{C}_{\hat{\sigma}}$) promolecules listed in Fig. 7 (except **23**). Note that these *RS*-stereoisomeric groups contain $\mathbf{C}_1$ as the maximum point group.
2. In accord with Eq. 143, the point group $\mathbf{C}_2$ corresponds to the type-III ($\mathbf{C}_2$) promolecules **98** and **99** shown in Fig. 12, the type-I ($\mathbf{C}_{2\hat{1}}$) promolecule **23** shown in Fig. 7, and the type-II ($\mathbf{C}_{2\tilde{\sigma}}$) promolecule **29** shown in Fig. 9. Note that these *RS*-stereoisomeric groups contain $\mathbf{C}_2$ as the maximum point group.

On the other hand, the set of achiral subgroups under the point-group symmetry (Eqs. 144–146) is correlated to stereoisograms of type IV and V, which are characterized by the achirality along the vertical direction under the *RS*-stereoisomeric-group symmetry.

1. In accord with Eq. 144, the point group $\mathbf{C}_s$ corresponds to the type-V ($\mathbf{C}_s$) promolecules **107**, **109**, and **110** shown in Fig. 16, the type-IV ($\mathbf{C}_{s\tilde{\sigma}\hat{1}}$) promolecule **101** shown in Fig. 14, and the type-IV ($\mathbf{C}'_{s\tilde{\sigma}\tilde{\sigma}}$) promolecule **104** shown in Fig. 14. Note that these *RS*-stereoisomeric groups contain $\mathbf{C}_s$ as the maximum point group.
2. In accord with Eq. 145, the point group $\mathbf{C}'_s$ corresponds to the type-V ($\mathbf{C}'_s$) promolecules **108**, **111**, and **112** shown in Fig. 16, the type-IV ($\mathbf{C}'_{s\tilde{\sigma}\hat{1}}$) promolecule **102** shown in Fig. 14, and the type-IV ($\mathbf{C}_{s\tilde{\sigma}\tilde{\sigma}}$) promolecule **103** shown in Fig. 14. Note that these *RS*-stereoisomeric groups contain $\mathbf{C}'_s$ as the maximum point group.
3. In accord with Eq. 146, the point group $\mathbf{C}_{2v}$ corresponds to the type-V ($\mathbf{C}_{2v}$) promolecule **113** shown in Fig. 16 and the type-IV ($\mathbf{C}_{2v\tilde{\sigma}\hat{1}}$) promolecule **105** shown in Fig. 14. Note that these *RS*-stereoisomeric groups contain $\mathbf{C}_{2v}$ as the maximum point group.

8.2 Enumeration of oxiranes under the *RS*-permutation group $\mathbf{C}_{2\tilde{\sigma}}$

8.2.1 The FPM method

Suppose that the oxirane skeleton **2** is considered to belong to the *RS*-permutation group $\mathbf{C}_{2\tilde{\sigma}}$ in place of the *RS*-stereoisomeric group $\mathbf{C}_{2v\tilde{\sigma}\hat{1}}$ and of the point group $\mathbf{C}_{2v}$. The four positions of **2** construct an orbit governed by the coset representation $\mathbf{C}_{2\tilde{\sigma}}(/\mathbf{C}_1)$ under the *RS*-permutation group $\mathbf{C}_{2\tilde{\sigma}}$ in place of the coset representation $\mathbf{C}_{2v\tilde{\sigma}\hat{1}}(/\mathbf{C}_{\hat{1}})$ under the *RS*-stereoisomeric group $\mathbf{C}_{2v\tilde{\sigma}\hat{1}}$ as well as in place of $\mathbf{C}_{2v}(/\mathbf{C}_1)$ under the point group $\mathbf{C}_{2v}$.

The *RS*-permutation group $\mathbf{C}_{2\tilde{\sigma}}$ has the following non-redundant set of subgroups (SSG):

$$\mathrm{SSG}_{\mathbf{C}_{2\tilde{\sigma}}} = \left\{ \overset{1}{\mathbf{C}}_1, \overset{2}{\mathbf{C}}_2, \overset{3}{\mathbf{C}}_{\tilde{\sigma}}, \overset{4}{\mathbf{C}}'_{\tilde{\sigma}}, \overset{15}{\mathbf{C}}_{2\tilde{\sigma}} \right\}, \tag{147}$$

which are type-II and type-III subgroups selected from Eq. 16 (cf. $\mathrm{SG}^{[\mathrm{II}]}$ in Eq. 18 and $\mathrm{SG}^{[\mathrm{III}]}$ in Eq. 19), where the subgroups are aligned in the ascending order of their orders and attached by the sequential numbers of the subgroups listed in Eq. 16. Because $\mathbf{C}_{2\tilde{\sigma}}$ is isomorphic to $\mathbf{C}_{2v}$, the mark table $M_{\mathbf{C}_{2\tilde{\sigma}}}$ and its inverse $M^{-1}_{\mathbf{C}_{2\tilde{\sigma}}}$ are identical with Eqs. 122 and 123, respectively.

The USCI-CFs corresponding to $\mathbf{C}_{2\tilde{\sigma}}(/\mathbf{C}_1)$ are obtained according to the USCI approach because of its isomorphism with the point group $\mathbf{C}_{2v}$ (Table E.5 of Ref. [23]), where all of the operations of the *RS*-permutation group $\mathbf{C}_{2\tilde{\sigma}}$ are determined to be exchiral. These USCI-CFs are regarded as SCI-CFs of the symmetry-restricted skeletons derived from **2**, so that the subduced-cycle-indices (SCI-CFs) are obtained to form the following row vector:

$$\text{SCI-CF}_{\mathbf{C}_{2\tilde{\sigma}}(/\mathbf{C}_1)} = \left(b_1^4, b_2^2, b_2^2, b_2^2, b_4 \right), \tag{148}$$

which consists of only hemispheric sphericity indices (b_1, b_2, and b_4) because of the exchirality of the *RS*-permutation group $\mathbf{C}_{2\tilde{\sigma}}$. Compare this vector with $\text{SCI-CF}_{\mathbf{C}_{2v}(/\mathbf{C}_1)}$ (Eq. 124) and with $\text{SCI-CF}_{\mathbf{C}_{2v\tilde{\sigma}\tilde{I}}(/\mathbf{C}_{\tilde{I}})}$ (Eq. 65).

Among the ligand-inventory functions (Eqs. 24–26), the last one (Eq. 26) is effective to the SCI-CF represented by Eq. 148. Thereby, the corresponding fixed-point matrices, FPM''_1 and FPM''_2 are obtained in a similar way to FPM'_1 (Eq. 125) and FPM'_2 (Eq. 126) as well as to FPM_1 (Eq. 60) and FPM_2 (Eq. 61). These FPM''_1 and FPM''_2 are multiplied by the inverse mark table $M^{-1}_{\mathbf{C}_{2\tilde{\sigma}}}$ (Eq. 123) to give the corresponding isomer-counting matrices, ICM''_1 and ICM''_2, respectively:

$$\mathrm{ICM}''_1 = \mathrm{FPM}''_1 \times M^{-1}_{\mathbf{C}_{2\tilde{\sigma}}}$$

$$\begin{matrix} [\theta]_1 \\ [\theta]_2 \\ [\theta]_3 \\ [\theta]_4 \\ [\theta]_5 \\ [\theta]_6 \\ [\theta]_7 \\ [\theta]_8 \\ [\theta]_9 \\ [\theta]_{10} \\ [\theta]_{11} \\ [\theta]_{12} \\ [\theta]_{13} \\ [\theta]_{14} \\ [\theta]_{15} \\ [\theta]_{16} \\ [\theta]_{17} \\ [\theta]_{18} \\ [\theta]_{19} \end{matrix}$$
$$= \begin{pmatrix} 1 & 1 & 1 & 1 & 1 \\ 4 & 0 & 0 & 0 & 0 \\ 4 & 0 & 0 & 0 & 0 \\ 6 & 2 & 2 & 2 & 0 \\ 6 & 2 & 2 & 2 & 0 \\ 12 & 0 & 0 & 0 & 0 \\ 12 & 0 & 0 & 0 & 0 \\ 12 & 0 & 0 & 0 & 0 \\ 12 & 0 & 0 & 0 & 0 \\ 24 & 0 & 0 & 0 & 0 \\ 24 & 0 & 0 & 0 & 0 \\ 12 & 0 & 0 & 0 & 0 \\ 24 & 0 & 0 & 0 & 0 \\ 24 & 0 & 0 & 0 & 0 \\ 4 & 0 & 0 & 0 & 0 \\ 12 & 0 & 0 & 0 & 0 \\ 12 & 0 & 0 & 0 & 0 \\ 24 & 0 & 0 & 0 & 0 \\ 24 & 0 & 0 & 0 & 0 \end{pmatrix} \begin{pmatrix} \frac{1}{4} & 0 & 0 & 0 & 0 \\ -\frac{1}{4} & \frac{1}{2} & 0 & 0 & 0 \\ -\frac{1}{4} & 0 & \frac{1}{2} & 0 & 0 \\ -\frac{1}{4} & 0 & 0 & \frac{1}{2} & 0 \\ \frac{1}{2} & -\frac{1}{2} & -\frac{1}{2} & -\frac{1}{2} & 1 \end{pmatrix} = \begin{matrix} [\theta]_1 \\ [\theta]_2 \\ [\theta]_3 \\ [\theta]_4 \\ [\theta]_5 \\ [\theta]_6 \\ [\theta]_7 \\ [\theta]_8 \\ [\theta]_9 \\ [\theta]_{10} \\ [\theta]_{11} \\ [\theta]_{12} \\ [\theta]_{13} \\ [\theta]_{14} \\ [\theta]_{15} \\ [\theta]_{16} \\ [\theta]_{17} \\ [\theta]_{18} \\ [\theta]_{19} \end{matrix} \begin{pmatrix} 0 & 0 & 0 & 0 & 1 \\ 1 & 0 & 0 & 0 & 0 \\ 1 & 0 & 0 & 0 & 0 \\ 0 & 1 & 1 & 1 & 0 \\ 0 & 1 & 1 & 1 & 0 \\ 3 & 0 & 0 & 0 & 0 \\ 3 & 0 & 0 & 0 & 0 \\ 3 & 0 & 0 & 0 & 0 \\ 3 & 0 & 0 & 0 & 0 \\ 6 & 0 & 0 & 0 & 0 \\ 6 & 0 & 0 & 0 & 0 \\ 3 & 0 & 0 & 0 & 0 \\ 6 & 0 & 0 & 0 & 0 \\ 6 & 0 & 0 & 0 & 0 \\ 1 & 0 & 0 & 0 & 0 \\ 3 & 0 & 0 & 0 & 0 \\ 3 & 0 & 0 & 0 & 0 \\ 6 & 0 & 0 & 0 & 0 \\ 6 & 0 & 0 & 0 & 0 \end{pmatrix} \tag{149}$$

$$
\begin{aligned}
\mathrm{ICM}_2'' &= \mathrm{FPM}_2'' \times M_{\mathbf{C}_{2\widetilde{\sigma}}}^{-1} \\
&= \begin{matrix}[\theta]_{20}\\ [\theta]_{21}\\ [\theta]_{22}\\ [\theta]_{23}\\ [\theta]_{24}\\ [\theta]_{25}\\ [\theta]_{26}\\ [\theta]_{27}\\ [\theta]_{28}\\ [\theta]_{29}\\ [\theta]_{30}\end{matrix}
\begin{pmatrix} 1 & 1 & 1 & 1 & 1 \\ 4 & 0 & 0 & 0 & 0 \\ 4 & 0 & 0 & 0 & 0 \\ 6 & 2 & 2 & 2 & 0 \\ 12 & 0 & 0 & 0 & 0 \\ 6 & 2 & 2 & 2 & 0 \\ 12 & 0 & 0 & 0 & 0 \\ 12 & 0 & 0 & 0 & 0 \\ 24 & 0 & 0 & 0 & 0 \\ 24 & 0 & 0 & 0 & 0 \\ 24 & 0 & 0 & 0 & 0 \end{pmatrix}
\begin{pmatrix} \frac{1}{4} & 0 & 0 & 0 & 0 \\ -\frac{1}{4} & \frac{1}{2} & 0 & 0 & 0 \\ -\frac{1}{4} & 0 & \frac{1}{2} & 0 & 0 \\ -\frac{1}{4} & 0 & 0 & \frac{1}{2} & 0 \\ \frac{1}{2} & -\frac{1}{2} & -\frac{1}{2} & -\frac{1}{2} & 1 \end{pmatrix} \\
&= \begin{matrix}[\theta]_{20}\\ [\theta]_{21}\\ [\theta]_{22}\\ [\theta]_{23}\\ [\theta]_{24}\\ [\theta]_{25}\\ [\theta]_{26}\\ [\theta]_{27}\\ [\theta]_{28}\\ [\theta]_{29}\\ [\theta]_{30}\end{matrix}
\begin{pmatrix} 0 & 0 & 0 & 0 & 1 \\ 1 & 0 & 0 & 0 & 0 \\ 1 & 0 & 0 & 0 & 0 \\ 0 & 1 & 1 & 1 & 0 \\ 3 & 0 & 0 & 0 & 0 \\ 0 & 1 & 1 & 1 & 0 \\ 3 & 0 & 0 & 0 & 0 \\ 3 & 0 & 0 & 0 & 0 \\ 6 & 0 & 0 & 0 & 0 \\ 6 & 0 & 0 & 0 & 0 \\ 6 & 0 & 0 & 0 & 0 \end{pmatrix}
\end{aligned} \tag{150}
$$

The columns of ICM_1'' (Eq. 149) or ICM_2'' (Eq. 150) are aligned in the order of subgroups listed in $\mathrm{SSG}_{\mathbf{C}_{2\widetilde{\sigma}}}$ (Eq. 147).

8.2.2 The PCI method

According to the PCI method of the USCI approach [23], the multiplication of the set of SCI-CFs (Eq. 148) by the inverse mark table (Eq. 123), i.e., $\text{SCI-CF}_{\mathbf{C}_{2\widetilde{\sigma}}(/\mathbf{C}_1)} \times M_{\mathbf{C}_{2\widetilde{\sigma}}}^{-1}$, gives the PCI-CFs as follows:

$$\text{PCI-CF}''(\mathbf{C}_1) = \frac{1}{4}b_1^4 - \frac{3}{4}b_2^2 + \frac{1}{2}b_4 \tag{151}$$

$$\text{PCI-CF}''(\mathbf{C}_2) = \frac{1}{2}b_2^2 - \frac{1}{2}b_4 \tag{152}$$

$$\text{PCI-CF}''(\mathbf{C}_{\widehat{\sigma}}) = \frac{1}{2}b_2^2 - \frac{1}{2}b_4 \tag{153}$$

$$\text{PCI-CF}''(\mathbf{C}'_{\widehat{\sigma}}) = \frac{1}{2}b_2^2 - \frac{1}{2}b_4 \tag{154}$$

$$\text{PCI-CF}''(\mathbf{C}_{2\widehat{\sigma}}) = b_4 \tag{155}$$

Among the ligand-inventory functions (Eqs. 24–26), the last one (Eq. 26) is introduced into the PCI-CFs (Eqs. 151–155). The resulting equations are expanded to give the following generating functions:

$$
\begin{aligned}
f''_{\mathbf{C}_1} = {} & \left\{(\mathrm{A}^3\mathrm{p} + \mathrm{A}^3\overline{\mathrm{p}}) + \cdots\right\}_{[\theta]_3} + 3(\mathrm{A}^2\mathrm{Bp} + \mathrm{A}^2\mathrm{B}\overline{\mathrm{p}}) + \cdots\Big\}_{[\theta]_7} \\
& + \left\{3(\mathrm{A}^2\mathrm{pq} + \mathrm{A}^2\overline{\mathrm{pq}}) + \cdots\right\}_{[\theta]_9} + \{6(\mathrm{ABXp} + \mathrm{ABX}\overline{\mathrm{p}}) + \cdots\}_{[\theta]_{11}} \\
& + \{6\mathrm{ABp}\overline{\mathrm{p}} + \cdots\}_{[\theta]_{13}} + \left\{3(\mathrm{ABp}^2 + \mathrm{AB}\overline{\mathrm{p}}^2) + \cdots\right\}_{[\theta]_{12}} \\
& + \{6(\mathrm{ABpq} + \mathrm{AB}\overline{\mathrm{pq}}) + \cdots\}_{[\theta]_{14}} + \left\{3(\mathrm{Ap}^2\overline{\mathrm{p}} + \mathrm{Ap}\overline{\mathrm{p}}^2) + \cdots\right\}_{[\theta]_{16}} \\
& + \left\{3(\mathrm{Ap}^2\mathrm{q} + \mathrm{A}\overline{\mathrm{p}}^2\overline{\mathrm{q}}) + \cdots\right\}_{[\theta]_{17}} + \left\{(\mathrm{Ap}^3 + \mathrm{A}\overline{\mathrm{p}}^3) + \cdots\right\}_{[\theta]_{15}}
\end{aligned}
$$

$$
\begin{aligned}
&+\{6(\mathrm{Ap\overline{p}q}+\mathrm{Ap\overline{pq}})+\cdots\}_{[\theta]_{18}}+\{6(\mathrm{Apqr}+\mathrm{A\overline{pqr}})+\cdots\}_{[\theta]_{19}}\\
&+\left\{(\mathrm{p^3\overline{p}}+\mathrm{p\overline{p}^3})+\cdots\right\}_{[\theta]_{21}}+\left\{(\mathrm{p^3q}+\mathrm{\overline{p}^3\overline{q}})+\cdots\right\}_{[\theta]_{22}}\\
&+\left\{3(\mathrm{p^2\overline{p}q}+\mathrm{p\overline{p}^2\overline{q}})+\cdots\right\}_{[\theta]_{24}}+\left\{3(\mathrm{p^2q\overline{q}}+\mathrm{\overline{p}^2q\overline{q}})+\cdots\right\}_{[\theta]_{26}}\\
&+\left\{3(\mathrm{p^2qr}+\mathrm{\overline{p}^2\overline{qr}})+\cdots\right\}_{[\theta]_{27}}+\{6(\mathrm{p\overline{p}qr}+\mathrm{p\overline{pqr}})+\cdots\}_{[\theta]_{29}}\\
&+\{6(\mathrm{pqrs}+\mathrm{\overline{pqrs}})+\cdots\}_{[\theta]_{30}}\\
&+\left\{3(\mathrm{A^2p\overline{p}})+\cdots\right\}_{[\theta]_8}+\{6(\mathrm{p\overline{p}q\overline{q}})+\cdots\}_{[\theta]_{28}}\\
&+\left\{(\mathrm{A^3B})+\cdots\right\}_{[\theta]_2}+\left\{3(\mathrm{A^2BX})+\cdots\right\}_{[\theta]_6}\\
&+\{6(\mathrm{ABXY})+\cdots\}_{[\theta]_{10}} \qquad (156)
\end{aligned}
$$

$$
\begin{aligned}
f''_{\mathbf{C}_2}=&\left\{(\mathrm{A^2p^2}+\mathrm{A^2\overline{p}^2})+\cdots\right\}_{[\theta]_5}+\left\{(\mathrm{p^2q^2}+\mathrm{\overline{p}^2\overline{q}^2})+\cdots\right\}_{[\theta]_{25}}\\
&+\left\{(\mathrm{p^2\overline{p}^2})+\cdots\right\}_{[\theta]_{23}}+\left\{(\mathrm{A^2B^2})+\cdots\right\}_{[\theta]_4} \qquad (157)
\end{aligned}
$$

$$
\begin{aligned}
f''_{\mathbf{C}_{\tilde{\sigma}}}=&\left\{(\mathrm{A^2p^2}+\mathrm{A^2\overline{p}^2})+\cdots\right\}_{[\theta]_5}+\left\{(\mathrm{p^2q^2}+\mathrm{\overline{p}^2\overline{q}^2})+\cdots\right\}_{[\theta]_{25}}\\
&+\left\{(\mathrm{A^2B^2})+\cdots\right\}_{[\theta]_4}+\left\{(\mathrm{p^2\overline{p}^2})+\cdots\right\}_{[\theta]_{23}} \qquad (158)
\end{aligned}
$$

$$
\begin{aligned}
f''_{\mathbf{C}'_{\tilde{\sigma}}}=&\left\{(\mathrm{A^2p^2}+\mathrm{A^2\overline{p}^2})+\cdots\right\}_{[\theta]_5}+\left\{(\mathrm{p^2q^2}+\mathrm{\overline{p}^2\overline{q}^2})+\cdots\right\}_{[\theta]_{25}}\\
&+\left\{(\mathrm{A^2B^2})+\cdots\right\}_{[\theta]_4}+\left\{(\mathrm{p^2\overline{p}^2})+\cdots\right\}_{[\theta]_{23}} \qquad (159)
\end{aligned}
$$

$$
f''_{\mathbf{C}_{2\tilde{\sigma}}}=\left\{(\mathrm{p^4}+\mathrm{\overline{p}^4})+\cdots\right\}_{[\theta]_{20}}+\left\{(\mathrm{A^4})+\cdots\right\}_{[\theta]_1} \qquad (160)
$$

Each pair of braces in the generating functions (Eqs. 156–160) contains terms having the same partition, which is shown in the subscript attached to the ending brace. The generating function $f''_{\mathbf{G}_j}$ for the subgroup $\mathbf{G}_j$ (j = 1–5, Eqs. 156–160) corresponds to the $\mathbf{G}_j$-columns (j = 1–5) of the isomer-counting matrices, ICM''_1 (Eq. 149) and ICM''_2 (Eq. 150).

8.2.3 The RS-stereoisomeric group $\mathbf{C}_{2v\tilde{\sigma}\hat{I}}$ versus the RS-permutation group $\mathbf{C}_{2\tilde{\sigma}}$

The PCI-CFs for the *RS*-permutation group $\mathbf{C}_{2\tilde{\sigma}}$ (Eqs. 151–155) can be derived by starting the PCI-CFs for the *RS*-stereoisomeric group $\mathbf{C}_{2v\tilde{\sigma}\hat{I}}$ (Eqs. 67–82). Each *RS*-permutation subgroup is constructed on the basis of the fact that a set of *RS*-stereoisomeric subgroups coalesces to give the common maximum *RS*-permutation subgroup. For example, $\overset{1}{\mathbf{C}}_1$, $\overset{5}{\mathbf{C}}_s$, $\overset{6}{\mathbf{C}}'_s$, $\overset{7}{\mathbf{C}}_{\hat{I}}$, and $\overset{8}{\mathbf{C}}_{\hat{\sigma}}$ coalesce to give the point group $\mathbf{C}_1$ as the common maximum subgroup.

It should be noted that enumeration under an *RS*-permutation group presumes that a pair of *RS*-diastereomers or an *RS*-astereogenic promolecule (as a pair of self-*RS*-diastereomers) is counted once. By referring to Fig. 6, each quadruplet of

type II or III under the *RS*-stereoisomeric group corresponds to two pairs of *RS*-diastereomers or two *RS*-astereogenic promolecules under the *RS*-permutation group, while each quadruplet of type I, IV, or V under the *RS*-stereoisomeric group corresponds to one pair of *RS*-diastereomers or one *RS*-astereogenic promolecule under the *RS*-permutation group. Hence, the PCI-CFs for the *RS*-permutation group $\mathbf{C}_{2\tilde{\sigma}}$ (Eqs. 151–155) are calculated from the PCI-CFs for the *RS*-stereoisomeric group $\mathbf{C}_{2v\tilde{\sigma}\hat{I}}$ (Eqs. 67–82) as follows:

$$\text{PCI-CF}''(\mathbf{C}_1) = 2\text{PCI-CF}\left(\overset{1}{\mathbf{C}}_1\right) + \text{PCI-CF}\left(\overset{5}{\mathbf{C}}_s\right) + \text{PCI-CF}\left(\overset{6}{\mathbf{C}}'_s\right) + \text{PCI-CF}\left(\overset{7}{\mathbf{C}}_{\hat{I}}\right) + \text{PCI-CF}\left(\overset{8}{\mathbf{C}}_{\hat{\sigma}}\right) \tag{161}$$

$$\text{PCI-CF}''(\mathbf{C}_2) = 2\text{PCI-CF}\left(\overset{2}{\mathbf{C}}_2\right) + \text{PCI-CF}\left(\overset{9}{\mathbf{C}}_{2v}\right) + \text{PCI-CF}\left(\overset{12}{\mathbf{C}}_{2\hat{I}}\right) \tag{162}$$

$$\text{PCI-CF}''(\mathbf{C}_{\tilde{\sigma}}) = 2\text{PCI-CF}\left(\overset{3}{\mathbf{C}}_{\tilde{\sigma}}\right) + \text{PCI-CF}\left(\overset{10}{\mathbf{C}}_{s\tilde{\sigma}\hat{I}}\right) + \text{PCI-CF}\left(\overset{13}{\mathbf{C}}_{s\tilde{\sigma}\hat{\sigma}}\right) \tag{163}$$

$$\text{PCI-CF}''(\mathbf{C}'_{\tilde{\sigma}}) = 2\text{PCI-CF}\left(\overset{4}{\mathbf{C}}'_{\tilde{\sigma}}\right) + \text{PCI-CF}\left(\overset{11}{\mathbf{C}}'_{s\tilde{\sigma}\hat{I}}\right) + \text{PCI-CF}\left(\overset{14}{\mathbf{C}}'_{s\tilde{\sigma}\hat{\sigma}}\right) \tag{164}$$

$$\text{PCI-CF}'(\mathbf{C}_{2\tilde{\sigma}}) = 2\text{PCI-CF}\left(\overset{15}{\mathbf{C}}_{2\tilde{\sigma}}\right) + \text{PCI-CF}\left(\overset{16}{\mathbf{C}}_{2v\tilde{\sigma}\hat{I}}\right) \tag{165}$$

In a parallel way, the generating functions for the *RS*-permutation group $\mathbf{C}_{2\tilde{\sigma}}$ (Eqs. 156–160) can be calculated from those for the *RS*-stereoisomeric group $\mathbf{C}_{2v\tilde{\sigma}\hat{I}}$ (Eqs. 83–98) as follows:

$$f''_{\mathbf{C}_1} = 2f_{\mathbf{C}_1} + f_{\mathbf{C}_s} + f_{\mathbf{C}'_s} + f_{\mathbf{C}_{\hat{I}}} + f_{\mathbf{C}_{\hat{\sigma}}} \tag{166}$$

$$f''_{\mathbf{C}_2} = 2f_{\mathbf{C}_2} + f_{\mathbf{C}_{2v}} + f_{\mathbf{C}_{2\hat{I}}} \tag{167}$$

$$f''_{\mathbf{C}_{\tilde{\sigma}}} = 2f_{\mathbf{C}_{\tilde{\sigma}}} + f_{\mathbf{C}_{s\tilde{\sigma}\hat{I}}} + f_{\mathbf{C}_{s\tilde{\sigma}\hat{\sigma}}} \tag{168}$$

$$f''_{\mathbf{C}'_{\tilde{\sigma}}} = 2f_{\mathbf{C}'_{\tilde{\sigma}}} + f_{\mathbf{C}'_{s\tilde{\sigma}\hat{I}}} + f_{\mathbf{C}'_{s\tilde{\sigma}\hat{\sigma}}} \tag{169}$$

$$f''_{\mathbf{C}_{2\tilde{\sigma}}} = 2f_{\mathbf{C}_{2\tilde{\sigma}}} + f_{\mathbf{C}_{2v\tilde{\sigma}\hat{I}}} \tag{170}$$

Each column of ICM''_1 (Eq. 149) or ICM''_2 (Eq. 150) can be calculated by summing up an appropriate set of columns of ICM_1 (Eq. 60) or ICM_2 (Eq. 61) in accord with Eqs. 166–170. For example, the first (duplicated), 5th, 6th, 7th, and 8th columns of ICM_1 (Eq. 60) or ICM_2 (Eq. 61) are summed up to give the first column of ICM''_1 (Eq. 149) or ICM''_2 (Eq. 150) in agreement with Eq. 166 (cf. Eq. 161).

The enumeration under the *RS*-permutation group $\mathbf{C}_{2\tilde{\sigma}}$ (Eqs. 166–170) are divided into two parts, i.e., *RS*-stereogenic subgroups (Eqs. 166 and 167) and *RS*-astereogenic subgroups (Eqs. 168–170). See the division by a vertical double line in Fig. 6.

The set of *RS*-stereogenic subgroups (Eqs. 166 and 167) under the *RS*-permutation-group symmetry is correlated to stereoisograms of type I, III, and V, which are

characterized by the *RS*-stereogenicity along the horizontal direction under the *RS*-stereoisomeric-group symmetry.

1. In accord with Eq. 166, the *RS*-permutation group $\mathbf{C}_1$ corresponds to all the type-III ($\mathbf{C}_1$) promolecules listed in Figs. 11 and 12 (except **98** and **99**), the type-V ($\mathbf{C}_s$ and $\mathbf{C}'_s$) promolecules shown in Fig. 16 (except **113**), and all the type-I ($\mathbf{C}_{\widehat{I}}$ and $\mathbf{C}_{\widehat{\sigma}}$) promolecules listed in Fig. 7 (except **23**).
2. In accord with Eq. 167, the *RS*-permutation group $\mathbf{C}_2$ corresponds to the type-III ($\mathbf{C}_2$) promolecules **98** and **99** shown in Fig. 12, the type-V ($\mathbf{C}_{2v}$) promolecule **113** shown in Fig. 16, and the type-I ($\mathbf{C}_{2\widehat{I}}$) promolecule **23** shown in Fig. 7.

On the other hand, the set of *RS*-astereogenic subgroups under the *RS*-permutation-group symmetry (Eqs. 168–170) is correlated to stereoisograms of type II and IV, which are characterized by the *RS*-astereogenicity along the horizontal direction under the *RS*-stereoisomeric-group symmetry.

1. In accord with Eq. 168, the *RS*-permutation group $\mathbf{C}_{\widetilde{\sigma}}$ corresponds to the type-II ($\mathbf{C}_{\widetilde{\sigma}}$) promolecules **25** and **27** listed in Fig. 9, the type-IV ($\mathbf{C}_{s\widetilde{\sigma}\widehat{I}}$) promolecule **101** shown in Fig. 14, and the type-IV ($\mathbf{C}_{s\widetilde{\sigma}\widehat{\sigma}}$) promolecule **103** shown in Fig. 14.
2. In accord with Eq. 169, the *RS*-permutation group $\mathbf{C}'_{\widetilde{\sigma}}$ corresponds to the type-II ($\mathbf{C}'_{\widetilde{\sigma}}$) promolecules **26** and **28** listed in Fig. 9, the type-IV ($\mathbf{C}'_{s\widetilde{\sigma}\widehat{I}}$) promolecule **102** shown in Fig. 14, and the type-IV ($\mathbf{C}'_{s\widetilde{\sigma}\widehat{\sigma}}$) promolecule **104** shown in Fig. 14.
3. In accord with Eq. 170, the *RS*-permutation group $\mathbf{C}_{2\widetilde{\sigma}}$ corresponds to the type-II ($\mathbf{C}_{2\widetilde{\sigma}}$) promolecule **29** listed in Fig. 9 and the type-IV ($\mathbf{C}_{2v\widetilde{\sigma}\widehat{I}}$) promolecule **105** shown in Fig. 14.

9 Conclusion

On the basis of the proligand–promolecule model applied to an oxirane skeleton, the *RS*-stereoisomeric group $\mathbf{C}_{2v\widetilde{\sigma}\widehat{I}}$ for the oxirane skeleton is defined by starting from the point group $\mathbf{C}_{2v}$. Each oxirane derivative as a promolecule, which belongs to a subgroup of $\mathbf{C}_{2v\widetilde{\sigma}\widehat{I}}$, is considered to generate a stereoisogram composed of a quadruplet of promolecules. Because the *RS*-stereoisomeric group $\mathbf{C}_{2v\widetilde{\sigma}\widehat{I}}$ is isomorphic to the point group $\mathbf{D}_{2h}$, the data necessary to combinatorial enumeration under $\mathbf{C}_{2v\widetilde{\sigma}\widehat{I}}$, e.g., the non-redundant set of subgroups, the subduction of coset representations, and the inverse of the mark table, are prepared by referring to the data of $\mathbf{D}_{2h}$. Thereby, the fixed-point-matrix (FPM) method and the partial-cycle-index (PCI) method, which have been originally developed to accomplish combinatorial enumeration under point groups in the unit-subduced-cycle-index approach [23], are extended to meet the combinatorial enumeration under the *RS*-stereoisomeric group $\mathbf{C}_{2v\widetilde{\sigma}\widehat{I}}$. The numbers of inequivalent quadruplets under $\mathbf{C}_{2v\widetilde{\sigma}\widehat{I}}$ are calculated by the FPM method and the PCI method, where each quadruplet contained in a stereoisogram is counted once during this combinatorial enumeration. Such quadruples are itemized with respect to the subgroups of $\mathbf{C}_{2v\widetilde{\sigma}\widehat{I}}$ and categorized into five types (type I to V). The enumeration of oxiranes under the point group $\mathbf{C}_{2v}$ as well as under the *RS*-permutation group $\mathbf{C}_{2\widetilde{\sigma}}$ is also conducted and the results are compared with those of the *RS*-stereoisomeric group $\mathbf{C}_{2v\widetilde{\sigma}\widehat{I}}$.

References

1. A.-H. Li, L.-X. Dai, V.K. Aggarwai, Chem. Rev. **97**, 2341–2372 (1997)
2. A. Padwa, S.S. Murphree, Arkivoc **3**, 6–33 (2006)
3. V.K. Aggarwai, D.M. Badine, V.A. Moorthie, in *Aziridines and Epoxides in Organic Synthesis, Chapter 1*, ed. by A.K. Yudin (Wiley-VCH, Weinheim, 2006), pp. 1–35
4. T. Katsuki, K.B. Sharpless, J. Am. Chem. Soc. **102**, 5974–5976 (1980)
5. Y. Gao, J.M. Klunder, R.M. Hanson, H. Masamune, S.Y. Ko, K.B. Sharpless, J. Am. Chem. Soc. **109**, 5765–5780 (1987)
6. R.A. Johnson, K.B. Sharpless, in *Comprehensive Organic Synthesis*, vol. 7, ed. by B.M. Trost (Pergamon Press, New York, 1991), pp. 389–436
7. E. Höft, Top. Curr. Chem. **164**, 63–77 (1993)
8. T. Katsuki, V. Martin, Organ. React. **48**, 1–299 (1996)
9. Q.-H. Xia, H.-Q. Ge, C.-P. Ye, Z.-M. Liu, K.-X. Su, Chem. Rev. **105**, 1603–1662 (2005)
10. K.B. Sharpless, Nobelprize.org. Novel Media AB2013. Web. 8 Apr 2014 (2001) Nobel lecture: searching for new reactivity. http://www.nobelprize.org/nobel_prizes/chemistry/laureates/2001/sharpless-lecture.html
11. S. Fujita, K. Imamura, H. Nozaki, Bull. Chem. Soc. Jpn. **44**, 1975–1977 (1971)
12. W. McCoull, F. A. Davis, Synthesis **2000**, 1347–1365 (2000)
13. I. Cano, E. Gómez-Bengoa, A. Landa, M. Maestro, A. Mielgo, I. Olaizola, M. Oiarbide, C. Palomo, Angew. Chem. Intern. Ed. **51**, 10856–10860 (2012)
14. S. Fujita, Theor. Chim. Acta **76**, 247–268 (1989)
15. S. Fujita, Bull. Chem. Soc. Jpn. **63**, 315–327 (1990)
16. S. Fujita, J. Am. Chem. Soc. **112**, 3390–3397 (1990)
17. S. Fujita, J. Org. Chem. **67**, 6055–6063 (2002)
18. S. Fujita, Chem. Rec. **2**, 164–176 (2002)
19. S. Fujita, Bull. Chem. Soc. Jpn. **75**, 1863–1883 (2002)
20. S. Fujita, J. Math. Chem. **5**, 121–156 (1990)
21. S. Fujita, Bull. Chem. Soc. Jpn. **63**, 203–215 (1990)
22. S. Fujita, Theor. Chim. Acta **82**, 473–498 (1992)
23. S. Fujita, *Symmetry and Combinatorial Enumeration in Chemistry* (Springer, Berlin, 1991)
24. S. Fujita, *Diagrammatical Approach to Molecular Symmetry and Enumeration of Stereoisomers* (Faculty of Science, University of Kragujevac, Kragujevac, 2007)
25. S. Fujita, Theor. Chem. Acc. **113**, 73–79 (2005)
26. S. Fujita, Theor. Chem. Acc. **113**, 80–86 (2005)
27. S. Fujita, Theor. Chem. Acc. **115**, 37–53 (2006)
28. S. Fujita, Theor. Chem. Acc. **117**, 353–370 (2007)
29. S. Fujita, J. Comput. Chem. Jpn. **6**, 59–72 (2007)
30. S. Fujita, J. Comput. Chem. Jpn. **6**, 73–90 (2007)
31. S. Fujita, Theor. Chem. Acc. **117**, 339–351 (2007)
32. S. Fujita, MATCH Commun. Math. Comput. Chem. **57**, 265–298 (2007)
33. S. Fujita, MATCH Commun. Math. Comput. Chem. **57**, 299–340 (2007)
34. S. Fujita, J. Math. Chem. **43**, 141–201 (2008)
35. S. Fujita, MATCH Commun. Math. Comput. Chem. **58**, 5–45 (2007)
36. S. Fujita, Bull. Chem. Soc. Jpn. **83**, 1–18 (2010)
37. S. Fujita, *Combinatorial Enumeration of Graphs, Three-Dimensional Structures, and Chemical Compounds* (Faculty of Science, University of Kragujevac, Kragujevac, 2013)
38. S. Fujita, Tetrahedron **47**, 31–46 (1991)
39. S. Fujita, J. Org. Chem. **69**, 3158–3165 (2004)
40. S. Fujita, J. Math. Chem. **35**, 265–287 (2004)
41. S. Fujita, J. Math. Chem. **33**, 113–143 (2003)
42. S. Fujita, Tetrahedron **60**, 11629–11638 (2004)
43. S. Fujita, MATCH Commun. Math. Comput. Chem. **54**, 39–52 (2005)
44. S. Fujita, Bull. Chem. Soc. Jpn. **84**, 1192–1207 (2011)
45. S. Fujita, Bull. Chem. Soc. Jpn. **85**, 793–810 (2012)
46. S. Fujita, Bull. Chem. Soc. Jpn. **85**, 811–821 (2012)
47. S. Fujita, J. Math. Chem. **52**, 508–542 (2014)

48. S. Fujita, J. Math. Chem. **52**, 543–574 (2014)
49. S. Fujita, J. Math. Chem. **50**, 2202–2222 (2012)
50. S. Fujita, J. Math. Chem. **50**, 2168–2201 (2012)
51. S. Fujita, Tetrahedron Asymmetry **23**, 623–634 (2012)
52. S. Fujita, MATCH Commun. Math. Comput. Chem. **61**, 71–115 (2009)
53. S. Fujita, Tetrahedron **46**, 365–382 (1990)
54. S. Fujita, J. Math. Chem. **32**, 1–17 (2002)